Identification and Characterization of natural products as dual inhibitors of microsomal Prostaglandin E$_2$ Synthase-1 and 5-Lipoxygenase

Identifizierung und Charakterisierung von Naturstoffen als duale Hemmstoffe der mikrosomalen Prostaglandin E$_2$ Synthase-1 und 5-Lipoxygenase

DISSERTATION

der Mathematisch-Naturwissenschaftlichen Fakultät

der Eberhard Karls Universität Tübingen

zur Erlangung des Grades eines

Doktors der Naturwissenschaften

(Dr. rer. nat.)

vorgelegt von

Julia Seegers

aus Heidelberg

Tübingen

2014

Identification and Characterization of natural products as dual inhibitors of microsomal Prostaglandin E₂ Synthase-1 and 5-Lipoxygenase

Identifizierung und Charakterisierung von Naturstoffen als duale Hemmstoffe der mikrosomalen Prostaglandin E₂ Synthase-1 und 5-Lipoxygenase

DISSERTATION

der Mathematisch-Naturwissenschaftlichen Fakultät
der Eberhard Karls Universität Tübingen

zur Erlangung des Grades eines
Doktors der Naturwissenschaften
(Dr. rer. nat.)

vorgelegt von
Julia Seegers
aus Heidelberg

Tübingen
2014

Tag der mündlichen Qualifikation: 13. Oktober 2014

Dekan: Prof. Dr. Wolfgang Rosenstiel

Erster Berichterstatter: Prof. Dr. O. Werz

Zweiter Berichterstatter: Prof. Dr. S. Laufer

ACKNOWLEDGEMENTS

PUBLICATIONS

List of publications

[1]   Oettl SK, Gerstmeier J, Khan SY, Wiechmann K, **Bauer J,** Atanasov AG, Malainer C, Awad EM, Uhrin P, Heiss EH, Waltenberger B, Remias D, Breuss JM, Boustie J, Dirsch VM, Stuppner H, Werz O and Rollinger JM, Imbricaric acid and perlatolic acid: multi-targeting anti-inflammatory depsides from Cetrelia monachorum. PLoS One, 2013. 8(10): p. e76929.

[2]   **Bauer J,** Waltenberger B, Noha SM, Schuster D, Rollinger JM, Boustie J, Chollet M, Stuppner H and Werz O, Discovery of depsides and depsidones from lichen as potent inhibitors of microsomal prostaglandin E_2 synthase-1 using pharmacophore models. Chem Med Chem. 2012 Dec;7(12):2077-81.

[3]   Elkady M, Nieß R, Schaible AM, **Bauer J**, Luderer S, Ambrosi G, Werz O and Laufer SA, Modified Acidic Nonsteroidal Anti-Inflammatory Drugs as Dual Inhibitors of mPGES-1 and 5-LOX. J Med Chem. 2012 Oct 25;55(20):8958-62.

[4]   De Simone R, Bruno I, Riccio R, Stadler K, **Bauer J**, Schaible AM, Laufer S and Werz O, Identification of new γ-hydroxybutenolides that preferentially inhibit the activity of mPGES-1. Bioorg Med Chem. 2012 Aug 15;20(16):5012-6.

[5]   **Bauer J,** Kuehnl S, Rollinger JM, Scherer O, Northoff H, Stuppner H, Werz O and Koeberle A. Carnosol and carnosic acids from Salvia officinalis inhibit microsomal prostaglandin E_2 synthase-1. J Pharmacol Exp Ther. 2012 Jul;342(1):169-76.

[6]   Minassi A, Cicione L, Koeberle A, **Bauer J**, Laufer S, Werz O and Appendino G. A Multicomponent Carba-Betti Strategy to Alkylidene

Heterodimers - Total Synthesis and Structure-Activity Relationships of Arzanol. European J Org Chem, 2012(4): p. 772-779.

[7]   Baumgartner L, Sosa S, Atanasov AG, Bodensieck A, Fakhrudin N, **Bauer J**, Favero GD, Ponti C, Heiss EH, Schwaiger S, Ladurner A, Widowitz U, Loggia RD, Rollinger JM, Werz O, Bauer R, Dirsch VM, Tubaro A and Stuppner H. Lignan derivatives from Krameria lappacea roots inhibit acute inflammation in vivo and pro-inflammatory mediators in vitro. J Nat Prod. 2011 Aug 26;74(8):1779-86.

[8]   Koeberle A, Rossi A, **Bauer J**, Dehm F, Verotta L, Northoff H, Sautebin L and Werz O. Hyperforin, an Anti-Inflammatory Constituent from St. John's Wort, Inhibits Microsomal Prostaglandin E(2) Synthase-1 and Suppresses Prostaglandin E(2) Formation in vivo. Front Pharmacol. 2011 Feb 18;2:7.

[9]   Waltenberger B, Wiechmann K, **Bauer J**, Markt P, Noha SM, Wolber G, Rollinger JM, Werz O, Schuster D and Stuppner H. Pharmacophore modeling and virtual screening for novel acidic inhibitors of microsomal prostaglandin E(2) synthase-1 (mPGES-1). J Med Chem. 2011 May 12;54(9):3163-74.

[10]   **Bauer J**, Koeberle A, Dehm F, Pollastro F, Appendino G, Northoff H, Rossi A, Sautebin L and Werz O. Arzanol, a prenylated heterodimeric phloroglucinyl pyrone, inhibits eicosanoid biosynthesis and exhibits anti-inflammatory efficacy in vivo. Biochem Pharmacol. 2011 Jan 15;81(2):259-68.

[11]   Koeberle A, Rossi A, Zettl H, Pergola C, Dehm F, **Bauer J**, Greiner C, Reckel S, Hoernig C, Northoff H, Bernhard F, Dötsch V, Sautebin L, Schubert-Zsilavecz M and Werz O. The molecular pharmacology and in vivo activity of 2-(4-chloro-6-(2,3-dimethylphenylamino)pyrimidin-2-ylthio)octanoic acid (YS121), a dual inhibitor of microsomal prostaglandin

E2 synthase-1 and 5-lipoxygenase. J Pharmacol Exp Ther. 2010 Mar;332(3):840-8.

[12]   Koeberle A, **Bauer J**, Verhoff M, Hoffmann M, Northoff H and Werz O. Green tea epigallocatechin-3-gallate inhibits microsomal prostaglandin E(2) synthase-1. Biochem Biophys Res Commun. 2009 Oct 16;388(2):350-4.

Manuscripts accepted

Werz O, **Seegers J**, Schaible AM, Weinigel C, Barz D, Koeberle A, Allegrone G, Pollastro F, Zampieri L, Grassi G and Appendino G. Cannflavins from hemp sprouts, a novel cannabinoid-free hemp food product, target microsomal prostaglandin E_2 synthase-1 and 5-lipoxygenase. (2014) PharmaNutrition

Manuscripts in preparation

Seegers, J., Boustie, J., Rollinger, J., Stuppner, H., Weinigel, C., Barz, D. and Werz, O. (2014) The pharmacological profile of perlatolic acid and physodic acid from *lichen species* as inhibitors of eicosanoid biosynthesis.

Presentations

Bauer, J., Kuehnl, S., Rollinger, J.M., Scherer, O., Northoff, H., Stuppner, H., Werz, O., Koeberle, A. (2012) Carnosol and carnosic acid from *Salvia officinalis* inhibit microsomal Prostaglandin E_2 synthase-1. Poster, *DPhG joint meeting 2012,* Greifswald (Germany)

Bauer, J., Dehm, F., Koeberle, A., Pollastro, F., Appendino, G., Rossi, A., Sautebin, L., Werz O. (2010) *In vitro* and *in vivo* evaluation of the anti-inflammatory effects of Arzanol from *Helichrysum italicum.* Poster, *58th International Congress and Annual Meeting of the Society for Medicinal Plant and Natural Product Research* 2010, Berlin (Germany)

Bauer, J., Dehm, F., Koeberle, A., Pollastro, F., Rossi, A., Appendino, G., Sautebin, L. and Werz, O. (2010) Arzanol, a dual inhibitor of 5-LO and mPGES-1. Poster, *III European Workshop on Lipid Mediators* 2010, Paris (France)

TABLE OF CONTENT

ABBREVIATION

12-HHT	12(S)-hydroxy-5-cis-8,10-trans-heptadecatrienoic acid
5-HEDH	5-hydroxyeicosanoid dehydrogenase
5-HETE	5(S)-hydroxy-6-trans-8,11,14-cis-eicosatetraenoic acid
5-HpETE	5(S)-hydroperoxy-6-trans-8,11,14-cis-eicosatetraenoic acid
5-oxo-ETE	5-oxo-eicosatetraenoic acid
A23187	Ca^{2+} ionophore A23187
AA	arachidonic acid
ATP	adenosine triphosphate
cAMP	cyclic adenosine monophosphate
CHM	chinese herbal medicine
CIA	collagen-induced arthritis
COX	cyclooxygenase
cPGES	cytosolic prostaglandin E_2 synthase
$cPLA_2$	cytosolic phospholipase A_2
DHA	docosahexaenoic acid
DMEM	Dulbecco's modified eagle's medium
DMSO	dimethylsulfoxide
DPPH	2,2-diphenyl-1-picrylhydrazyl
EDTA	ethylenediaminetetraacetic acid
ELISA	enzyme linked immunosorbent assay
EPA	eicosapentaenoic acid
ERK	extracellular signal-regulated kinase
FCS	fetal calf serum
FLAP	5-lipoxygenase-activating protein
fMLP	formyl-methionyl-leucyl-phenylalanine

GBE	Ginkgo biloba extract
GPCR	G protein-coupled receptor
GSH	glutathione
HPLC	high performance liquid chromatography
IL-1ß	interleukin-1ß
iNOS	inducible nitric oxide synthase
JAK	janus kinase
LDLR	low-densitiy lipoprotein receptor
LO	lipoxygenase
LPA	lysophosphatidic acid
LPC	lysophospholipids
LPS	lipopolysaccharide
LT	leukotriene
LTA4H	LTA_4 hydrolase
LTC4S	LTC_4 synthase
MAPEG	Membrane-associated proteins involved in eicosanoid and glutathione metabolism
MAPK	mitogen-activated protein kinase
MDA	malondialdehyde
MGST	microsomal glutathione S-transferase
mPGES-1	microsomal prostaglandin E_2 synthase-1
mPGES-2	microsomal prostaglandin E_2 synthase-2
MRP	multidrug resistance protein
MTT	3-(4,5-dimethylthiazol-2-Yl)-2,5-diphenyltetrazolium bromide
NFκB	nuclear factor kappa B
NO	nitric oxide
NSAID	non-steroidal anti-inflammatory drug
PAF	platelet-activating factor

PBMC	peripheral blood mononucelar cells
PBS	phosphate-buffered saline
PG	prostaglandin
PKA	protein kinase A
PMNL	polymorphonuclear leukocytes
PUFA	polyunsaturated fatty acid
S1P	sphingosine-1-phosphate
SAR	structure activity relationship
SDS	sodiumdodecylsulfate
SDS-PAGE	sodiumdodecylsulfate polyacrylamide gel electrophoresis
TBH	tert-butyl hydroperoxide
TLR	toll like receptor
TNF	tumor necrosis factor
TXAS	thromboxane A_2 synthase

1   INTRODUCTION

1.1   Role of lipid mediators in inflammation

Inflammation is a complex physiological mechanism in response to tissue injury and/or infection and contemporaneously the initiation of the healing process. The cardinal signs of inflammation are swelling, pain, heat, redness and loss of function (tumor, dolor, calor, rubor and functio laesa) [1].

Bioactive lipids play important roles as signalling and regulatory mediators in the body, see **Fig. 1.1** for overview. Various lipid mediators derived from polyunsaturated fatty acids (PUFAs), arachidonic acid (AA) or lysophospholipids (LPC) and can be structurally classified into three groups, see **Table 1.1** [2].
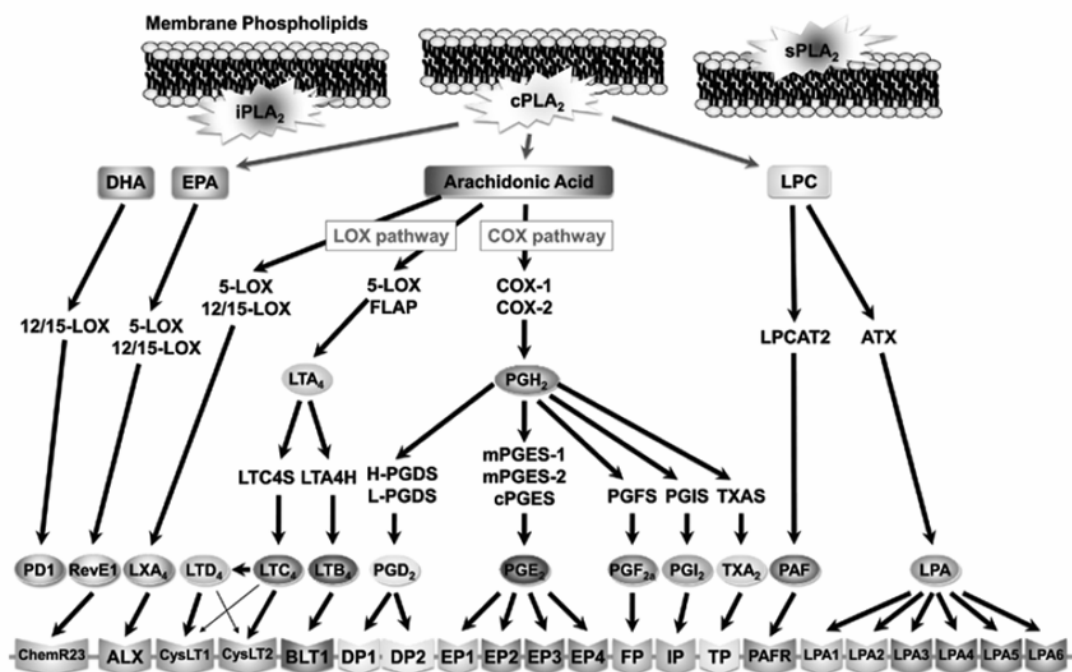
Fig. 1.1: Overview on lipid mediator pathways [2]

Phospholipases, mainly cPLA$_2$ but also iPLA$_2$ and sPLA$_2$, release polyunsaturated fatty acids (AA, DHA and EPA) or lysophospholipids (LPC) from the membrane. AA is

converted through the COX or 5-LO pathway to prostanoids or leukotrienes. AA, DHA and EPA are converted by 5-LO and 12/15-LO to the anti-inflammatory mediators lipoxin A_4 (LXA$_4$), resolvin E_1 (RevE$_1$) and protectin D1 (PD$_1$). LPC is converted to PAF or LPA. Incurred lipid mediators act via their corresponding G protein-coupled receptors (GPCR). Abbreviations: iPLA$_2$, inhibitory phospholipase A$_2$; sPLA$_2$, secretory phospholipase A$_2$; cPLA$_2$, cytosolic phospholipase A$_2$; DHA, docosahexaenoic acid; EPA, eicosapentaenoic acid; LPC, lysophosphatidylcholine; LO, lipoxygenase; COX, cyclooxygenase; FLAP, 5-lipoxygenase-activating protein; LPCAT2, lysophosphatidylcholine acetyltransferase 2; ATX, autotoxin; LTC4S, LTC$_4$ synthase; LTA4H, LTA$_4$ hydrolase; H-/L-PGDS, hematopoetic or lipocalin-type prostaglandin D$_2$ synthase; mPGES-1/-2, microsomal prostaglandin E$_2$ synthase 1/2; cPGES, cytosolic prostaglandin E$_2$ synthase; PAF, platelet activating factor; LPA, lysophosphatidic acid

Table 1.1: classification of lipid mediators [2]

1	arachidonic acid-derived eicosanoids	e.g. prostaglandins (PGs), leukotrienes (LTs)
2	lysophospholipids and endocannabinoids	e.g. platelet-activating factor (PAF), lysophosphatidic acid (LPA), sphingosine-1-phosphate (S1P)
3	ω-3-polyunsaturated fatty acids derived anti-inflammatory mediators	e.g. resolvins, protectins

1.1.1 Acute inflammation

Tissue damage provokes three types of acute signals. Hyperalgesia is mediated by PGE$_2$ and in response to pain. Cytokine production is induced as a consequence of broken cells that release their intracellular proteins to the vicinity, and pathogens are sensed by the complement system and cell-surface receptors, such as toll like receptors (TLR). Responding to these

signals, leukocytes are recruited from the blood. Histamine and eicosanoids released from perivascular mast cells cause vasodilatation (heat and redness) and extravasation of fluid (swelling). In addition, platelet-activating factor (PAF) is released to amplify leukocyte emigration. Neutrophils, activated by tumor necrosis factor (TNF) and leukotrienes degranulate and gear the inflammatory process. Monocytes and tissue macrophages are chemotactically attracted and lymphocytes as well as dendritic cells are recruited by prostaglandins, leukotrienes, chemokines and defensins to mature and activate macrophages. The acute inflammatory process requires ongoing signals in a positive feedback-loop from every newly recruited cell after contact to pathogens or broken cells. If the initiating factor is removed, the inflammatory reaction will resolve. During resolution of inflammation PGE_2 turns to anti-inflammatory properties, as rising PGE_2 levels inhibit the pro-inflammatory enzymes cyclooxygenase-2 (COX-2) and 5-lipoxygenase (5-LO) and additionally induce 15-lipoxygenase (15-LO) expression in neutrophils. Neutrophil-derived arachidonic acid (AA) is then metabolized to anti-inflammatory lipoxins via 12- and 15-LOs leading to resolution of inflammation. Macrophages and lymphocytes return to pre-inflammatory numbers and phentotypes and tissue repair is accomplished [1, 3].

1.1.2 Chronic inflammation and cancer

If the initiating factors persist or inflammatory responses are dysregulated, inflammation becomes chronic and leads to inflammatory disorders, such as Alzheimer disease, asthma, atherosclerosis, chronic obstructive pulmonary disease (COPD), multiple sclerosis (MS) or rheumatoid arthritis (RA).

Moreover, a connection between chronic inflammation and cancer is evident [4, 5]. For example, several studies have shown that inflammatory cells and mediators are present in the tumour microenvironment [6-8]. Triggers of chronic inflammation, such as microbial or viral infections, autoimmune diseases or other inflammatory conditions of unknown origin, are associated with different types of cancer development [4]. In line, treatment with non-steroidal anti-inflammatory drugs (NSAIDs) or coxibes was shown to decrease the risk of cancer development [9-11]. However, inflammatory processes in tumours do not have to be causally related to a classical inflammation [12].

1.1.3 Eicosanoids

In 1982, the Nobel Prize in Physiology or Medicine was awarded to Samuelsson, Bergstrom (Sweden) and Vane (UK) *"for their discoveries concerning prostaglandins and related biologically active substances"* [13]. Eicosanoids, including PGs, LTs and derivatives, act as autocrine or paracrine lipid mediators. They are derived from 20-carbon unsaturated fatty acids such as AA via the COX or LO pathway and are involved in various physiological and pathological actions in the body (see **Table 1.2** for overview) [2, 3, 14-16].

Table 1.2: overview of biological actions of eicosanoids [17]

Organ	function	eicosanoids
vessels and sphincter	Vasodilatation	PGE_2, PGD_2, PGI_2
	Vasoconstriction	PGE_2, PGD_2, $PGF_{2\alpha}$, TXA_2, LTC_4, LTD_4, LTE_4
	Permeability ↑	LTB_4, LTC_4, LTD_4, LTE_4
Stomach and gastrointestinal tract	Relaxation of smooth muscle	PGE_2
	Contraction of smooth muscle	PGE_2, $PGF_{2\alpha}$, PGI_2, TXA_2, LTC_4, LTD_4, LTE_4
	secretory volume, acidity and pepsin ↓	PGE_2, PGI_2
	mucus secretion ↑	PGE_2, PGI_2
heart	blood flow ↑	PGE_2
	Cardiac output ↑	PGE_2, $PGF_{2\alpha}$, PGI_2
	Cardiac contractility ↑	$PGF_{2\alpha}$
	Modulation of cardiac rhythm	$PGF_{2\alpha}$
kidney	Diuresis, natriuresis and kaliuresis ↑	PGE_2, PGI_2
	Renin secretion ↑	PGE_2, PGD_2, PGI_2
	Glomerular filtration ↓	TXA_2
lung and bronchia	Relaxation of smooth muscle	PGE_2, PGI_2
	Contraction of smooth muscle	PGD_2, $PGF_{2\alpha}$, LTC_4, LTD_4, LTE_4
	Mucosal edema	LTC_4, LTD_4, LTE_4
	Secretion of mucus and glycoproteins	LTC_4, LTD_4, LTE_4

immune system	chemotaxis	LTB_4
	Aggregation of neutrophils	LTB_4
	Recruitment, migration, adhesion of leukocytes	LTB_4
	Degranulation of leukocytes	LTB_4
	Cytokine production ↑	LTB_4
	Proliferation, activation and immunoglobulin production of B lymphocytes	LTB_4
nervous system	Hyperalgesia	PGE_2, PGI_2, LTB_4
	Nociceptive modulation	PGD_2
uterus	Relaxation of smooth muscle	PGE_2
	Contraction of smooth muscle	$PGF_{2\alpha}$, TXA_2
Endocrine system	ACTH, growth hormone, prolactin, gonadotropin ↑	PGE_2

1.2 PGE_2 as prominent bioactive lipid mediator

1.2.1 Prostanoids

Five endogenously produced bioactive prostanoids are known to date: prostaglandin E_2 (PGE_2), prostaglandin D_2 (PGD_2), prostaglandin F_{2a} (PGF_{2a}), prostacyclin (PGI_2) and thromboxane A_2 (TXA_2). They are generated via the COX pathway, see **Fig. 1.2**. As prostanoids cannot be stored, they are synthesized *de novo* in most cells of the body either constitutively or after certain stimuli. Here, phospholipases, mainly cytosolic phospholipase A_2 ($cPLA_2$), release arachidonic acid (AA) from membrane glycerophospholipids. AA is further oxygenated via the activity of either COX-1 or -2 to PGG_2 and subsequently reduced to the instable

intermediate PGH_2. Terminal synthases isomerize PGH_2 into different prostanoids, depending on the cellular constitution of the respective cell. Then, prostanoids are released from the cell and act via their corresponding G protein-coupled receptors (GPCR). These receptors are highly selective for the individual prostanoids [2, 14].
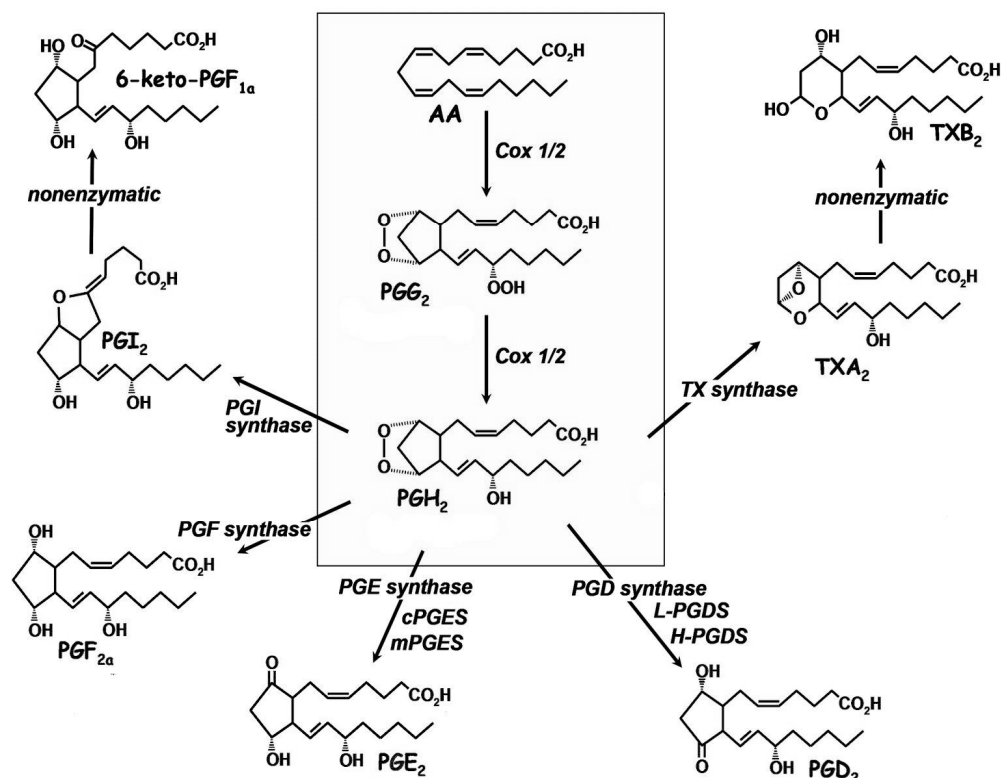
Fig. 1.2: Biosynthesis of PGI$_2$, PGF$_{2\alpha}$, PGE$_2$, PGD$_2$ and TXA$_2$ via the cyclooxygenase pathway [18], modified.

Inhibition of PGE_2 biosynthesis has been an effective pharmacological strategy in the therapy of inflammation for more than 100 years [19]. Due to the fact that inhibition of COX-1 and -2 by NSAIDs or selective COX-2 inhibition by coxibs is associated with severe side-effects such as gastrointestinal toxicity and cardiovascular complications, there is still a strongly need for further development of anti-inflammatory drugs. Gastrointestinal toxicity is predominantly attributed to the suppression of constitutively COX-1-derived prostanoid formation. Based on the fact that

constitutive COX-2 expression is essentially restricted to the brain and kidney and pathogenic PGE_2 levels are generated via the inducible COX-2 isoform, selective COX-2 inhibitors (coxibs) have been developed. COX-2 is inducible and expressed in response to pro-inflammatory stimuli, whereas COX-1 is constitutively active and rather responsible for physiological housekeeping functions. Coxibs possess an improved gastrointestinal tolerance, but studies reveal an increased risk for cardiovascular complications due to an imbalance of COX-1 derived pro-thrombotic TXA_2 and COX-2 derived anti-thrombotic PGI_2. Therefore, several coxibs have been withdrawn from the market [2, 14].

Since long-term application is required for therapy of chronic inflammation, there is still a strong need for the development of anti-inflammatory drugs with an improved safety profile. Thus, suppression of selective microsomal prostaglandin E_2 synthase-1 (mPGES-1)-derived PGE_2 has been considered as an alternative strategy for the treatment of inflammation [20].

1.2.2 PGE_2

PGE_2 is among the most powerful lipid mediators and exerts various physiological and pathological effects depending (I) on the amount of PGE_2 and (II) the subtype of receptor (EP1-4) available within the respective tissue [15]. Several basic homeostatic functions are known for PGE_2 like gastrointestinal mucosa protection and motility [21], blood pressure control, airway homeostasis, female reproduction and kidney function [22]. On the other hand, PGE_2 is also involved in pathological actions, basically inflammation, fever and pain.
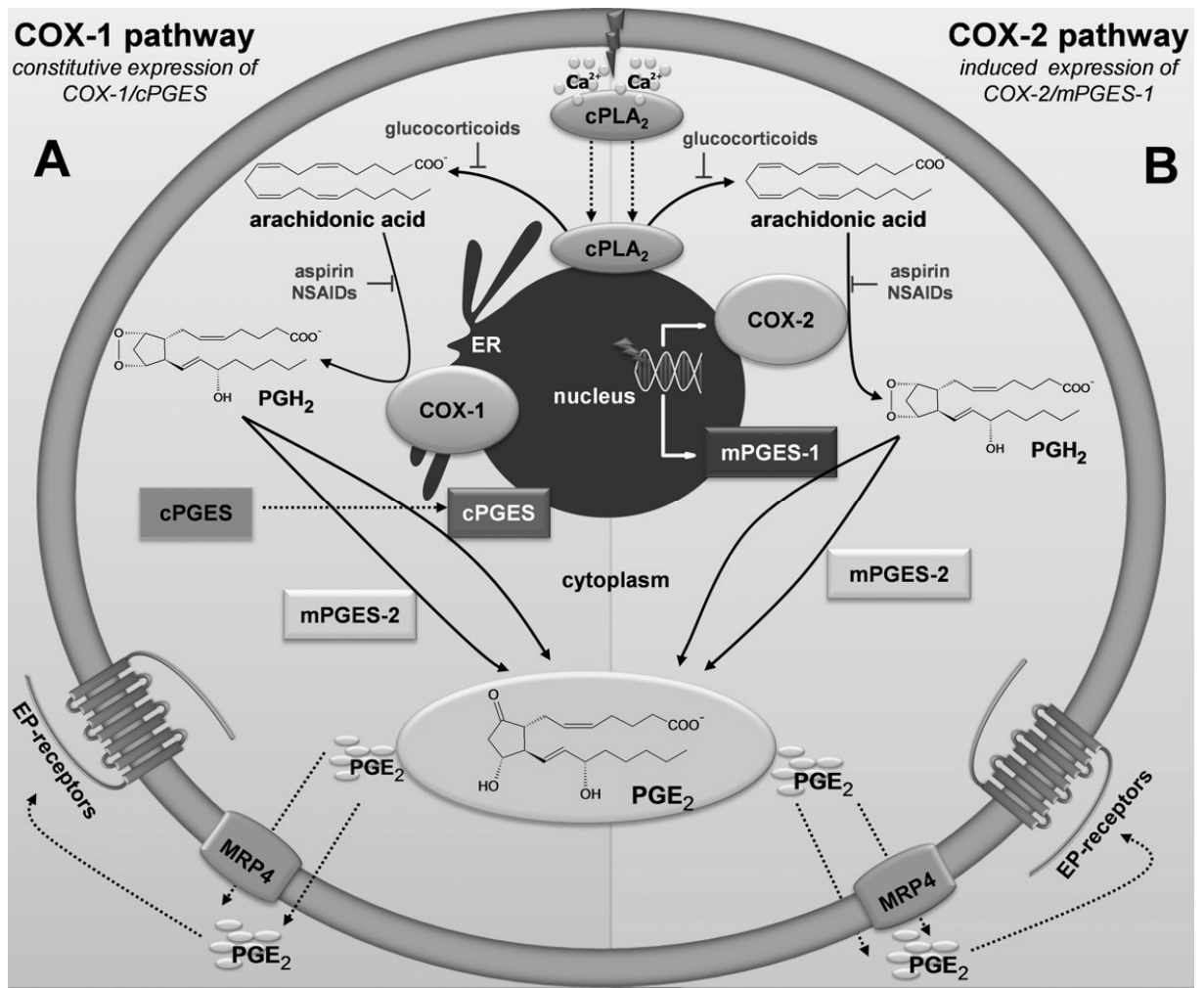
Fig. 1.3: PGE$_2$ biosynthesis (from [15], modified)

Abbreviations: cPLA$_2$, cytosolic phospholiase A$_2$; COX, cyclooxygenase; mPGES-1/-2, microsomal prostaglandin E$_2$ synthase-1/-2; cPGES, cytosolic prostaglandin E$_2$ synthase; MRP4, multidrug resistance protein 4

Three terminal synthases that catalyze PGE$_2$ formation from COX-derived PGH$_2$ are known, namely the cytosolic PGE$_2$ synthase (cPGES) and the two membrane-bound PGE$_2$ synthases mPGES-1 and mPGES-2 (**Fig. 1.3**) [23-25].

cPGES and mPGES-2 are structurally and biologically distinct from mPGES-1. They are constitutively expressed and therefore more likely involved in homeostatic processes in the body [26-28]. mPGES-2 can use PGH$_2$ as a substrate from both COX-1 and -2, whereas cPGES is mainly

coupled to COX-1. However, mPGES-1 is inducible and functionally coupled to COX-2 [25].

mPGES-1 (16kDa) was discovered by Jakobsson et al. in 1999 and belongs to the MAPEG (membrane-associated proteins involved in eicosanoid and glutathione metabolism) family. This superfamily also contains leukotriene C_4 (LTC$_4$) synthase, 5-lipoxygenase-activating protein (FLAP) and three different glutathione-transferases 1-3 (MGST1-3). The structure forms a homotrimer consisting of twelve transmembrane helices (four for each monomer) with a large cone-shaped cavity in the center of the trimer [29], which is similar to other MAPEG members. Glutathione (GSH) is required as cofactor for the activity [30]. It is coordinated by hydrogen bonds involving the side chains of helices I, II and IV and π-stacking interactions of Tyr130 in a horseshoe conformation. The catalysis of PGH$_2$ to PGE$_2$ has not yet been fully determined, but it is likely that glutathione, Asp49 and Ser127 are involved to initiate the catalytic cycle [31]. Its regulation is still under investigation.

The human gene for mPGES-1 (18.3 kb) contains three exons and is localized to chromosome 9q34.3 [32]. Although there is no obvious similarity of the mPGES-1 and COX-2 promoters, their expression is generally co-regulated [25, 33]. Constitutive expression levels of mPGES-1 are low and as mPGES-1 is primarily linked to COX-2 it can be strongly upregulated by pro-inflammatory stimuli, such as interleukin-1β (IL-1ß), tumor necrosis factor-α (TNFα), or LPS. Studies reveal the concomitant induction of COX-2 and mPGES-1 in various cultured cells, i.e. human lung carcinoma A549 cells [30], macrophages [34] or endothelial cells [35] in response to pro-inflammatory stimuli and its prevention by glucocorticoids [32-34, 36, 37]. PGE$_2$ formation was significantly

increased in HEK293 cells, cotransfected with mPGES-1 and COX-2, in response to A23187 (induces acute inflammatory response) or IL-1ß (mediator of the delayed response) [34]. These observations could not be shown for HEK293 cells cotransfected with COX-1 and mPGES-1.

Increased mPGES-1 expression was found in various diseases related to inflammation, i.e. synovial tissue of patients with rheumatoid arthritis [38], in the cartilage and chondrocytes of osteoarthritic patients [39-42] in inflamed intestinal mucosa from patients with inflammatory bowel disease [43], in atherosclerotic carotid plaques [44-46], in Alzheimer disease tissues [47], in muscle tissue of patients with idiopathic inflammatory mypathies [48], in endothelial cells, smooth muscle cells and immune cells from patients with periodontitis [49], in chronic active lesions localized to microglia/macrophages from patients with multiple sclerosis [50], and various cancer types including gastrointestinal, lung, stomach, brain, breast, pancreas, prostate, cervix, papillary thyroid, head and neck squamous carcinoma [51].

In vivo experiments with wild-type rats and mice support the role of mPGES-1 in inflammation *in vivo* [52]. Constitutive expression of mPGES-1 resulted in small amounts of PGE_2 levels, whereas addition of LPS could significantly increase the PGE_2 production [36, 53, 54]. Moreover, mPGES-1 RNA and protein was observed in carrageenan-induced and adjuvant-induced paw edema in rats [55, 56].

mPGES-1 knockout mice exhibit normal phenotype, life period and fertility compared to their littermates. They show significantly reduced PGE_2 levels in response to pro-inflammatory stimuli, such as LPS, TNFα or interleukin-6/-12 compared to wild type mice in different models of inflammation [57, 58]. Several studies demonstrate a pathogenic role of mPGES-1 in collagen-induced arthritis [57], atherosclerosis [59], LPS–induced pyresis [60], pain hypersensitivity [54], experimental autoimmune

encephalomyelitis [50], infection-induced neonatal hypoxia [61], Alzheimer´s disease [62] and several types of cancer [63, 64].

PGE_2 is secreted by the ATP-dependent multidrug resistance protein-4 (MRP4) or by diffusion and acts nearby through binding to one or more of the PGE_2 receptor (EP) subtypes EP1 to EP4 [23, 65]. EP receptors are GPCR receptors and for signal transduction cAMP, Ca^{2+} and inositol phosphates act as second messenger, depending on the subtype of EP receptor. EP1 regulates Ca^{2+} influx without relevant levels of a phosphatidylinositide response, suggesting that it is coupled to an unidentified G protein. The EP2 and EP4 receptor subtypes are coupled to G_s and mediate increase in cAMP concentrations. In contrast, EP3 is G_i coupled and reduces cAMP concentrations [65].

EP1 has been reported to be involved in mediating hyperalgesia on peripheral sensory neurones [66] and acute pain response in acetic acid-induced writhing test [67]. EP2 and EP3 are described to participate in inflammatory exudation [68]. In addition development of paw swelling associated with collagen induced arthritis [69] is also contributed to EP2. EP4 is known to have a pro-inflammatory role in pathogenesis of rheumatoid arthritis [70] and in the development of paw swelling associated with collagen induced arthritis [69].

Besides its pro-inflammatory properties, EP2-4 receptors can also contribute to the resolution of inflammation [71-75].

1.2.3 Drug discovery of mPGES-1 inhibitors

The story of coxibs has taught us what might happen if the sensitive balance of prostanoids (here PGI_2 and TXA_2) is affected by drugs. Concerns about cardiotoxicity of potential mPGES-1 inhibitors could not

be confirmed, since deletion of mPGES-1 did not result in any impact on blood pressure when mice were crossed with low-density lipoprotein receptor (LDLR) knockout mice [59]. Moreover, reduced levels of myocardial damage after coronary occlusion and no alteration of PGI_2 and TXA_2 after myocardial infarct were observed in mPGES-1 knockout mice [76, 77].

By now, multiple diverse structures of mPGES-1 inhibitors are described in literature, but no selective mPGES-1 inhibitor is available for clinical use. Chang and Meuillet [78] characterized them into four groups: (I) endogenous lipids, fatty acids and PGH_2 analogues (II) known anti-inflammatory drugs and/or inhibitors of LT biosynthesis (III) natural compounds and (IV) further development.

Endogenous lipids, fatty acids and PGH_2 analogues

LTC_4 (IC_{50} = 5 µM) [33], identified as inhibitor of mPGES-1, was first shown to inhibit MGST-1 [79]. Since MGST-1 and mPGES-1 are structural homologues that both belong to the MAPEG superfamily, the mode of inhibition might be similar by competing with GSH. Also other lipids could be identified as mPGES-1 inhibitors, i.e. 15-deoxy-Δ12,14-PGJ_2 (IC_{50} = 0.3 µM) and a number of fatty acids, including AA, DHA, EPA (IC_{50} = 0.3 µM each) and palmitic acid (IC_{50} = 2 µM) [80]. As 15-deoxy-Δ12,14-PGJ_2, DHA and EPA have anti-inflammatory properties, mPGES-1 inhibition might contribute to their anti-inflammatory effects. Among stable PGH_2 analogues, U-51605 was shown to inhibit mPGES-1 activity [33, 80].

Table 1.3: structures of endogenous lipids, fatty acids and PGH$_2$ analogues identified as mPGES-1 inhibitors

LTC$_4$

15-deoxy-Δ12,14-PGJ$_2$

DHA

EPA

AA

palmitic acid

U-51605
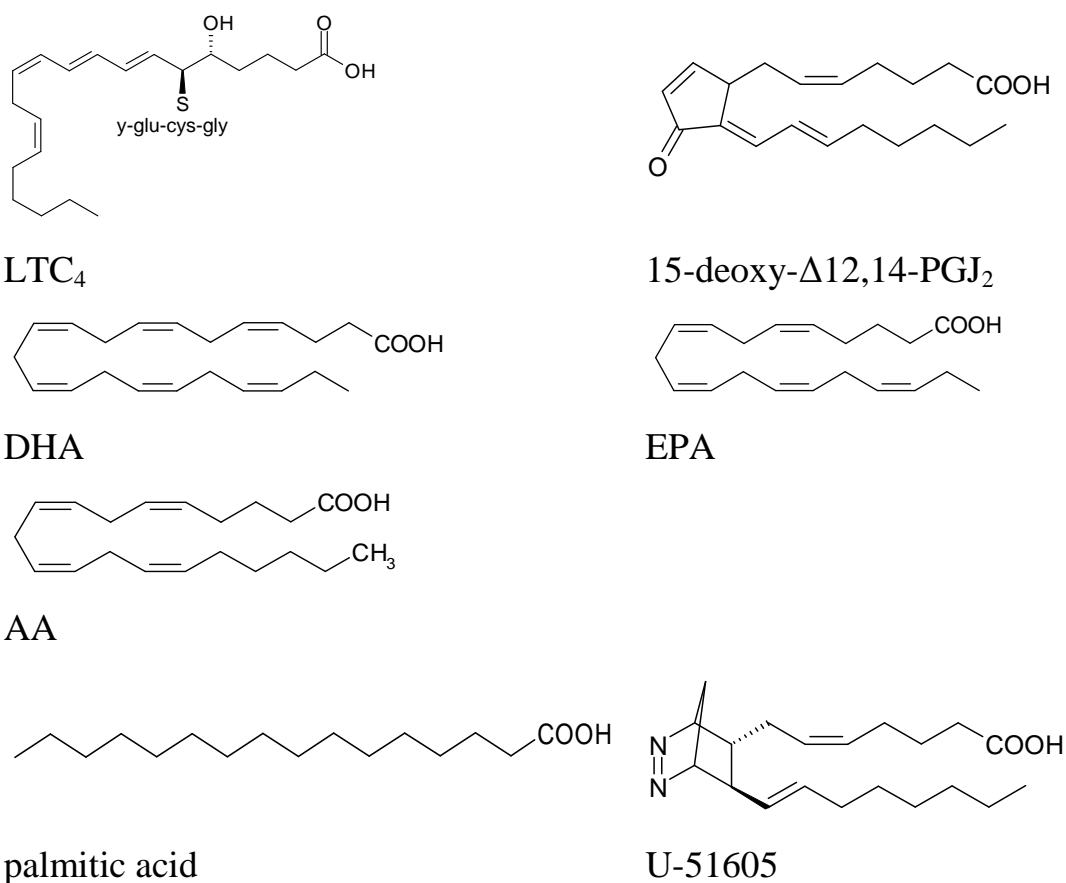
Known anti-inflammatory drugs and/or inhibitors of LT biosynthesis

Several NSAIDs and coxibs were identified as mPGES-1 inhibitors, including sulindac sulfide (IC$_{50}$ = 80 µM), NS-398 (IC$_{50}$ = 20 µM) [33], celecoxib (IC$_{50}$ = 22 µM), dimethylcelecoxib (IC$_{50}$ = 16 µM), lumiracoxib (IC$_{50}$ = 33 µM) and valdecoxib (IC$_{50}$ = 75 µM) [81]. The well-known FLAP inhibitor MK-886 also inhibits mPGES-1 (IC$_{50}$ = 2.4 µM) [56]. As FLAP also belongs to the MAPEG superfamily, inhibition might be due to similarities in the structure. Furthermore, licofelone, a proposed dual COX/5-LO inhibitor, was identified as inhibitor of mPGES-1 (IC$_{50}$ = 6 µM) [82].

Table 1.4: structures of anti-inflammatory drugs identified and/or inhibitors of LT biosynthesis identified as mPGES-1 inhibitors

| sulindac sulfide | NS-398 | celecoxib | dimethylcelecoxib |

| lumiracoxib | valdecoxib | MK-886 | licofelone |
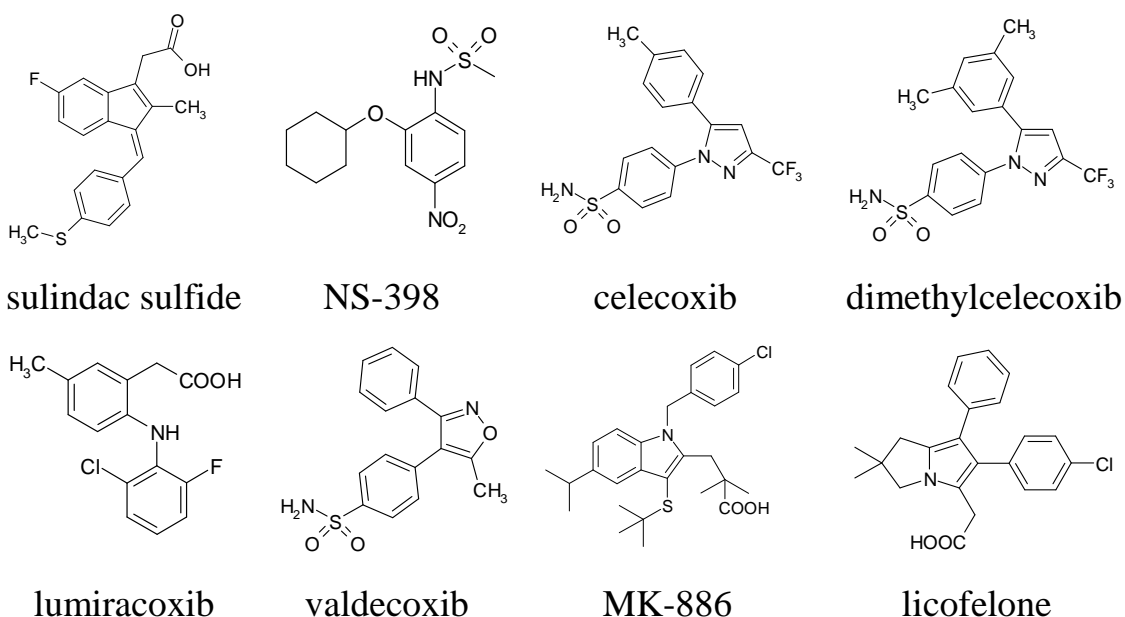
Natural compounds

A series of anti-inflammatory natural mPGES-1/5-LO inhibitors from our group have been described in literature, such as curcumin from turmeric (IC_{50} = 0.3 µM) [83], epi-gallocatechin gallate (EGCG) from green tea (IC_{50} = 1.8 µM) [84], garcinol from the fruit rind of *Guttiferae* species (IC_{50} = 0.3 µM) [85], myrtucommulone from myrtle (IC_{50} = 1 µM) [86], several boswellic acids from frankincense (IC_{50} = 3–10 µM) [87], and the acylphloroglucinol hyperforin from St. John's wort (IC_{50} = 1 µM) [88].

Table 1.5: structures of natural compounds identified as mPGES-1 inhibitors

| curcumin | EGCG | garcinol |

myrtucommulone   boswellic acids   hyperforin
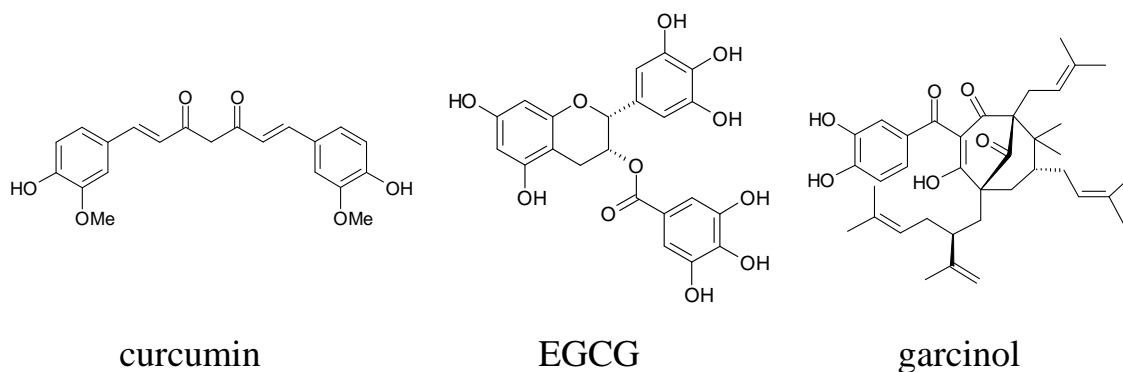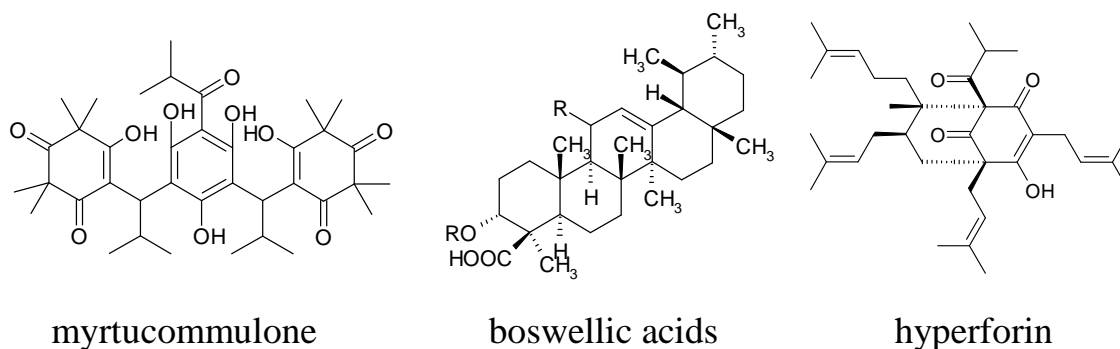
Further development of mPGES-1 inhibitors [89]

Based on the structure and cellular activities some compounds were further improved, resulting in a heterologue field of synthetic mPGES-1 inhibitors. These scaffolds include carboxylic acids from MK-886 [90], phenanthrene imidazoles from the JAK inhibitor azaphenanthrenone [91], biarylimidazoles from MF63 [92], pirinixic acid derivatives [93], 2-mercaptohexanoic acids from 2-mercaptohexanoic [94], arylpyrrolizines from licofelone [95], benzo[g]indol-3-carboxylates [96], oxicames from a screening series of benzo-thiopyran S-dioxides [97, 98], trisubstituted ureas from high-throughput screening campaign [99] and carbazole benzamide from a series of carbazole benzamides [100].

1.3   The dual inhibition concept

In 1996, the group of Nickerson-Nutter demonstrated the effects of 5-LO and/or COX inhibitor administration in a mouse model of collagen-induced arthitis (CIA) [101]. Surprisingly, a significant reduction of CIA was only observed in the dual approach of 5-LO and COX inhibitors and no effect could be observed when administered alone.

COX inhibition might redirect available AA towards 5-LO, leading to an increased formation of pro-inflammatory leukotrienes [14] and therefore increase the risk of gastric damage. Comedication of NSAIDs with 5-LO inhibitors or leukotriene receptor antagonists was shown to be superior

over single NSAID administration not only in the treatment of inflammation and pain as they have an improved side-effect profile [102]. COX-1 is constitutively expressed in nearly all tissues and considered to mediate physiological responses, such as cytoprotection of the stomach, platelet aggregation and renal function. COX-2 on the other hand is known to be inducible and highly upregulated in inflammatory cells during pathological processes [103]. Classical NSAIDs have no selectivity for COX-1 or -2 and mostly inhibit both enzymes with a similar potency. As the anti-inflammatory action results from COX-2 inhibition, unwanted side-effects, mainly gastrointestinal and renal toxicity, are ascribed to COX-1 inhibition [104]. Consequently, selective COX-2 inhibitors, known as coxibs, were developed in order to improve the safety profile and potency. To this knowledge dual COX-2/5-LO inhibition seems to be favored in the development of safer anti-inflammatory drugs. Several studies demonstrate that selective COX-2 inhibition indeed causes significantly less ulceration, but renal and cardiovascular toxicity were observed [105]. Since synthesis or end actions of LTs are unaffected by NSAIDs, "targeting of these enzyme systems suggested a promising pharmacological approach in the post-COX-2 era to reduce the cardiovascular events of selective COX-2 inhibition without gastric side effects of non-specific inhibition of COX" [103].

Because mainly PGE_2 among the COX products is responsible for inflammatory events, current research outcomes propose the dual inhibition of mPGES-1/5-LO as a promising strategy to avoid ordinary side effects of NSAIDs or coxibs and to improve the safety of anti-inflammatory drugs [93].

1.4   5-LO products and their role in inflammation

1.4.1 Leukotrienes

Besides the COX pathway, released AA can be converted via the LO pathway into leukotrienes and other hydroxylated derivatives, see **Fig. 1.4**. Five human LOs are known by now, i.e., 5-(S)-LO, platelet-type 12-(S)-LO, epidermis-type 12(R)-LO, reticulocyte type 15-(S)-LO (15-LO-1) and epidermis-type 15(R)-LO (15-LO-2) [106]. Of these LOs, 5-LO seems to play a critical role in inflammatory events.

5-LO is the key enzyme in the LO pathway and catalyzes the incorporation of molecular oxygen into AA yielding LTA_4. LTA_4 can be either hydrolysed to LTB_4 by LTA_4-hydrolase (LTA4H) or conjugated with glutathione to LTC_4 by LTC_4 synthase (LTC4S), depending on the cellular facilities. LTB_4 and LTC_4 are secreted from the cell. Extracellular metabolism can form the cysteinyl leukotrienes (CysLTs) LTD_4 and LTE_4 out of LTC_4 [107], see **Fig. 1.4**. Leukotrienes exert their biological actions via their corresponding GPCR receptors. They have multiple biologic actions and are involved in several pathologies, including allergic and inflammatory diseases [108]. At least, combined action of 5-LO and 12-LO or 15-LO can form anti-inflammatory bioactive lipoxins, which act through the ALX receptor and are involved in resolution of inflammation [107]. The CysLT1 receptor antagonist montelukast is used as drug for the therapy of asthma. No other "leukotriene pharmaceuticals" are available on the European market by now [14]. Zafirlukast, Pranlukast as leukotriene receptor antagonists and Zileuton, a FLAP inhibitor, are available on the Japanese and/or US market.
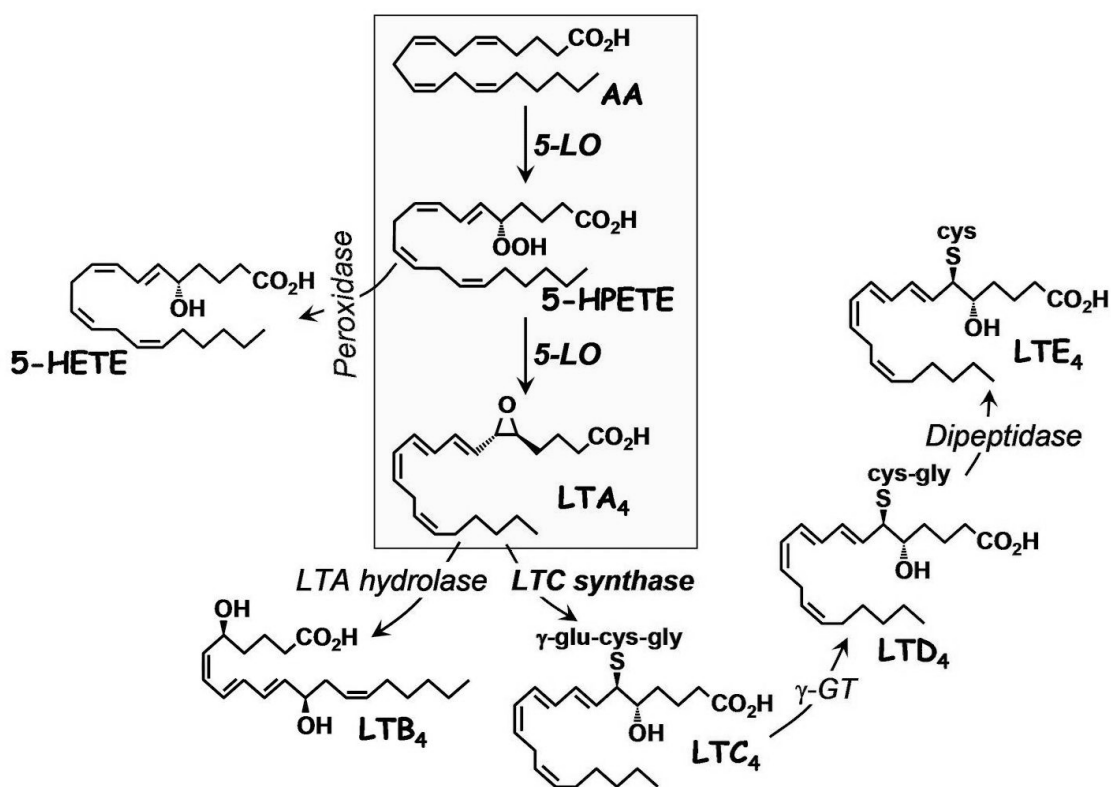
Fig. 1.4: Biosynthesis of leukotrienes via the LO pathway (from [18], modified)
Abbreviations: AA, arachidonic acid; 5-HpETE, 5(S)-hydroperoxy-6-trans-8,11,14-cis-
eicosatetraenoic acid; 5-HETE, 5(S)-hydroxy-6-trans-8,11,14-cis-eicosatetraenoic
acid; LO, lipoxygenase

1.4.2 5-LO

5-LO (78 kDa) is a nonheme iron dioxygenase and is located in the soluble
compartment of the cell. It is expressed primarily in leukocytes. The 5-LO
enzyme possesses a large catalytic domain, which binds the iron and a
regulatory C2-like domain, which binds Ca^{2+} [14].

$cPLA_2$ and 5-LO are activated by immune complexes, bacterial peptides
and other certain stimuli, whereupon they translocate to the nuclear
envelope. There, AA is released from phospholipids and metabolized by 5-

LO aided by FLAP, which facilitates the transfer of AA to 5-LO. Cellular activation of 5-LO is known to be predominantly mediated by Ca^{2+}, ATP and phosphorylation. Ca^{2+} either stimulates 5-LO activation and the association to the nuclear membrane [109]. The catalytic activity of 5-LO is stimulated by ATP, which binds to 5-LO and seems to have a stabilizing effect [110]. Phosphorylation by p38 mitogen-activated protein kinase (MAPK)-regulated MAPK-activated protein kinase (MK)-2/3 [111] or extracellular signal-regulated kinase (ERK) 1/2 at Ser271 and Ser663 [112] activates 5-LO, promoted by unsaturated fatty acids [113]. In contrast, phosphorylation of Ser523 by protein kinase A (PKA) results in inhibition of 5-LO activity. Essential for activation is the degree of oxidation of the nonheme iron in the catalytic centre of 5-LO. The ferrous state (Fe^{2+}) is the inactive iron conformation. Oxidation by lipid hydroperoxides forms the active ferric state (Fe^{3+}) [114].

Activated 5-LO catalyzes the oxygenation of AA to 5(S)-hydroperoxy-6-*trans*-8,11,14-*cis*-eicosatetraenoic acid (5-HpETE) and further dehydration to the epoxide LTA_4. Besides the formation of LTA_4, 5-HpETE can be reduced to its corresponding alcohol 5-HETE and further oxidized to 5-oxo-ETE by 5-HEDH in eosinophils. After synthesis, 5-LO products are released from the cell. LTB_4 efflux is facilitated through a LTB_4 transporter and LTC_4 is secreted by MRP1 [107].

LTB_4 acts through its specific BLT1 or non-specific BLT2 receptor and is involved in the regulation of the immune response, as it is known to be a chemotactic mediator and enhances phagocyctic activity and secretion of immunoglobulins [14, 107]. CysLTs that act through the receptors CysLT1 or CysLT2, are involved in asthma as they induce smooth muscle contraction, mucus secretion and vasoconstriction [14, 107]. Also 5-

H(p)ETE and 5-oxo-ETE exert pharmacological effects through their GPCR receptors, termed OXE, which may be involved in asthma and allergic diseases [115].

Studies with 5-LO knockout mice confirmed the participation of 5-LO in inflammatory events, including AA-induced ear inflammation, zymosan- or immune-complex-induced peritonitis, allergic airway inflammation and PAF-induced shock [116].

1.4.3 5-LO inhibitors

Suppression of 5-LO product biosynthesis can be implemented by direct inhibition of 5-LO or antagonism of FLAP or $cPLA_2$ [107]. Different categories of inhibitors according to the mode of action are classified. FLAP inhibitors interfere with the transfer of the substrate AA and thus reduce AA availability for 5-LO. Redox-active inhibitors keep the active site iron in the ferrous state and thereby uncouple the catalytic cycle of 5-LO. Many of this inhibitor class comprise lipophilic antioxidants from plant origin, such as flavonoids or polyphenols. As redox type 5-LO inhibitors often interfere with other redox systems, leading to severe side effects such as methemoglobin formation and possess mostly poor selectivity; no substance has entered the market yet. Iron ligand inhibitors chelate the active site iron with hydroxamic acid or N-hydroxyurea derivative structures. Zileuton (Zyflo$^{®}$) is approved in the US for the prophylaxis and chronic treatment of asthma. Nonredox type inhibitors compete with AA or hydroperoxides for binding to 5-LO. Note that phosphorylation of 5-LO and/or elevated hydroperoxide levels (present in inflammatory reactions) were shown to strongly reduce the efficacy of nonredox type inhibitors [107].
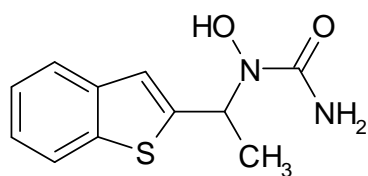
zileuton

1.5   Compounds from plant origin with historical use in the treatment of inflammatory diseases

1.5.1 Helichrysum italicum

Helichrysum italicum is a widespread Mediterranean plant that has been traditionally used in folk medicine to treat inflammatory diseases [117, 118]. It is a member of the Asteracaeae family and is domestic along the east coast and on the islands of the Adriatic Sea [119]. Extracts of *H. italicum* are known to exhibit anti-inflammatory, antioxidant [117], antibacterial [120], antifungal [121] and antiviral [122] properties.

Several constituents of *H. italicum* have been reported by now, including α-amyrin, uvaol [123], ß-diketones [124], kaempferol-3-glucoside, naringenin-glycoside [125], gnaphaliin, pinocembrin, tiliroside [126], eudesm-5-en-11-ol [127], *iso*-italicene epoxide, ß-costol, (*Z*)-α-*trans*-bergamotol [128], and the phloroglucinol α-pyrone arzanol [118]. Among these, the acylphloroglucinol arzanol (**Fig. 1.5**), which was first identified in 2007, was recently suggested as the active constituent responsible for the anti-inflammatory effects of *H. italicum* [118].
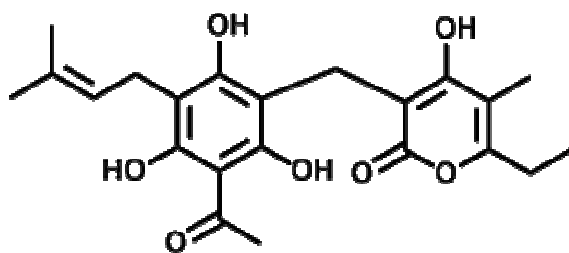
Fig. 1.5: chemical structure of arzanol from the plant Helichrysum italicum

Arzanol was already shown to inhibit the release of pro-inflammatory mediators, such as interleukin (IL)-1ß, IL-6, IL-8, TNFα and PGE$_2$ in LPS-stimulated monocytes [118]. In addition, activation of NFκB and HIV-1 replication in T-cells could be blocked by arzanol [118]. Antioxidant and cytotoxic effects of arzanol were studied in various systems of lipid peroxidation *in vitro* and protected VERO cells against tert-butyl hydroperoxide (TBH)-induced oxidative stress [129].

This study describes structure activity relationship (SAR) of arzanol and 24 synthetic derivatives thereof on mPGES-1 and 5-LO [130]. Furthermore, mPGES-1, 5-LO and TXAS were addressed as molecular targets of arzanol. In a rat model of carrageenan-induced pleurisy arzanol confirmed the anti-inflammatory potential with a significantly reduced inflammatory response and reduced PGE$_2$ levels in the pleural exudate [131].

1.5.2 Cannabis sativa

Cannabis sativa, a member of the Cannabaceae family, has been cultivated as a source of industrial fibre, seed oil, food, recreation and medicine for millennia. Depending on the purpose of its use, different parts of the plant are used. *Cannabis sativa L.* (hemp) preparations have traditionally been used in folk medicine [132]. Concerns over addiction and abuse led to the banning of the medicinal use in most countries in the 1930s [133].

Many inflammatory disorders, such as inflammation, pain, MS, Alzheimer´s disease, osteoporosis, cancer, cardiovascular disorders and metabolic syndrome-related disorders have been treated by *Cannabis sativa* preparations [133].

Several hundred secondary metabolites were identified by now with widespread biological actions. *Cannabis sativa* is the exclusive natural source of its cannabinoid constituents, except cannabigerol, which was shown to occur also in a *Helichrysum* species [134]. In addition to the well-known psychotropic properties of THC, cannabinoids and non-cannabinoids have been reported to possess anti-inflammatory properties [135]. THC was shown to reduce inter alia airway inflammation in mice [136] and the development of experimental atherosclerosis [137]. cannabidiol (CBD), which is the most abundant non-psychoactive cannabinoid in the plant, reduces joint inflammation in collagen-induced arthritis (CIA) in mice [138] and carrageenan induced paw edema in rats [139]. cannflavin (CF), a non-cannabinoid, was shown to be 30-fold more potent than aspirin in TPA-induced PGE_2 release from cultured synovial cells [140]. However, only few molecular targets of phytocannabinoids or non-cannabinoids within the AA cascade have been described in literature so far, namely COX-1 at rather high concentrations (>10 µM) [141], COX-2 [142] and 15-LO [143]. This thesis addresses mPGES-1 and/or 5-LO as potent molecular targets of several phytocannabinoids and non-cannabinoids. The molecular pharmacology of CFA was intensively studied.

1.5.3 Lichen spec.

Lichens are symbiotic organisms of fungi and algae and extracts of certain *lichen species* have been traditionally used as remedies in folk medicine

[144]. Due to various algalfungal combinations and the variable ecological and climatic growth conditions, *lichens* differ widely in appearance and produce a vast diversity of secondary metabolites, such as mono- and diaromatics, terpenoids, steroids, anthraquinones, naphthoquinones, xanthones, and furans [145]. These secondary metabolites were proposed to exhibit anti-inflammatory, antipyretic, and analgesic properties [144]. Among the secondary metabolites, the exclusively occurring depsides and depsidones in *lichens*, seem to have interesting properties. Only one study has reported that lichen depsides and depsidones interfere with COX activity in a cell-free assay using rabbit renal microsomes [146]. Furthermore, little is known about the bioactivities of lichen compounds on the PG biosynthetic pathway.
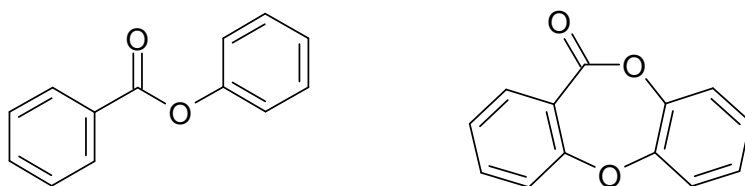
Fig. 1.6: chemical core structures of depsides and depsidones from Lichen spec.

Some molecular targets of depsides and depsidones have been identified. For example, several depsides were shown to act as nonredox-type inhibitors of LTB_4 formation in Ca^{2+}-ionophore-activated bovine polymorphonuclear leukocytes (PMNL) [147, 148], and blocked acetic-acid-induced writhing and hypothermia after oral administration in mice [149]. Similarly, depsidones were shown to inhibit 5-LO from porcine leukocytes and the formation of cys-LTs in human smooth muscle cells [150]. Moreover, for depsides, a selective inhibition of MAO-B [151, 152], inhibition of rat brain homogenate auto-oxidation [153], and suppression of the growth of human keratinocytes could be demonstrated [154]. This study adresses new molecular targets of depsides and depsidones within the AA-cascade.

1.5.4 Ginkgo biloba

Ginkgo biloba is called a "living fossil", as it is a member of the gymnosperms that has flourished 150 million years ago. Ginkgo seeds and leafs have been used in traditional Chinese medicine to treat pulmonary disorders, bladder inflammation, heart dysfunctions and skin infections [155-159]. Nowadays, several *Ginkgo biloba* preparations are available on the market. Among these the standard extract formulation *Ginkgo biloba* extract (GBE) or EGb 761 (Tebonin®) of Dr. Wilmar Schwabe GmbH & Co has shown to be beneficial in the treatment of Alzheimer´s disease, cardiovascular disease, cancer, stress, memory loss and psychiatric disorders [158, 160, 161]. The standardized extract contains 24% flavonoid glycosides (e.g. ginketin, isoginkgetin, bilobetin), 6% terpene lactones (mainly ginkgolides and bilobalides) and less than 5 ppm ginkgolic acids, since ginkgolic acids are considered to be toxic and cause gastrointestinal and allergic reactions [156, 162]. Administration of EGb 761 resulted in a decrease of platelet aggregation, allergic reaction, general inflammatory response, oxygen radical discharge and other pro-inflammatory functions of macrophages [163, 164] these anti-inflammatory effects are ascribed to mainly ginkgolides and flavonoids. PAF, COX and LO could be addressed as molecular targets of flavonoids [165, 166]. Besides, flavonoids exert antioxidant activity [167], whereas ginkgolides and bilobalides have antioxidant [168] and antimicrobial activities [169].

Another interesting class are the ginkgolic acids. Ginkgolic acids are 2-hydroxy-6-alkylbenzoic acids with a varying alkyl side chain from 13 to 17 carbons with zero to two double bonds [170]. They are considered to be toxic and cause gastrointestinal and allergic reactions, but have low cytotoxicity [171]. Ginkgolic acid, which is the main component of the nutshells and leaves of *Ginkgo biloba* [172], has been reported to show

antioxidant, radical-captivated, anti-inflammatory and antiallergic properties and is not allergenic as long as the carboxylic acid group is intact, either in free or conjugated form [173, 174].
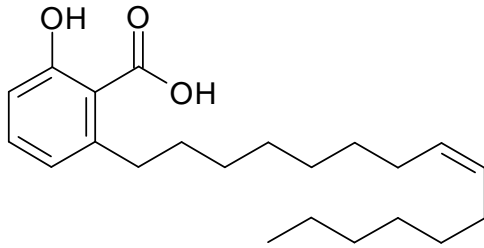
Fig. 1.7: chemical structure of ginkgolic acid from the plant Ginkgo biloba

This thesis will address several enzymes, i.e. mPGES-1, 5-LO and TXAS within the AA-cascade as molecular targets of ginkgolic acid.

1.6   Aim of this work

Nonsteroidal anti-inflammatory drugs (NSAID) and selective COX-2 inhibitors (coxibs) suppress the biosynthesis of prostanoids via inhibition of COX activity. Because not only pathogenic formed prostanoids, mainly PGE_2, but also physiologically important prostanoids are suppressed, long-term application can lead to severe side effects. Targeting COX-1 primarily leads to gastrointestinal and renal complications while COX-2 inhibition has been linked to cardiovascular incidents due to an imbalance of prothrombotic TXA_2 and antithrombotic PGI_2. Therefore, selective targeting of terminal PG synthases to inhibit individual prostanoids has been considered as an improved alternative in the treatment of inflammation and pain. The discovery of mPGES-1, a terminal synthase of PGE_2 biosynthesis that is believed to regulate pathogenic PGE_2 formation is of great interest. As mPGES-1 is known to be upregulated in pathogenic events and only low constitutive levels are present, mPGES-1 inhibitors may achieve anti-inflammatory efficacy of NSAIDs, while avoiding adverse side effects.

Discovery of mPGES-1 inhibitors started in 1999 and to date no selective inhibitors are available for clinical use. This discrepancy might be explained by the lack of suitable cell-based models for analysis of mPGES-1 inhibition [175]. Another reason was the lack of lead structures and structural models of mPGES-1, making it difficult to discover mPGES-1 inhibitors. Furthermore, problems and challenges in the development of mPGES-1 inhibitors occurred, leading to only few inhibitors that exhibit also *in vivo* activity.

The aim of this study was to discover natural and synthetic mPGES-1 inhibitors and to characterize the pharmacological profile of promising candidates towards their potency *in vitro* and *in vivo*, their selectivity within several enzymes (cPLA$_2$, 5-LO, COX, TXAS) of the eicosanoid pathway and their mechanistic properties.

2   MATERIALS AND METHODS

2.1   Materials

2.1.1 Compounds

Arzanol was isolated from *H. italicum* [118] and arzanol derivatives were prepared as described [130]. Phytocannabinoids and non-cannabinoids were synthesized by Prof. G. Appendino, Italy, unpublished data. Lignan derivatives from the dichloromethane extract of *K. lappacea* roots were isolated as described [176]. Depsides and depsidones were obtained from plant material as described [177]. Ginkgolic acid was kindly provided by Prof. H. Stuppner, Innsbruck, unpublished data. NSAID derivatives were synthesized by Prof. S. Laufer, Tübingen [178].

All compounds were dissolved in dimethyl sulfoxide (DMSO) and kept in the dark at −20°C and freezing/thawing cycles were kept to a minimum.

2.1.2 Materials

The TXAS inhibitor CV4151 and celecoxib were generous gift by Prof. S. Laufer (University of Tuebingen, Germany). BWA4C was a generous gift by Dr. L. G. Garland (Wellcome Res. Laboratories, Kent, UK). COX-2 antibody was obtained from Enzo Life Sciences (Loerrach, Germany). DMEM/HighGlucose (4.5 g/l) medium, penicillin, streptomycin, trypsin/EDTA solution, PAA Laboratories (Linz, Austria); λ-Carrageenan type IV isolated from *Gigartina aciculaire* and *Gigartina pistillata* and indomethacin were purchased from Sigma–Aldrich (Milan, Italy); PGH_2, Larodan (Malmo, Sweden); 11b-PGE_2, PGB_1, MK-886 (3-[1-(4-chlorobenzyl)-3-t-butyl-thio-5-isopropylindol-2-yl]-2,2-

dimethylpropanoicacid), human recombinant COX-2, ovine isolated COX-1, Cayman Chemical (AnnArbor, MI); UltimaGoldTM XR, PerkinElmer (Boston, MA); [³H]-PGE$_2$ was from Perkin Elmer Life Sciences (Milan, Italy) and PGE$_2$ antibody from Sigma–Aldrich (Milan, Italy). All other chemicals were obtained from Sigma–Aldrich (Deisenhofen, Germany) unless stated otherwise.

2.2   Methods

2.2.1 Cells and cell viability assay

A549 cells were cultured in DMEM/High Glucose (4.5 g/l) medium supplemented with heat-inactivated fetal calf serum (10%, v/v), penicillin (100 U/ml), and streptomycin (100 µg/ml) at 37 °C in a 5% CO$_2$ incubator. After 3 days, confluent cells were detached using 1 × trypsin/EDTA solution and reseeded at 2 x 10^6 cells in 20 ml medium in 175 cm^2 flasks. Blood cells were freshly isolated from leukocyte concentrates obtained at the Blood Center of the University Hospital Tuebingen (Germany) as described [179]. In brief, venous blood was taken from healthy adult donors that did not take any medication for at least 7 days, and leukocyte concentrates were prepared by centrifugation (4000 x g, 20 min, 20 °C). Cells were immediately isolated by dextran sedimentation and centrifugation on Nycoprep cushions (PAA Laboratories, Linz, Austria). Platelet-rich-plasma was obtained from the supernatants, mixed with phosphate-buffered saline (PBS) pH 5.9 (3:2 v/v), centrifuged (2100 x g, 15 min, room temperature), and the pelleted platelets were resuspended in PBS pH 5.9/0.9% NaCl (1:1, v/v). Washed platelets were finally resuspended in PBS pH 7.4 and 1 mM CaCl$_2$. Neutrophils were immediately isolated from the pellet after centrifugation on Nycoprep cushions, and hypotonic lysis of erythrocytes was performed as described

[179]. Cells were finally resuspended in PBS pH 7.4 containing 1 mg/ml glucose and 1 mM $CaCl_2$ (PGC buffer) (purity > 96-97%). For isolation of human monocytes, peripheral blood mononuclear cells (PBMC) were promptly isolated from leukocyte concentrates by dextran sedimentation and centrifugation on Nycoprep cushions. PBMC were washed three times with cold PBS and then monocytes were separated by adherence for 1 h at 37 °C to culture flasks (Greiner, Nuertingen, Germany; cell density was 2 x 10^7 cells/ml of RPMI 1640 medium containing 2 mM L-glutamine and 50 µg/ml penicillin/streptomycin), which finally gave a purity of > 85%, defined by forward- and side-light scatter properties and detection of the CD14 surface molecule by flow cytometry (BD FACS Calibur). Monocytes were finally resuspended in ice-cold PBS plus 1 mg/ml glucose (PG buffer) or in PG buffer supplemented with 1 mM $CaCl_2$ (PGC buffer).

For analysis of acute cytotoxicity during pre-incubation periods, viability was analyzed by light microscopy and trypan blue exclusion. For analysis of cytotoxicity of A549 cells, the MTT assay was used. In brief, cells (100 µl cell suspension corresponding to 3 x 10^5 A549 cells) were incubated for 24 h and 48 h at 37 °C with vehicle (0.3% DMSO) or the indicated compounds. After 24 h or 48 h, 20 µl of a sterile filtered solution of 3-(4,5-dimethyl-2-thiazolyl)-2,5-diphenyl-2H-tetrazolium bromide (MTT) in PBS (5 mg/ml) was added and samples were incubated for 4 h at 37 °C. Then, 100 µl of 10% SDS in 20 mM HCl (pH 4.5; SDS lysis buffer) was added and samples were shaken for 15 h at RT in the dark and the absorption was measured at 570 nm. Results are reported as percentage of viable cells as compared to vehicle control. A statistically significant impairment of MTT reduction to formazan was considered cytotoxic.

2.2.2 Animals

Male adult Wistar Han rats (200 – 220 g, Harlan, Milan, Italy) were housed in a controlled environment and provided with standard rodent chow and water. Animal care complied with Italian regulations on protection of animals used for experimental and other scientific purpose (Ministerial Decree 116192) as well as with the European Economic Community regulations (Official Journal of E.C. L 358/1 12/18/1986).

2.2.3 DPPH assay

The radical scavenger capability was assessed by measuring the reduction of the stable free radical 2,2-diphenyl-1-picrylhydrazyl (DPPH). Briefly, an ethanol solution of a sample at various concentrations (100 µl) was mixed with an acetate-buffered (pH 5 - 6.5) DPPH solution (final concentration 50 µM). After incubation for 30 min in the dark the absorbance of the mixture was measured at 520 nm. Ascorbic acid and L-cysteine were used as reference compounds. All analyses were performed in triplicates.

2.2.4 Preparation of crude mPGES-1 in microsomes of A549 cells and determination of PGE$_2$ synthase activity

Preparations of A549 cells and determination of mPGES-1 activity was performed as described previously [82]. In brief, cells were treated with 1 ng/ml Il-1β for 48 h at 37 °C, 5% CO_2. Cells were harvested, sonicated and the homogenate was subjected to differential centrifugation at 10,000 x g for 10 min and 174,000 x g for 1 h at 4 °C. The pellet (microsomal fraction) was resuspended in 1 ml homogenization buffer (0.1 M potassium phosphate buffer, pH 7.4, 1 mM phenylmethanesulfonyl fluoride, 60 µg/ml

soybean trypsin inhibitor, 1 µg/ml leupeptin, 2.5 mM glutathione, and 250 mM sucrose), and the total protein concentration was determined. Microsomal membranes were diluted in potassium phosphate buffer (0.1 M, pH 7.4) containing 2.5 mM glutathione. Test compounds or vehicle were added, and after 15 min at 4 °C reaction (100 µl total volume) was initiated by addition of PGH_2 at the indicated concentration. After 1 min at 4 °C, the reaction was terminated using stop solution (100 µl; 40 mM $FeCl_2$, 80 mM citric acid, and 10 µM 11β-PGE_2 as internal standard. PGE_2 formation was analyzed using PGE_2-ELISA according to the manufactures protocol (1 and 5 µM PGH_2) or separated by solid-phase extraction and analyzed by RP-HPLC (20 and 50 µM PGH_2) as described previously [82].

2.2.5 COX-2 and mPGES-1 expression in LPS stimulated human monocytes

Freshly isolated monocytes (10^6/ml) were cultured in RPMI medium supplemented with heat-inactivated fetal calf serum (0.5%, v/v) stimulated with 1 µg/ml LPS and the indicated compounds at 37 °C in a 5% CO_2 incubator. After 20 or 24 h monocytes were harvested, lysed and expression of COX-2 or mPGES-1 was detected by SDS-PAGE and Western blot.

2.2.6 Expression and purification of human recombinant 5-LO

E.coli MV1190 was transformed with pT3-5-LO plasmid and recombinant 5-LO protein was expressed at 27 °C as described [180]. Cells were lysed in 50 mM triethanolamine/HCl pH 8.0, 5 mM EDTA, soybean trypsin inhibitor (60 µg/ml), 1 mM phenylmethanesulphonyl fluoride, and lysozyme (500 µg/ml), homogenized by sonication (3 x 15 sec), and

centrifuged at 40,000 x g for 20 min at 4 °C. The 40,000 x g supernatant (S40) was applied to an ATP-agarose column to partially purify 5-LO as described previously [180]. Semi-purified 5-LO was immediately used for activity assays.

2.2.7 Determination of 5-LO activity in cell-free assay

Aliquots of semi-purified 5-LO were diluted with ice-cold PBS containing 1 mM EDTA, and 1 mM ATP was added. Samples were pre-incubated with the test compounds as indicated. After 10 min at 4 °C, samples were pre-warmed for 30 sec at 37 °C, and 2 mM $CaCl_2$ plus 20 µM AA was added to start 5-LO product formation. The reaction was stopped after 10 min at 37 °C by addition of 1 ml ice-cold methanol, and the formed metabolites were analyzed by RP-HPLC as described [181]. 5-LO products include the all-trans isomers of LTB_4 and 5(S)-hydro(pero)xy-6-trans-8,11,14-cis-eicosatetraenoic acid (5-HETE).

2.2.8 Determination of 5-LO product formation in intact cells

For determination of LO products in intact PMNL, 5×10^6 cells were resuspended in 1 ml PG-buffer containing 1 mM $CaCl_2$, pre-incubated for 15 min at 37 °C with test compounds or vehicle (0.3% DMSO), and incubated for 10 min at 37 °C with the indicated stimuli. Thus, the Ca^{2+}-ionophore A23187 (2.5 µM) was added with or without 20 µM AA and 10 min later the reaction was stopped on ice by addition of 1 ml of methanol. 30 µl 1 N HCL and 500 µl PBS, and 200 ng prostaglandin B1 were added and the samples were subjected to solid phase extraction on RP18-columns (100 mg, UCT, Bristol, PA, USA). 5-LO products (LTB_4, trans-isomeres, 5-HETE) were analyzed by HPLC and quantities calculated on the basis of

the internal standard PGB_1. Alternatively, cells were first primed at 37 °C with lipopolysaccharide (LPS, 1 µg/ml) plus adenosine deaminase (Ada, 0.3 U/ml) for 30 min. Formation of 5-LO products was started by addition of 1 µM formyl-methionyl-leucyl-phenylalanine (fMLP) and after 5 min the reaction was stopped on ice. Supernatants were collected after centrifugation at 600 x g for 10 min at 4 °C. LTB_4 levels were measured by ELISA according to the manufacturer´s (Assay Designs, Ann Arbor, MI) protocol.)

For determination of 5-LO products in cell homogenates, cell suspensions were resuspended in PBS containing 1 mM EDTA for 5 min at 4 °C and sonicated (4 x 10 sec, 4 °C). After addition of 1 mM ATP, homogenates corresponding to 5×10^6 cells/ml were incubated with the test compounds or vehicle (0.3% DMSO) for 15 min at 4 °C, pre-warmed for 30 sec at 37 °C and the reaction was started by the addition of 2 mM $CaCl_2$ and 20 µM AA. The reaction was stopped after 10 min at 37 °C and the samples were analyzed as described for intact cells above.

2.2.9 Activity assays of isolated COX-1, COX-2 and TXAS

Inhibition of the activities of isolated ovine COX-1 and human COX-2 was performed as described [82]. In brief, purified COX-1 (ovine, 50 units) or COX-2 (human recombinant, 20 units) were diluted in 1 ml reaction mixture containing 100 mM Tris buffer pH 8, 5 mM glutathione, 5 µM haemoglobin, and 100 µM EDTA at 4 °C and pre-incubated with the test compound for 5 min. Samples were pre-warmed for 60 sec at 37 °C, and AA (5 µM for COX-1, 2 µM for COX-2) was added to start the reaction. After 5 min at 37 °C, the reaction was stopped on ice by addition of 1 ml of methanol. 30 µl 1 N HCL and 500 µl PBS, and 200 ng prostaglandin B_1 were added and the samples were subjected to solid phase extraction on

RP18-columns (100 mg, UCT, Bristol, PA, USA). 12-HHT was analyzed by HPLC and quantities calculated on the basis of the internal standard PGB_1. Indomethacin (10 µM) was used as well-recognized reference inhibitor of COX-1 and celecoxib (5 µM) for COX-2 to control the assays. For analysis of the activity of TXAS in platelet homogenates (10^8/ml), cells were resuspended in PBS/EDTA for 5 min at 4 °C and sonicated (4 x 10 sec, 4 °C). Freshly prepared platelet homogenates were pre-incubated with test compounds or vehicle. After 15 min at 4 °C the reaction (100 µl total volume) was initiated by addition of 20 µM PGH_2 for 1 min at 4 °C and reaction was terminated using stop solution (100 µl; 40 mM $FeCl_2$, 80 mM citric acid). The formation of TXB_2 was measured via TXB_2-ELISA according to the manufactures protocol.

2.2.10 Determination of COX-1 product formation in human washed platelets

Freshly isolated human platelets (10^8/ml PGC buffer) were pre-incubated with the indicated compounds for 4 min at room temperature. Samples were pre-warmed for 60 sec at 37 °C and AA (5 µM) was added to start the reaction. After 10 min at 37 °C the reaction was stopped on ice or by the addition of 1 ml ice-cold methanol. The formation of TXB_2 was measured via TXB_2-ELISA according to the manufactures protocol and 12-HHT was analyzed by HPLC as described [182].

2.2.11 Determination of MAPK activation

Neutrophils (10^7/100 µl of PGC buffer) were pre-warmed for 3 min at 37 °C and pre-incubated with the indicated compounds at 37 °C for 15 min. The reaction was started by the addition of 0.1 µM fMLP and stopped after

1.5 min with 100 µl of ice-cold SDS-loading buffer and heated for 6 min at 95 °C. Total cell lysates were analyzed for ERK1/2, phosphorylated ERK1/2 (Thr-202/Tyr-204), phosphorylated p38 MAPK (Thr-180/Tyr-182), by SDS/PAGE and western blotting.

2.2.12 SDS–PAGE and Western blotting

Monocytes (5 x 10^6 cells) or neutrophils (10^7 cells) were resuspended in 50 µl PBS buffer pH 7.2, mixed with the same volume of 2 x SDS/PAGE sample loading buffer (20 mM Tris–HCl, pH 8, 2 mM EDTA, 5% (m/v) SDS, and 10% (v/v) β-mercaptoethanol), 20 µl glycerol/0,1% bromophenol blue (1:1, v/v) and boiled for 5 min at 95 °C. Proteins were separated by SDS-PAGE. Correct loading of the gel and transfer of proteins to the nitrocellulose membrane was confirmed by Ponceau staining. After electroblotting to nitrocellulose membrane (GE Healthcare, Munich, Germany) and blocking with 5% BSA for 1 h at room temperature, membranes were washed and incubated with primary antibodies overnight at 4 °C. The membranes were washed and incubated with a 1:1000 dilution of alkaline phosphatase-conjugated immunoglobulin G for 1 h at room temperature. After washing, proteins were visualized with nitro blue tetrazolium and 5-bromo-4-chloro-3-indolylphosphate.

2.2.13 Determination of activity of isolated human recombinant cPLA$_{2\alpha}$ in a cell-free assay

The cPLA$_{2\alpha}$ coding sequence was cloned from pVL1393 plasmid (kindly provided by Dr. Wonhwa Cho, University of Illinois at Chicago) into pFastBacTM HT A containing a 6 x his-tag coding sequence. The recombinant plasmid was transformed into DH10BacTM E. coli. Sf9 cells

were transfected with recombinant bacmid DNA using Cellfectin® Reagent and the generated baculovirus was amplified. Overexpression of His-tagged cPLA$_2$ in baculovirus-infected Sf9 cells and isolation using Ni-NTA agarose beads was performed as described [183].

Multilamelar vesicles (MLVs) were prepared by drying 1-palmitoyl-2-arachidonyl-sn-glycero-3-phosphocholine (PAPC) and 1-palmitoyl-2-oleoyl-sn-glycerol (POG) in a ratio of 2:1 (nn-1, in chloroform) under nitrogen in glass vials. After addition of 20 mM Tris buffer (pH 7.4) containing 134 mM NaCl and 1 mg/mL fatty acid free BSA, the MLV suspension was disrupted by several freeze-thaw cycles (liquid nitrogen) and then extruded 11 times with a mini-extruder (Avanti Polar Lipids, Inc.) through a polycarbonate membrane (100 nm pore diameter) at room temperature (above transition temperature of the lipids) to produce LUV (large unilamelar vesicles). Final total concentration of lipids was 250 µM in 200 µL. Test compounds and 1 mM CaCl$_2$ were added to the vesicles, and the reaction was started by addition of 500 ng his-tagged cPLA$_2$ (in 10 µL buffer). After 1 h at 37 °C, 1.6 mL CH$_3$OH was added, and AA was extracted by RP-18 solid phase extraction. Following derivatisation with p-anisidinium chloride, the resulting derivate was analyzed by RP-HPLC at 249 nm as described [183].

2.2.14 5-LO activity in human whole blood

Peripheral blood from healthy adult volunteers, who had not received any medication for at least 2 weeks under informed consent, was obtained by venipuncture and collected in syringes containing heparin (20 U/ml). 2 mL aliquots were pre-incubated with the indicated compounds and stimulated with A23187 (30 µM) for 10 min at 37 °C. After stimulation, the reaction was stopped on ice and the samples were centrifuged at 600 x g, 10 min, 4

°C. Aliquots of plasma (500 μL) were mixed with 2 mL of methanol and 200 ng PGB_1 were added as internal standard. The samples were put at -20 °C for 2 h and centrifuged (600 x g, 15 min, 4 °C). The supernatants were collected and diluted with 2.5 mL PBS + 75 μL HCl 1N. Formed 5-LO metabolites were extracted and analyzed by HPLC as described before.

2.2.15 Prostanoid formation in human whole blood

Peripheral blood from healthy adult volunteers, who had not received any medication for at least 2 weeks under informed consent, was obtained by venipuncture and collected in syringes containing heparin (20 U/ml) or citrate (0.106 mol/l trisodium citrate solution).

Stimulation for 5 h with LPS (10 μg/ml)

Aliquots of whole blood (for PGE_2: 0.8 ml, for 6-ketoPGF_{1a}: 0.4 ml) were mixed with CV4151 (1 μM) and with aspirin (50 μM) for determination of PGE_2 and with CV4151 (1 μM) for analysis of 6-ketoPGF_{1a}, respectively. For determination of TXB_2, aliquots of whole blood (0.4 ml) were used without additives. A total volume of 1 ml or 0.5 ml was adjusted with sample buffer (10 mM potassium phosphate buffer pH 7.4, 3 mM KCl, 140 mM NaCl and 6 mM D-glucose). After pre-incubation with the indicated compounds for 5 min at room temperature, the samples were stimulated with LPS (10 μg/ml) for 5 h at 37 °C. Prostanoid formation was stopped on ice, the samples were centrifuged (2300 x g, 10 min, 4 °C) and 6-ketoPGF_{1a} and TXB_2 were quantified in the supernatant using High Sensitivity EIA Kits (Assay Designs, Ann Arbor, MI), respectively, according to the manufacturer's protocols. PGE_2 was determined as described. In brief, the supernatant was acidified with citric acid (30 μl, 2 M), and after

centrifugation (2300 x g, 10 min, 4 °C), solid phase extraction and separation by RP-HPLC was performed to isolate PGE_2. The PGE_2 peak (3 ml), identified by co-elution with the authentic standard, was collected and acetonitrile was removed under a nitrogen stream. The pH was adjusted to 7.2 by addition of 10 x PBS buffer pH 7.2 (230 µl) before PGE_2 contents were quantified using a PGE_2 High Sensitivity EIA Kit (Assay Designs, Ann Arbor, MI) according to the manufacturer's protocol.

Stimulation for 24 h with LPS (10 µg/ml)

Aliquots of heparinized whole blood (1 ml) were pre-incubated with the indicated compounds for 5 min at room temperature and the samples were stimulated with LPS (10 µg/ml) for 24 h at 37 °C. Prostanoid formation was stopped on ice and the samples were centrifuged (2300 x g, 10 min, 4 °C). 6-ketoPGF_{1a} was quantified in the supernatant using High Sensitivity EIA Kits (Assay Designs, Ann Arbor, MI) according to the manufacturer's protocols.

Stimulation with thrombin (2 U/ml)

For determination of TXB_2 levels citrated human whole blood was pre-incubated with the indicated compounds for 15 min at 37 °C and the reaction was initiated with thrombin (2 U/ml). After 10 min the reaction was stopped on ice and TXB_2 levels were detected in the supernatant using a TXB_2 High Sensitivity EIA Kit according to the manufacturer's protocol.

2.2.16 Carrageenan-induced pleurisy in rats

Test compounds at the indicated concentration or indomethacin (5 mg/kg) were given i.p. 30 min before carrageenan. A group of male rats received the vehicle (DMSO, 4%, i.p.) 30 min before carrageenan. Rats were anaesthetized with enflurane 4% mixed with O_2, 0.5 l/min, N_2O 0.5 l/min and submitted to a skin incision at the level of the left sixth intercostal space. The underlying muscle was dissected, and saline (0.2 ml) or λ-carrageenan type IV 1% (w/v, 0.2 ml) was injected into the pleural cavity. The skin incision was closed with a suture, and the animals were allowed to recover. At 4 h after the injection of carrageenan, the animals were killed by inhalation of CO_2. The chest was carefully opened, and the pleural cavity was rinsed with 2 ml saline solution containing heparin (5 U/ml). The exudates and washing solution were removed by aspiration, and the total volume was measured. Any exudate that was contaminated with blood was discarded. The amount of exudates was calculated by subtracting the volume injected (2 ml) from the total volume recovered. Leukocytes in the exudates were resuspended in PBS and counted with an optical light microscope in a Burker's chamber after vital trypanblue staining. The amounts of PGE_2, LTB_4 and 6-ketoPGF_{1a} in the supernatant of centrifuged exudates (800 x g for 10 min) were assayed by radioimmunoassay (PGE_2) and enzyme immunoassay (LTB_4, 6-ketoPGF_{1a}), respectively (Cayman Chemical, Ann Arbor, MI) according to manufacturer's protocol. The results are expressed as ng per rat and represent the mean $\pm$ S.E. of 10 rats.

2.2.17 Statistics

Data are expressed as mean $\pm$ S.E. IC_{50} values were graphically calculated from averaged measurements at 3 - 5 different concentrations of the compounds using SigmaPlot 9.0 (Systat Software Inc., San Jose, USA). Statistical evaluation of the data was performed by one-way ANOVA followed by Tukey-Kramer post-hoc test for multiple comparisons respectively. A p value < 0.05 (*) was considered significant.

3   RESULTS

The design of novel mPGES-1 inhibitors is of great interest, since mPGES-1 inhibitors are considered as a promising alternative to NSAIDs in the therapeutic strategy of inflammatory diseases.

To enhance the benefit in pharmacotherapy, a dual inhibition concept of mPGES-1 and 5-LO might have synergistic effects and a reduced side effect profile compared to classical NSAIDs.
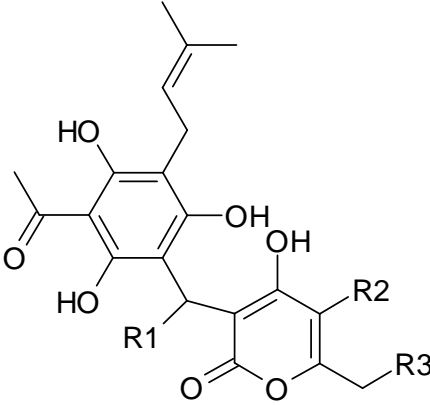
3.1   Discovery of mPGES-1 or dual mPGES-1/ 5-LO inhibitors from plant-origin that are traditionally used in folk medicine

3.1.1 Arzanol (1) from *Helichrysum italicum* as lead structure for structure activity relationship (SAR)

Arzanol (**1**), a constituent of *Helichrysum italicum,* was suggested to highly contribute to the anti-inflammatory potential of the plant. Arzanol (**1**) significantly inhibited (I) PGE_2 formation in microsomal preparations of IL-1ß-stimulated A549 cells as a source of mPGES-1¶ (IC_{50}= 0.4 µM) and (II) 5-LO product formation in the semi-purified 5-LO¶ assay (IC_{50}= 3.1 µM). SAR studies were performed to enhance the anti-inflammatory potential [131]. The basic structure consists of a prenylated heterodimeric acylphloroglucinol with an α-pyrone and a phloroglucinol core. As arzanol (**1**) is instable to acids and bases and exhibit high functionalization, the possibilities of chemical modification are restricted. Therefore, focus for the improvement of the pharmacophore of arzanol (**1**) was placed on the alkylidene linker and/or the pyrone moiety (**1a-g**), as well as on
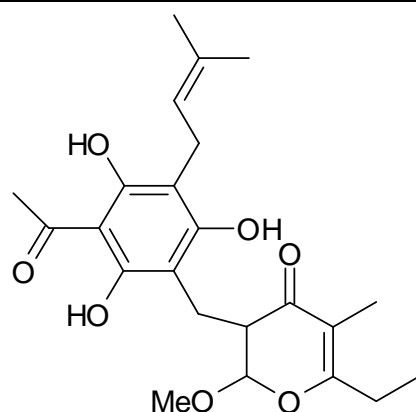
homodimeric analogues from both structural moieties (Helipyron, **2a-i** and **4a-d**). To check whether the basic structure elements itself influence the enzymatic activity of mPGES-1, a prenylated acylphloroglucinol core (**5**) and alkyl-substituted pyrones (**6, 7**) were tested for their ability to block mPGES-1 derived PGE_2 and 5-LO derived LT formation under cell-free conditions (**Table 3.6**).

*Table 3.6: Biological evaluation of arzanol (**1**) and its derivatives on product formation of cell-free mPGES-1 and semi-purified 5-LO. Mean values (n = 3-5) (IC$_{50}$ [μM] or % remaining activity at 10 μM)*

#	structure			Cell-free **mPGES-1**	Semipurified 5-LO
	R1	R2	R3		
arzanol (**1**)	H	CH$_3$	CH$_3$	0.4 μM	3.1 μM
1a	H	H	H	1.0 μM	9.5 μM
1b	CH$_3$	CH$_3$	CH$_3$	2.1 μM	5.9 μM
1c	CH$_3$	H	H	2.4 μM	7.9 μM
1d	nC$_6$H$_{13}$	CH$_3$	CH$_3$	0.3 μM	1.6 μM
1e	nC$_6$H$_{13}$	H	H	0.2 μM	1.2 μM
1f	Phenyl	CH$_3$	CH$_3$	0.8 μM	4.9 μM
1g	Phenyl	H	H	1.1 μM	8.4 μM
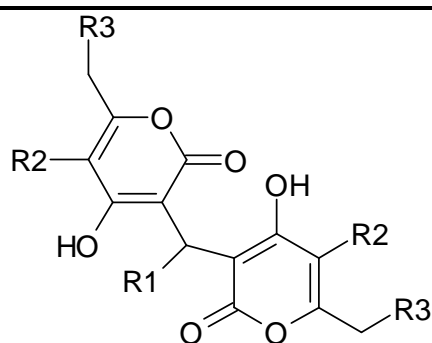
	R1	R2	R3		
helipyron (**2**)	H	CH$_3$	CH$_3$	6 µM	n.i.
2a	H	H	H	99.8±1.3	93.0±9.3
2b	CH$_3$	CH$_3$	CH$_3$	102.7±15.8	83.5±5.7
2c	CH$_3$	H	H	98.9±8.1	88.5±1.8
2d	nC$_6$H$_{13}$	CH$_3$	CH$_3$	0.84 µM	56.1±7.2
2e	nC$_6$H$_{13}$	H	H	79.2±11.8	7.8 µM
2f	Phenyl	CH$_3$	CH$_3$	66.6±4.6	86.1±12.8
2g	Phenyl	H	H	92.8±16.7	81.8±2.3
2h	2-furyl	CH$_3$	CH$_3$	80.3±6.6	71.2±16.8
2i	2-furyl	H	H	102.3±7.9	93.1±20.1

3 99.3±15.9 5 µM
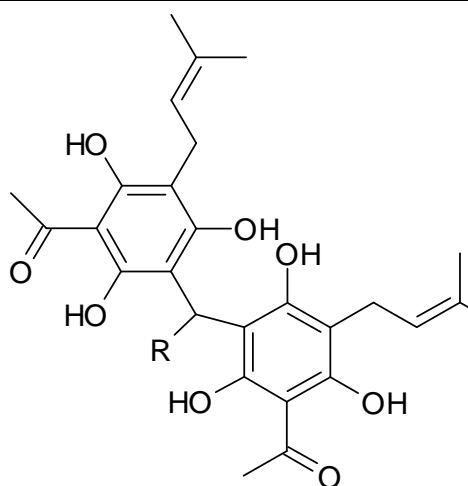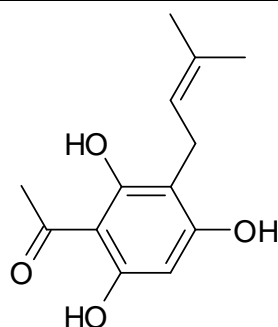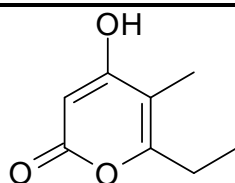
	R		
	R		
4a	H	0.5 µM	1.4 µM
4b	CH$_3$	0.7 µM	1.2 µM
4c	nC$_6$H$_{13}$	0.6 µM	0.6 µM
4d	Phenyl	1.5 µM	0.7 µM
5		62.4±5.8	5.1 µM
6		107.7±3.5	111.7±10.8
7		107.1±11.1	129.8±25.7
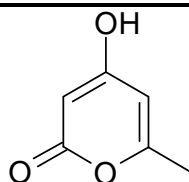
The reference drugs MK886 (standard mPGES-1 inhibitor [56]) and BWA4C (standard 5-LO inhibitor [184]) suppressed product formation as expected (not shown).

First, the pyrone substitution pattern was simplified which resulted in the bis-nor derivative **1a**. Compound **1a** basically retained activity towards mPGES-1 and 5-LO with IC_{50} values of 1 and 9.5 µM, respectively, suggesting that substitution of the pyrone pattern is not essential for the inhibitory potential. Introduction of a methyl on the alkylidene linker (**1b** and **1c**) slightly decreased the inhibitory potency of mPGES-1 and 5-LO with IC_{50} values of 2.1 and 5.9 µM as well as 2.4 and 7.9 µM, respectively. Interestingly, the derivatives **1d** and **1e,** which both possess n-hexyl residues on the alkylidene linker, increased the inhibitory potential of mPGES-1 and 5-LO product formation with IC_{50} values of 0.3 and 1.6 µM as well as 0.2 and 1.2 µM, respectively, suggesting that lipophilic substituents on the alkylidene linker enhance the efficacy towards mPGES-1 and 5-LO. However, introduction of a phenyl residue on the alkylidene linker (**1f** and **1g**) resulted in IC_{50} values of 0.8 and 4.9 µM as well as 1.1 and 8.4 µM, respectively. Moreover, **1f** and **1g** increased the inhibitory potential towards both enzymes compared to derivatives with the methyl residue **1b** and **1c**, but were less efficient compared to **1d** and **1e** which possess the lipophilic n-hexyl residue.

Next, the basic structure elements were investigated for their ability to suppress cell-free mPGES-1 and 5-LO product formation. The alkyl-substituted pyrones **6** and **7** did not inhibit mPGES-1 and 5-LO activity, whereas the prenylated acylphloroglucinol core **5** slightly inhibited mPGES-1 derived PGE_2 formation (62.4% remaining activity at 10 µM) and potently inhibited 5-LO product formation in the semi-purified 5-LO assay ($IC_{50}= 5.1$ µM). These findings suggest that **5** might be essential for the inhibitory potential whereas **6** and **7** (and **1a**) might have no influence on the inhibitory potential of the natural product arzanol (**1**).

Surprisingly, the enolether derivative **3** did not suppress mPGES-1 derived PGE_2 formation (99.3% remaining activity at 10 µM) but mainly sustained

5-LO inhibition (IC_{50}= 5 µM). These unexpected findings imply that the existence of an acidic group might be crucial for mPGES-1 inhibition.

To further investigate the significance of the heterodimeric structure of the natural compound arzanol (**1**), homodimeric pyrone- (Helipyron and **2a–2i**) and phloroacetophenon-derivatives (**4a-4d**) were tested for their ability to block the formation of mPGES-1-derived PGE_2 and 5-LO-derived LT formation.

The homodimeric pyrone helipyron (**2**) is known to occur in *Helichrysum italicum* [118]. Helipyron (**2**) is much less potent on mPGES-1 inhibition (IC_{50}= 6 µM) compared to arzanol (**1**) and even inactive towards 5-LO inhibition. Consistent with the results of the heterodimeric derivatives (arzanol (**1**) and **1a-1g**) introduction of n-hexyl residue to the methylene linker (**2d** and **2e**) increased the potency towards mPGES-1 and 5-LO inhibition whereas helipyron and the corresponding bis-nor derivatives (**2a** and **2e**) were less efficient. Methyl, phenyl or 2-furyl residues on the methylene linker resulted in completely inactive compounds (**2b, c, f, g, h, i**) towards mPGES-1 and 5-LO inhibition.

As the prenylated acylphloroglucinol core **5** already implied, homodimeric phloroacetophenon derivatives (**4a-4d**) potently suppressed the formation of mPGES-1 derived PGE_2 and 5-LO derived LTs. In line with other results, introduction of n-hexyl residue (**4c**) resulted in the most potent derivative of group **4** with IC_{50} values of 0.6 µM, each.
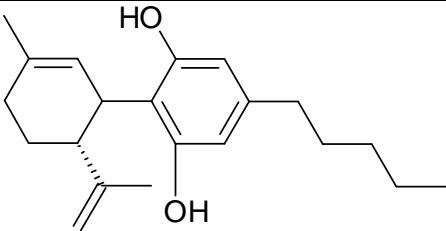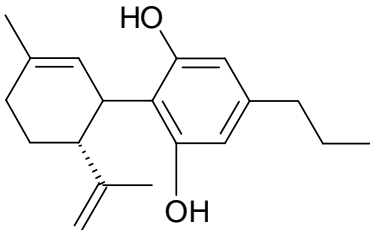
Taken together, arzanol (**1**) could be identified as a dual inhibitor of mPGES-1/5-LO and the performed SAR studies yield that introduction of lipophilic elements (especially n-hexyl residues) to the alkylidene linker enhance the potency towards mPGES-1 and 5-LO inhibition compared to the natural compound arzanol (**1**). Furthermore, the α-pyrone core is apparently not crucial for the inhibition potential which could be verified by the corresponding bis-nor derivatives and the homodimeric pyrone- and
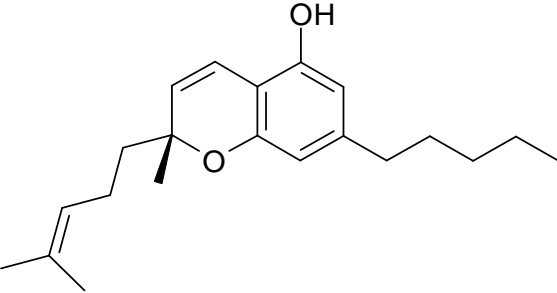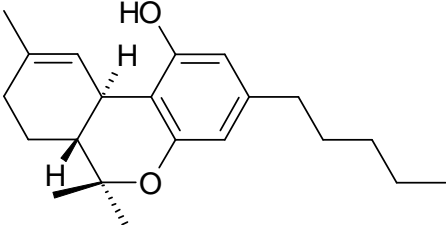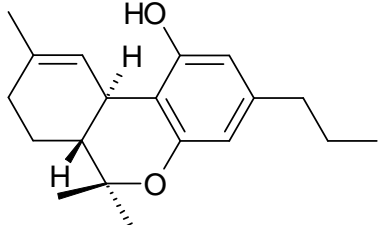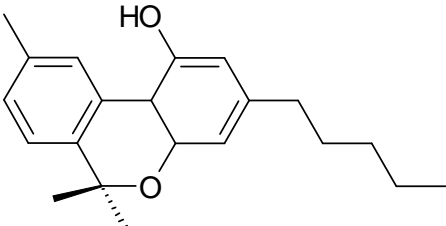
phloroacetophenon-derivatives. **1e,** as the most promising derivative, with potent properties will be further investigated on its molecular pharmacology within the eicosanoid pathway (see chapter **3.4.1**)

3.1.2 Phytocannabinoids and non-cannabinoids from *Cannabis sativa*

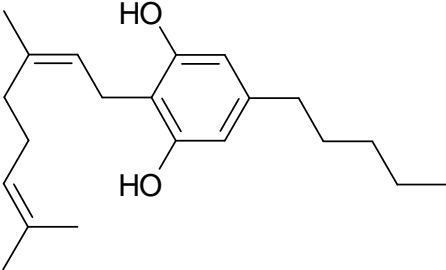Phytocannabinoids as well as non-cannabinoids from *Cannabis sativa* have been shown to interfere with the AA cascade [140-143]. Thus, little is known about the molecular targets. To screen for inhibition of mPGES-1, seven phytocannabinoids and eight non-cannabinoids were tested in microsomal preparations of interleukin-1β-stimulated A549 cells for their ability to block the formation of PGE_2 (see **Table 3.7** and **Table 3.8**).
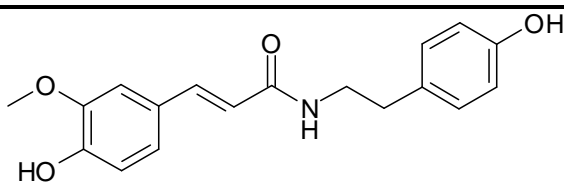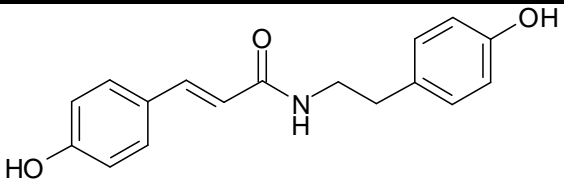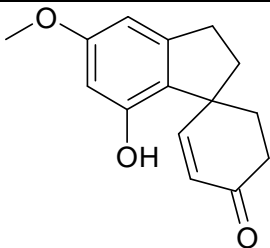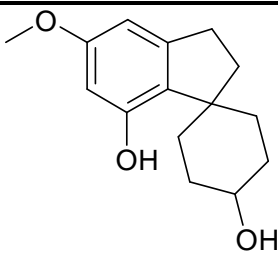
Table 3.7: Biological evaluation of phytocannabinoids on cell-free mPGES-1 product formation. Mean values (n = 3-4) (IC_{50} [µM] or % remaining activity at 10 µM)

#	Structure	Cell-free mPGES-1
cannabidiol (CBD) (**8**)		65.0±3.5
cannabidiol-viridine (CBD vir) (**9**)		62.5±4.1

cannabigerol (CBG) (**10**)		0.9 μM
cannabi- chromene (CBCr) (**11**)		84.0±5.6
tetrahydro- cannabinol (THC) (**12**)		70 μM
tetrahydro- cannabinol- viridine (THCvir) (**13**)		77.7±1.6
cannabinol (CBN) (**14**)		70.3±5.9

The standard reference inhibitor MK-886 blocked PGE_2 formation as expected ($IC_{50} = 2.1$ μM, data not shown). CBG (**10**) could be identified as a potent inhibitor of mPGES-1 with an IC_{50} value of 0.9 μM. Furthermore, THC (**12**) ($IC_{50} = 70$ μM) could be identified as weak inhibitor of mPGES-1 derived PGE_2 formation. All other cannabinoids (**8, 9, 11, 13, 14**) did not inhibit mPGES-1 activity up to 10 μM.

Table 3.8: Biological evaluation of non-cannabinoids on cell-free mPGES-1 and semi-purified 5-LO product formation. Mean values (n = 2-3) (IC_{50} [μM], % remaining activity at 10 μM, n.i. no inhibition)

#	Structure	Cell-free mPGES-1	Semipurified 5-LO
feruloyl-tyramine (**15**)		81.4±3.4	85.5±7.1
cumaroyl-tyramine (**16**)		89.3±5.0	114.9±4.8
cannabis-pyrenone (**17**)		n.i.	8.6 μM
cannabis-pyranol (**18**)		88.2±6.9	118.1±3.8
cann-flavin A (**19**)		1.8 μM	0.95 μM
cann-flavin B (**20**)		3.7 μM	0.9 μM
oxylipin (**21**)		57.5±5.6	6.0 μM

| canni-prene (**22**) | | 10 µM | 0.4 µM |

The references MK886 (standard mPGES-1 inhibitor [56]) and BWA4C (standard 5-LO inhibitor [184]) suppressed product formation as expected (not shown). Of all tested non-cannabinoids, the prenylated flavonoids cannflavin (CF) A (**19**) and B (**20**) and the dihydrostilbene canniprene (**22**) potently inhibited cell-free mPGES-1 and semi-purified 5-LO product formation with IC_{50} values of 1.8 and 0.95 µM for CFA (**19**), 3.7 and 0.9 µM for CFB (**20**) and 10 and 0.4 µM for canniprene (**22**), respectively. The endocannabinoid-related oxylipin (**21**) and the "spiro compound" cannabis-pyrenone (**17**) selectively blocked 5-LO products with IC_{50} values of 8.6 and 6.0 µM, respectively. The tyramine derivatives (**15**, **16**) as well as the "spiro compound" cannabispyranol (**18**) did not influence PGE_2 formation or 5-LO product formation in semi-purified 5-LO up to 10 µM.

As CFA (**19**) could be identified as a potent dual inhibitor of mPGES-1/5-LO, further experiments were performed to disclose the pharmacological profile within the AA cascade (see chapter **3.4.2**).
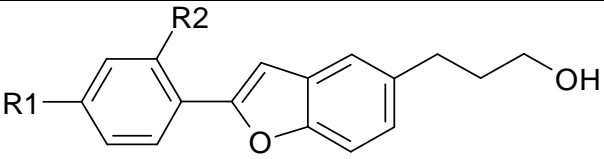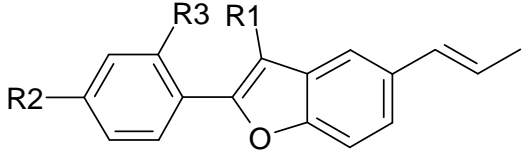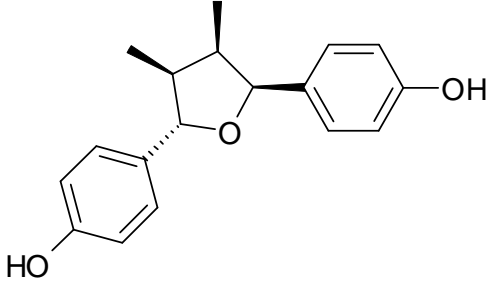
3.1.3 Lignan derivatives from *Krameria lappacea*
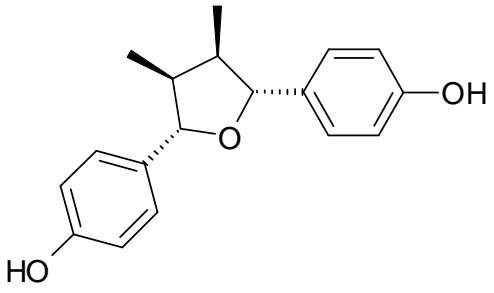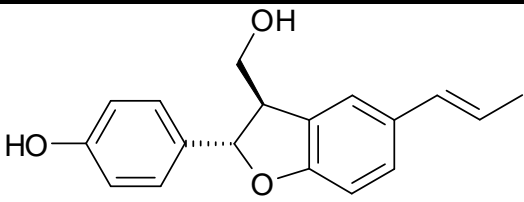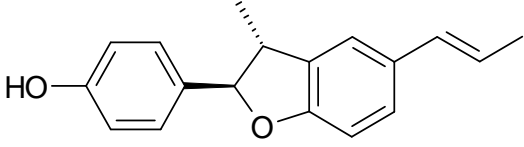
Lignan derivatives rank among the phenolic constituents of the South American plant *Krameria lappacea* (Dombey) Burdet et Simpson. The dried roots (syn. rhatany) are traditionally used in folk medicine to treat inflammation-related diseases predominantly of the mouth [185-188].

As lignans are already known to act as anti-inflammatory agents [189, 190], eleven lignan derivatives comprising neolignans, norneolignans, and

7,70-epoxy lignans were investigated for their ability to block mPGES-1 derived PGE$_2$ formation in a cell-free system (**Table 3.9**).
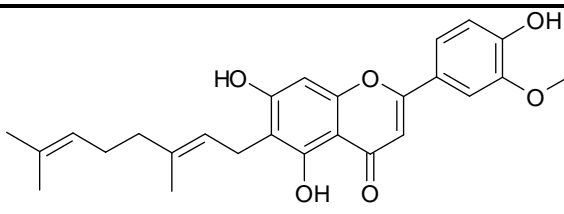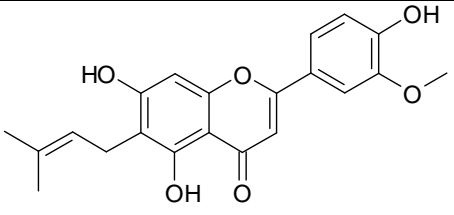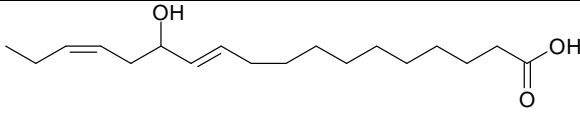
Table 3.9: Biological evaluation of lignan derivatives on cell-free mPGES-1 product formation. Mean values (n = 3) (IC$_{50}$ [µM] or % remaining activity at 50 µM)
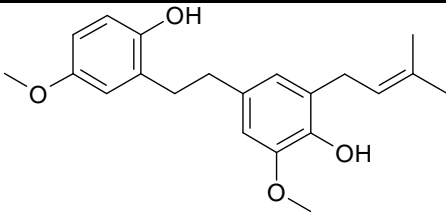

#	R1	R2	Cell-free mPGES-1
23a	OH	OCH$_3$	56.5±3.0
23b	OCH$_3$	OH	42 µM

#	R1	R2	R3	Cell-free mPGES-1
24a	H	OH	OH	7.4 µM
24b	H	OH	H	5.3 µM
24c	H	OH	OCH$_3$	13.5 µM
24d	H	OCH$_3$	OH	13 µM
24e	CH$_3$	OH	H	11 µM

#	structure	Cell-free mPGES-1
25		77.6±3.1

26		75.7±2.9
27		39.5 µM
28		19.5 µM

The standard reference inhibitor MK-886 blocked PGE_2 formation as expected (IC_{50} = 2.1 µM, data not shown). Compound **24a** and **24b** could be identified as potent inhibitors of mPGES-1 with IC_{50} values of 7.4 and 5.3 µM, respectively. The 7,7′-epoxy lignans (**25**, **26**) as well as compound **23a** did not show any inhibition up to 50 µM. All other compounds (**23b**, **24c-e**, **27**, **28**) moderately inhibited mPGES-1 with IC_{50} values between 11 and 42 µM [176].

3.2   Discovery of novel mPGES-1/5-LO inhibitors by pharmacophore model and virtual screening

Pharmacophore model and virtual screening

The pharmacophore model was developed by the group of Prof. Hermann Stuppner (Univ. Innsbruck) for acidic mPGES-1 inhibitors and was based

on highly potent indole derivatives as mPGES-1 inhibitors with IC_{50} values in the nanomolar range.

The pharmacophore model M1 consists of four hydrophobic features, one aromatic ring, one negatively ionizable feature and a shape restriction to limit the size of fitting compounds.

The second pharmacophore model M2 is a partial query of M1, in which the aromatic feature or one of the hydrophobic features is allowed to be omitted during the screening. While M1 achieved a more favorable enrichment of active compounds in a virtual screening, M2 correctly recognized chemically diverse mPGES-1 inhibitors for which M1 was too restrictive [191].
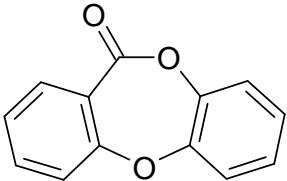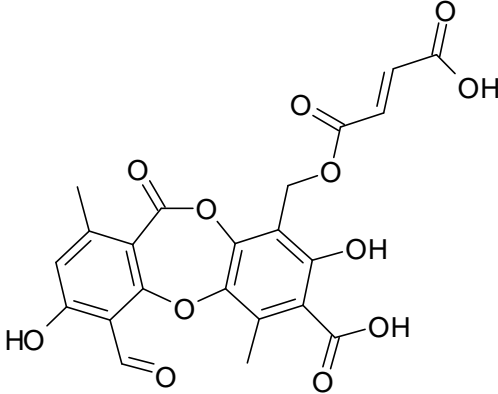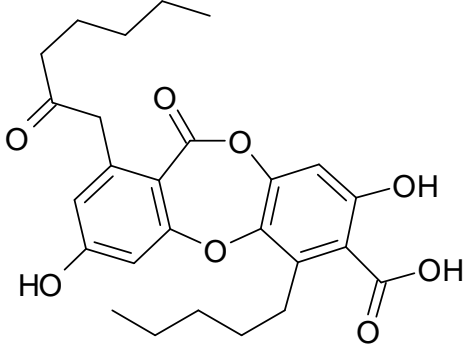
3.2.1 Depsides and depsidones from *lichen spec*.
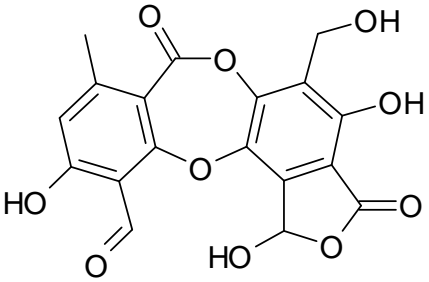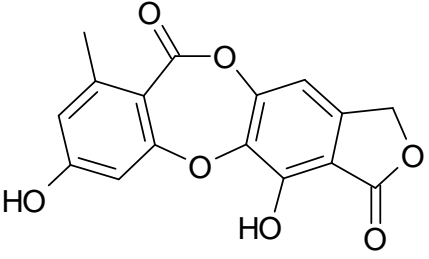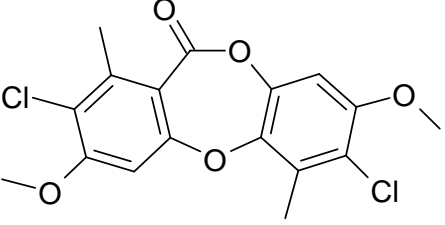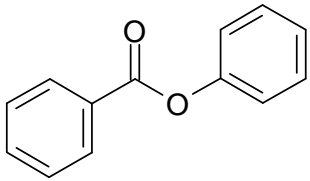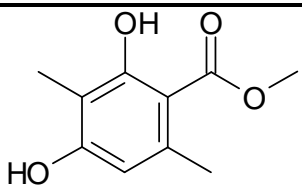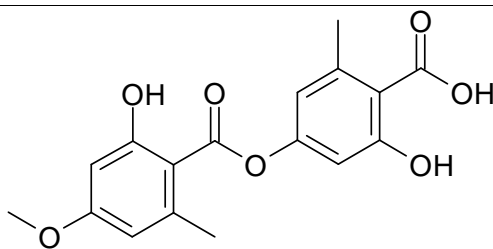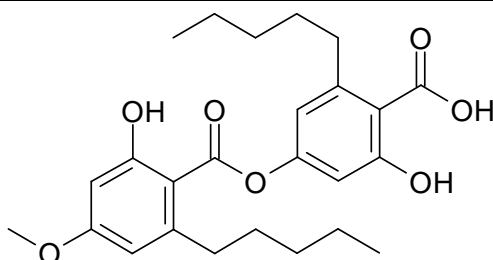
The Chinese herbal medicine (CHM) database consists of 10,216 compounds that are common in the traditional Chinese medicine [192]. Therefore, it was used for *in silico* screening with the pharmacophore models M1 and M2. More than 10% of the virtual hits could be identified as constituents of *lichen spec*. A set of ten different depsides and the related group of depsidones was composed and a virtual screening with the pharmacophore models M1 and M2 was disposed. Physodic acid (**29b),** perlatolic acid (**30c**), evernic acid (**30b)** and olivetoric acid (**30d)** were identified as virtual hits, whereas all other compounds in **Table 3.10** did not map the features of M1 or M2. [177]
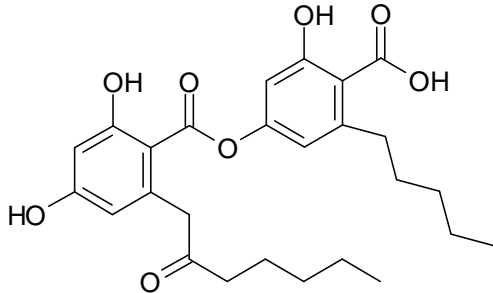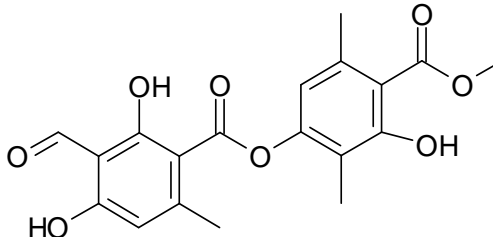
Multifaceted biological activities are known for depsides and depsidones, e.g. antioxidant, antibiotic, antiviral, antitumor properties [152]. As physodic acid (**29b**) is known to inhibit PG biosynthesis in rabbit renal microsomes [146] the selected depsides and depsidones (**Table 3.10**) were

tested for their ability to interfere with mPGES-1 derived PGE_2 formation and semi-purified 5-LO product formation.

Table 3.10: biological evaluation of depsides and depsidones on cell-free mPGES-1 and semi- purified 5-LO product formation. Mean values (n = 3-4) (IC_{50} [μM] or % remaining activity at 10 μM)

#	structure	Cell-free **mPGES-1**	Semi-purified **5-LO**
Depsidone (**29**) basic structure			
fumarproto-cetraric acid (**29a**)		74.6±10.7	82.6±9.4
physodic acid (**29b**)		0.43 μM	2.4 μM

salazinic acid (**29c**)		60.8±10.7	85.0±5.1
variolaric acid (**29d**)		75.5±12.9	96.2±7.3
scensidin (**29e**)		73.3±9.7	7.3 µM
Depside (**30**) basic structure			
methylbeta-orcinolcarboxylate (**30a**)		89.1±12.5	92.1±8.2
evernic acid (**30b**)		53.9±2.7	9.9 µM
perlatolic acid (**30c**)		0.4 µM	0.4 µM

olivetoric acid (**30d**)		1.15 µM	2.4 µM
atranorin (**30e**)		87.5±13.2	66.3±4.4

The reference inhibitors MK886 (mPGES-1 inhibitor [56]) and BWA4C (5-LO inhibitor [184]) worked as expected. The virtual hits physodic acid (**29b**), evernic acid, perlatolic acid and olivetoric acid (**30b-d**) from model M1 and M2 could be identified as inhibitors of mPGES-1 and 5-LO, in which physodic acid (**29b**), perlatolic acid (**30c**) and olivetoric acid (**30d**) strongly suppressed mPGES-1 and 5-LO product formation with IC_{50} values in the low micromolar range of 0.4 to 2.4 µM. Evernic acid (**30b**) moderately inhibited mPGES-1 and 5-LO product formation with IC_{50} values of >10 and 9.9 µM, respectively. Salazinic acid (**29c**) acts as a weak mPGES-1 inhibitor and scensidin (**29e**) and atranorin (**30e**) could be identified as moderate inhibitors of 5-LO (IC_{50} = 7.3 µM and >10 µM, respectively). All other compounds (fumarproto-cetraric acid (**29a**), variolaric acid (**29d**) and methylbeta-orcinolcarboxylate (**30a**)) were completely inactive towards mPGES-1 and 5-LO inhibition.

Interestingly, lipophilic residues seem to be crucial for the strong suppression of mPGES-1 and 5-LO derived product formation as the potent dual inhibitors **29b**, **30c** and **30d** all possess a long lipophilic alkyl chain at position 6 and 6'. **30b**, consisting of small alkyl residues at these positions, could be identified as a weak dual inhibitor of mPGES-1 and 5-LO.

In addition, also a free acidic group seems to be essential as all inactive compounds except **29a** lack a carboxylic group in position 1'.
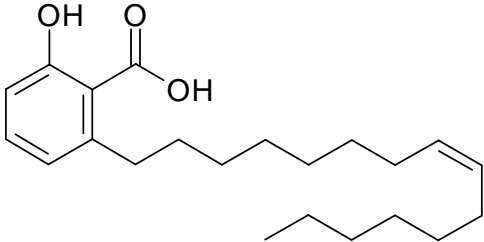
Taken together, (I) an acidic moiety in position 1' and (II) lipophilic chains in position 6 and 6' seem to be essential for the inhibition potential of depsides and depsidones on mPGES-1 and 5-LO product formation. Fitting studies with the potent compounds **29b**, **30c** and **30d** into pharmacophore model M2 pointed out that two of the hydrophobic features are mapped by the lipophilic alkyl chains. Moreover, the data of pharmacophore model M1 indicate that the aromatic ring feature is not essential for the inhibition potential towards mPGES-1 and 5-LO as **29b** and **30d** do not map this feature and **29b** is considered equally potent compared to **30c** which maps all features of M1 [177].

So far, only few natural compounds could be identified as equally potent dual inhibitors compared to **29b** and **30c.** For this reason their molecular pharmacology on the eicosanoid biosynthesis will be further investigated (see chapter **3.4.3**).

3.2.2 Ginkgolic acid from *Ginkgo biloba*

Another virtual hit of the Chinese herbal medicine (CHM) database using the pharmacophore models M1 and M2 was ginkgolic acid from *ginkgo biloba*. As ginkgolic acid has been reported to show antioxidant, radical-captivating, anti-inflammatory properties [173], it has been tested in a cell-free model for its ability to block the product formation of microsomal preparations of IL-1ß stimulated A549 cells as a source of mPGES-1 as well as semi-purified 5-LO product formation (**Table 3.11**).

Table 3.11: biological evaluation of ginkgolic acid (31) on cell-free mPGES-1 and semipurified 5-LO product formation. Mean values (n = 3) (IC_{50} [μM])

#	structure	Cell-free **mPGES-1**	Semi-purified **5-LO**
ginkgolic acid (**31**)		0.7 µM	0.2 µM

Ginkgolic acid (**31**) could be identified as a potent dual mPGES-1 and 5-LO inhibitor with IC_{50} values of 0.7 and 0.2 µM, respectively, compared to the standard reference inhibitors MK886 (mPGES-1 inhibitor IC_{50}= 2.1 µM) and BWA4C (5-LO inhibitor IC_{50}=0.16 µM).

Since only few natural compounds are known to potently block the product formation of both enzymes (mPGES-1 and 5-LO), the molecular pharmacology of ginkgolic acid on the arachidonic acid pathway was further analysed (see chapter **3.4.4**).
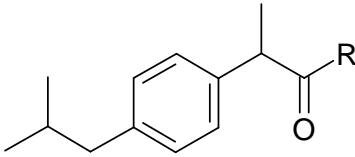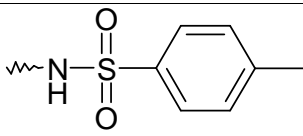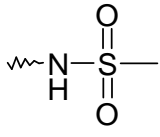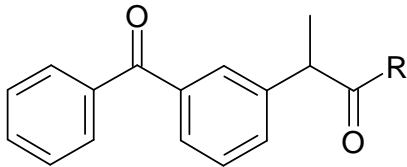
3.3   Synthetic-derivatives of acid-modified NSAIDs as new leads of mPGES-1 inhibitors

Modification of the acidic carboxylic group from the anti-inflammatory drug licofelone to sulfonamides was recently shown to impair COX activity and increase the potency of mPGES-1 inhibition [82].
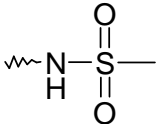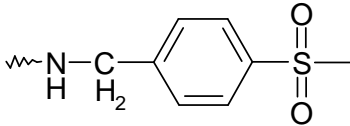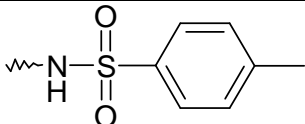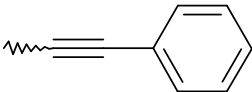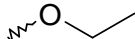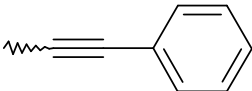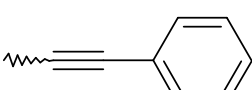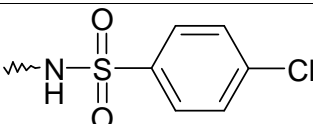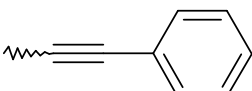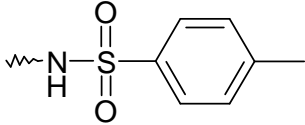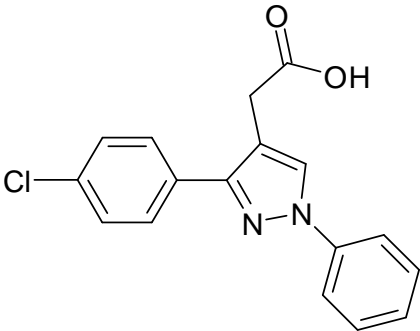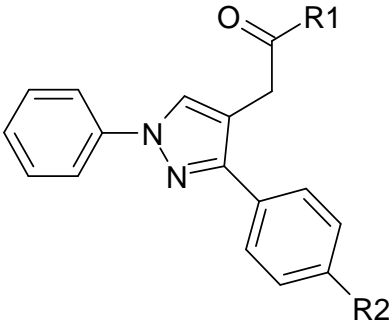
Studies on the classical NSAIDs ibuprofen, ketoprofen, naproxen, indomethacin and lonazolac were performed in the same line of action. Preparations of IL-1ß stimulated A549 cells were used as source for
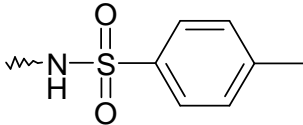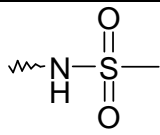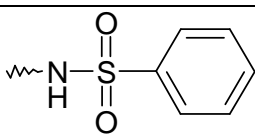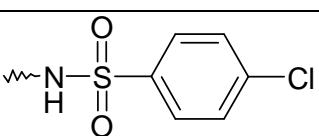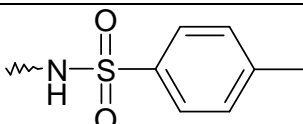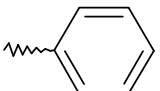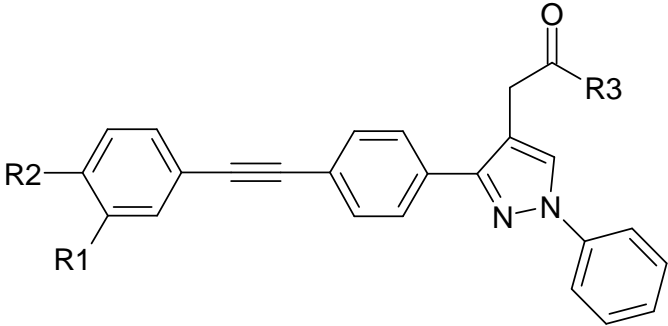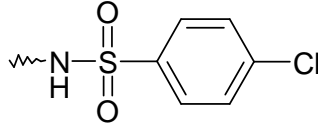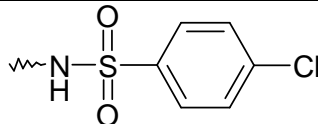
mPGES-1. Synthesized NSAID derivatives (by Prof. Stefan Laufer, Univ. Tuebingen) were tested for their ability to block the formation of PGE_2 using PGH_2 as substrate [178].
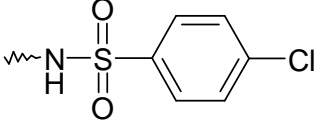
Table 3.12: biological evaluation of NSAID derivatives on cell-free mPGES-1 product formation. Mean values (n = 3) (IC_{50} [μM] or % remaining activity at 10 μM) (Experiments were partially conducted by Giulia Ambrosi, University of Tuebingen)

#	structure	Cell-free mPGES-1
	R	
ibuprofen (**32**)	OH	81.2±2.7
32a		78.6±6.4
32b		67.9±15.8
	R	
keto- profen (**33**)	OH	n.i.

33a		76.3±10.0
33b		78.6±2.1

R

	R	
naproxen (**34**)	OH	n.i.
34a		72.8±6.9
34b		92.5±4.8

	R1	R2	
indo-methacin (**35**)		OH	40.6 µM
35a			6.4 µM

35b	methoxy	NH-SO₂-CH₃	73.6±14.5
35c	methoxy	NH-CH₂-C₆H₄-SO₂-CH₃	68.7±3.5
35d	Br	NH-SO₂-C₆H₄-CH₃	1.75 µM
35e	phenylethynyl	O-ethyl	86.1±3.1
35f	phenylethynyl	OH	2.5 µM
35g	phenylethynyl	NH-SO₂-C₆H₄-Cl	1.8 µM
35h	phenylethynyl	NH-SO₂-C₆H₄-CH₃	2.8 µM

lonazolac

(**36**)

45 µM

	R1	R2	
36a		Cl	3.4 µM
36b		Cl	98.0±26.9
36c		Cl	5.9 µM
36d		Cl	2.3 µM
36e			1.7 µM

	R1	R2	R3	
36f	H	H	OH	0.4 µM
36g	H	Cl	OH	0.16 µM
36h	Cl	H	OH	0.18 µM
36i	H	H		0.2 µM
36j	H	Cl		0.35 µM

| **36k** | Cl | H | | 0.8 µM |

The mPGES-1 inhibitor MK886 was used a reference [56] and inhibited mPGES-1 derived PGE$_2$ formation as expected (data not shown). Comparable to the classical NSAIDs ibuprofen (**32**), ketoprofen (**33**) and naproxen (**34**) also the corresponding sulfonamides (**32a-b**, **33a-b**, **34a-b**) did not inhibit mPGES-1 up to 10 µM.

Introduction of a p-tolylsulfonamide residue to indomethacin (IC$_{50}$ = 40.6 µM) resulting in compound **35a** highly increased the potency towards mPGES-1 (IC$_{50}$ = 6.4 µM), whereas the methansulfonamide residue (**35b**) was less active, suggesting that a lipophilic residue is required at this position. The phenylacetylene-substituted derivatives **35e–h** further enhanced the efficacy towards mPGES-1 inhibition. Introduction of a bromide led to the most potent indomethacin derivative **35d** (IC$_{50}$ = 1.75 µM). Furthermore, derivatives of lonazolac (**36a-k**) were prepared and tested for their ability to block mPGES-1 derived PGE$_2$ formation. Consistent with the results of the indomethacin derivatives (**35a-h**), introduction of phenylsulfonamide residues (**36a**, **36c-e**, **36i-k**) increased the inhibitory potential of mPGES-1 activity whereas the methansulfonamide analogue (**36b**) decreased the potency of mPGES-1 inhibition. Replacing the methyl group from toluensulfonamide with chlorine (**36d**, **36i-k**) and/or introduction of substituted phenylacetylene moieties (**36f-k**) further enhanced the inhibitory potential towards mPGES-1 resulting in the most potent lonazolac derivative **36g** (IC$_{50}$ = 0.16 µM), that inhibited mPGES-1 with IC$_{50}$ value in the nanomolar range [178].

3.4 Molecular pharmacology of promising dual mPGES-1/5-LO inhibitors

3.4.1 Pharmacological profile of arzanol (1) and its promising derivative 1e on eicosanoid biosynthesis

3.4.1.1   Arzanol (1) and 1e inhibit 5-LO product formation

Arzanol (**1**) and its derivative **1e** potently suppressed the activity of semi-purified 5-LO in a cell-free assay with IC_{50} values of 3.1 and 1.2 µM, respectively (**Fig. 3.8A**). In addition, the IC_{50} value shifted to 5.7 µM when 5-LO inhibition of **1e** was analyzed in crude neutrophil homogenates under the same experimental conditions, suggesting that cellular components present in the homogenates may hamper 5-LO inhibition. Washout experiments demonstrated that this effect was reversible, as incubation of 5- LO with 10 µM arzanol (**1**) or 3 µM **1e** and a subsequent dilution to 1 or 0.3 µM (final concentration, respectively) fully abolished 5-LO inhibition (**Fig. 3.8B**). BWA4C was used as reference inhibitor and blocked the formation of 5-LO products as expected (not shown).

A
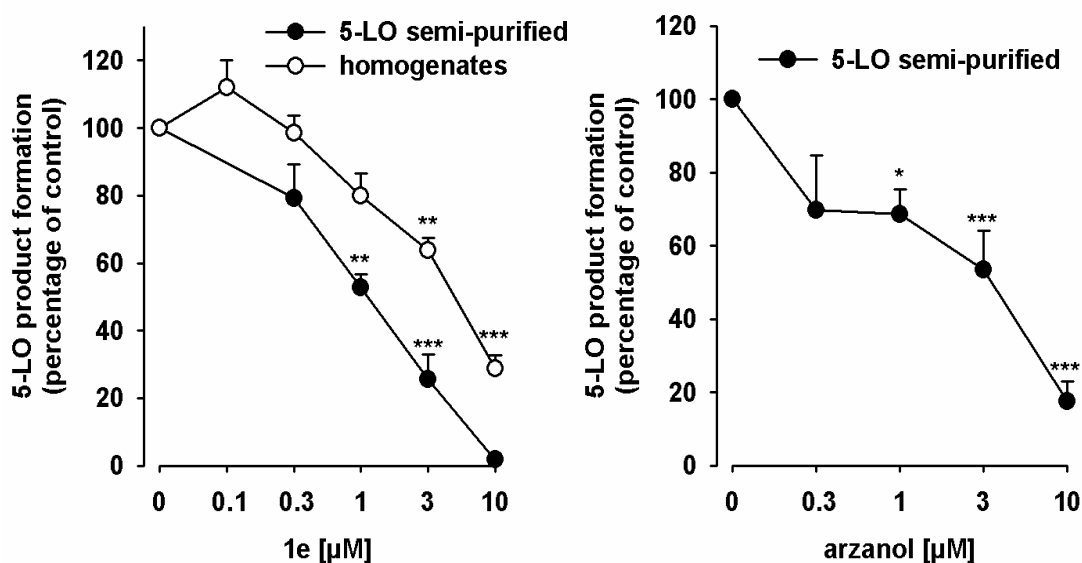
B
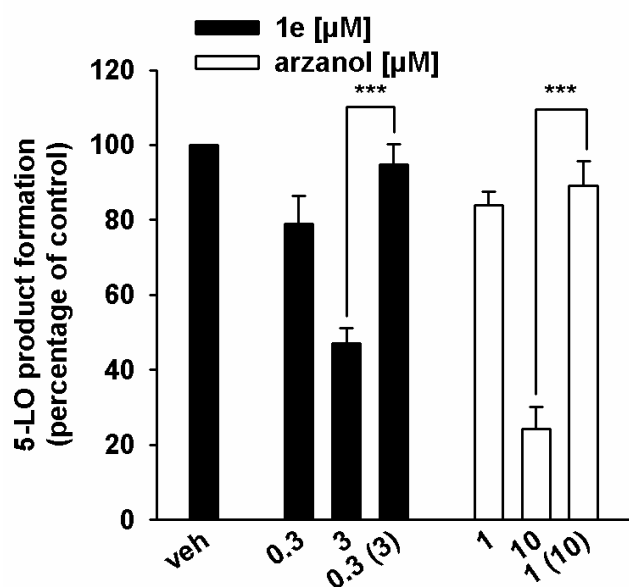
Fig. 3.8: Effects of arzanol[¶] (1) and 1e on isolated 5-LO (A) Inhibition of isolated 5-LO. Semi purified, human recombinant 5-LO or PMNL homogenates (5 x 10^{6} cells/exp.) were pre-incubated with 1e, arzanol[¶], BWA4C (0.3 µM) or vehicle (DMSO) in the presence of 1 mM ATP for 10 min. 5-LO product formation was initiated by addition of 2mM Ca^{2+} and 20 µM AA for 10 min at 37 °C. Reaction was stopped with methanol on ice and 5-LO products were analyzed by RP-HPLC. Data are given as mean + S.E., n = 3, *p < 0.05, **p < 0.01 and ***p < 0.001 vs. vehicle (DMSO) control, ANOVA + Tukey HSD post-hoc tests. (B) Reversibility of 5-LO inhibition. Semi purified, human recombinant 5-LO was pre-incubated in the presence of 1 mM ATP for 10 min and an aliquot was diluted 10-fold to obtain an inhibitor concentration of 0.3 or 1 µM. 5-LO product formation was initiated by addition of 2mM Ca^{2+} and 20 µM AA for 10 min at 37 °C. Reaction was stopped with methanol on ice and 5-LO products were analyzed by RP-HPLC. Data are given as mean + S.E., n = 3-6, ***p < 0.001; 3 or 10 µM vs. diluted sample, ANOVA + Tukey HSD post-hoc tests.

Many plant-derived 5-LO inhibitors are lipophilic reducing agents that act by uncoupling the redox cycle of the active-site iron of 5-LO or by radical scavenging activity [193]. Previous studies already revealed antioxidant properties of arzanol (**1**) [129] that could be confirmed for arzanol (**1**) and **1e** in the DPPH assay. Arzanol (**1**) and **1e** caused a concentration dependent reduction of DPPH with similar efficiency as the well recognized antioxidants cysteine or ascorbic acid (**Fig. 3.9**).
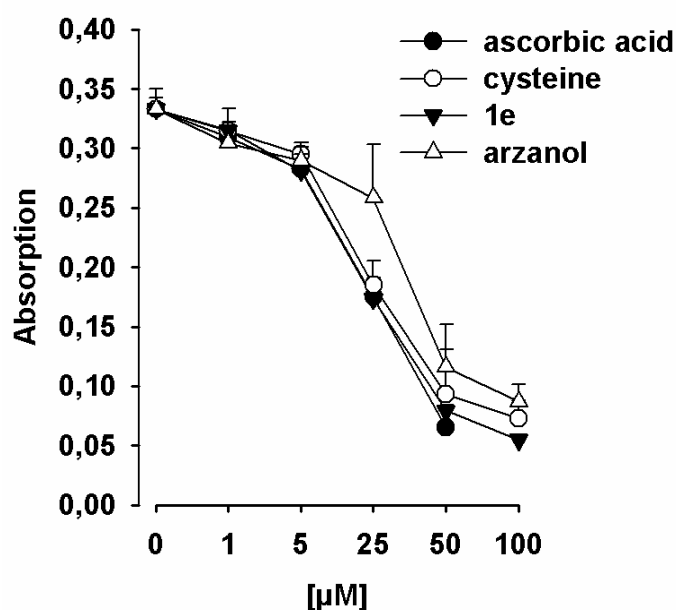
Fig. 3.9: radical scavenger properties of arzanol (1) and 1e. Arzanol, 1e, vehicle and controls were mixed with DPPH solution and incubated for 30 min in the dark. The absorbance was measured at 520 nm. Data are given as mean + S.E. n=3.

Next, investigation of arzanol (**1**) and **1e** on 5-LO activity in intact human neutrophils was performed. A concentration-dependent inhibition of 5-LO product synthesis for both compounds was evident in intact neutrophils stimulated with A23187 in the absence (IC_{50} = 2.4 and 2.6 µM, respectively) and presence (IC_{50} = 2.9 and 0.9 µM, respectively) of exogenous AA (20 µM) as well as for neutrophils primed with LPS (1 µg/ml) and stimulated with fMLP (IC_{50} = 8.1 and 2.8 µM, respectively, **Fig. 3.10**). The product formation of 12- and 15-LO was not inhibited by arzanol (not shown). The 5-LO inhibitor BWA4C (0.3 µM), used as reference compound, blocked 5-LO activity in all assays as expected (inhibition >90%, not shown).
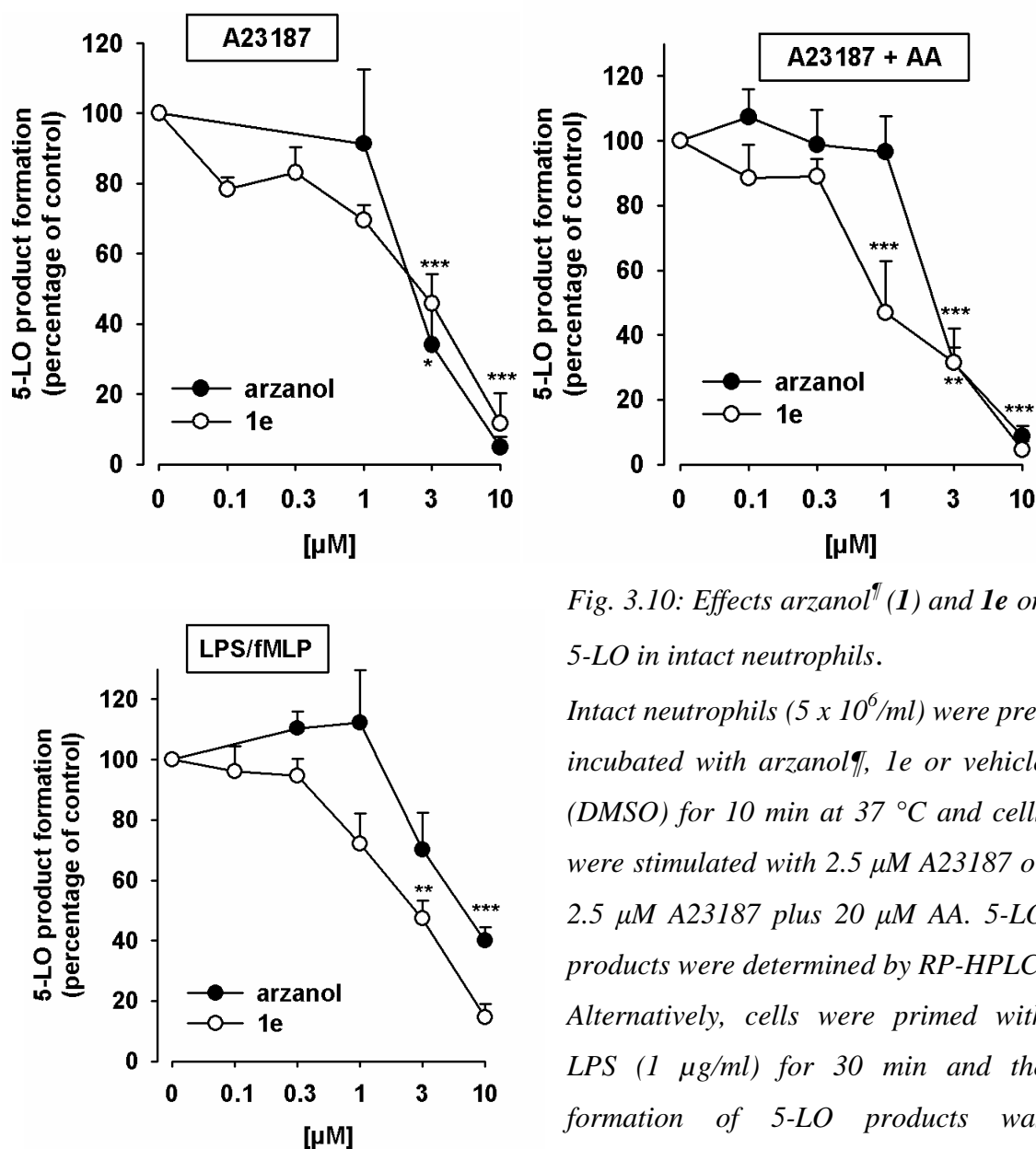
Fig. 3.10: Effects arzanol[¶] (1) and 1e on 5-LO in intact neutrophils.

Intact neutrophils (5 x 10^6/ml) were pre-incubated with arzanol¶, 1e or vehicle (DMSO) for 10 min at 37 °C and cells were stimulated with 2.5 μM A23187 or 2.5 μM A23187 plus 20 μM AA. 5-LO products were determined by RP-HPLC. Alternatively, cells were primed with LPS (1 μg/ml) for 30 min and the formation of 5-LO products was initiated by addition of 1 μM fMLP.

*LTB_4 levels were detected using a TXB_2 High Sensitivity EIA Kit according to the manufacturer's protocol. Data are given as mean + S.E. n=3-7, *p < 0.05, **p< 0.01 and ***p < 0.001 vs. vehicle (DMSO) control, ANOVA + Tukey HSD post-hoc tests.*

An interference at the level of AA supply, e.g. by inhibition of cPLA_2 can be excluded, as arzanol (1) and 1e failed to significantly inhibit isolated recombinant human cPLA_2 up to 10 μM, whereas the pyrrolidine inhibitor (5 μM) blocked AA release as expected (**Fig. 3.11**).
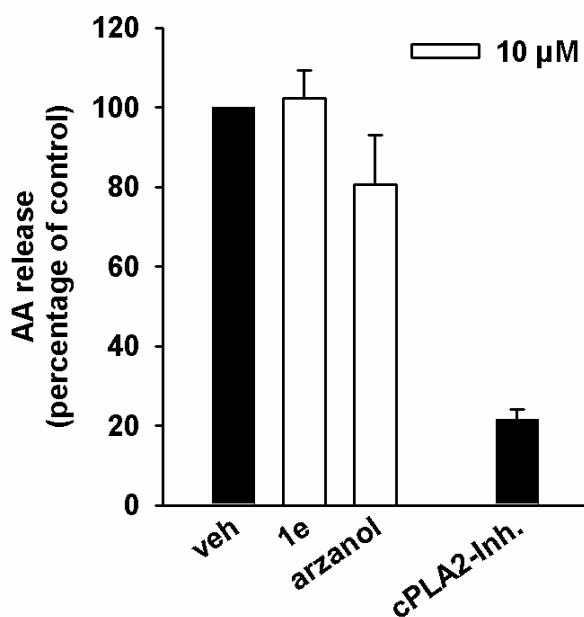
Fig. 3.11: arzanol (1) and 1e do not inhibit cPLA$_2$.

Freshly prepared large unilamelar vesicles were incubated with cPLA$_2$ enzyme, 1 mM Ca^{2+} and the indicated compounds for 1 h at 37 °C. Reaction was stopped using methanol. Following derivatisation with p-anisidinium chloride, the resulting derivate was analyzed by RP-HPLC. Data are given as mean + S.E., n = 3. Performed by Marius Melzer in the lab of Prof. Dr. O. Werz (University of Jena, Germany).

5-LO activity is tightly regulated in the cell [111], i.e. phosphorylation via the ERK-1/2 or p38 MAPK pathway leads to a strong upregulation of 5-LO activity. Therefore, **1e** was analyzed for its ability to interfere with the ERK-1/2 or p38 MAPK pathway. As can be seen in **Fig. 3.12**, **1e** did not influence the phosphorylation state compared to the reference inhibitor U0126. Thus, an influence on 5-LO regulation by phosphorylation can be excluded for **1e**.
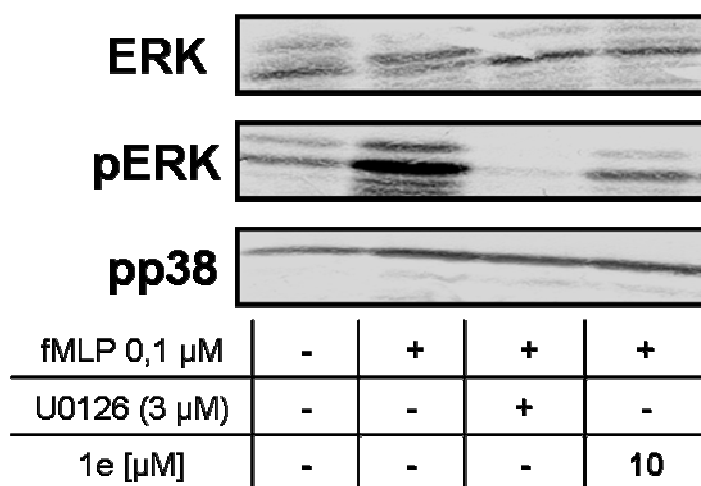
Fig. 3.12: Effects on ERK and p38 MAPK pathway of 1e.

Neutrophils (10^7) were pre-warmed for 3 min at 37 °C and pre-incubated with 1e or vehicle (DMSO) at 37 °C for 15 min. The reaction was started by the addition of 0.1 µM fMLP, stopped after 1.5 min with SDS-b and heated for 6 min at 95 °C. Total cell lysates were analyzed for ERK1/2, phosphorylated ERK1/2

(Thr-202/Tyr-204) and phosphorylated p38 MAPK (Thr-180/Tyr-182) by SDS/PAGE and western blotting. Results are representative of 2-3 independent experiments.

Experiments performed in human whole blood focussing on 5-LO inhibition revealed a loss of efficacy for arzanol (**1**) and **1e.** Both failed to block 5-LO product formation up to 10 µM (**Fig. 3.13**) in whole blood stimulated with A23187 for 10 min, whereas the standard inhibitor BWA4C suppressed 5-LO product formation as expected.
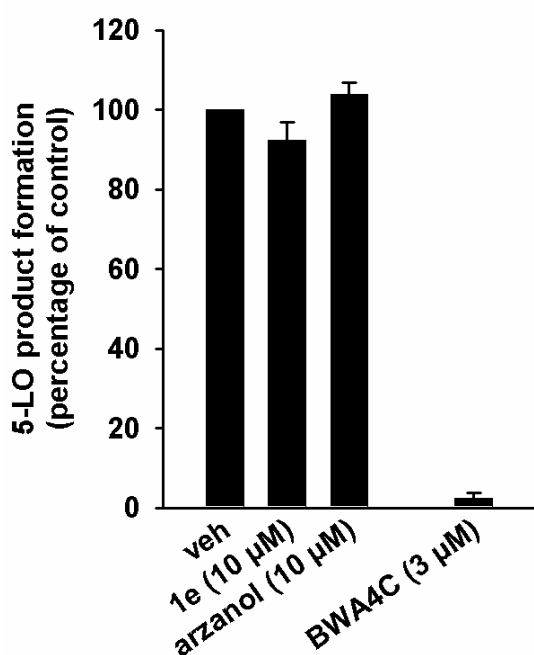
*Fig. 3.13: Effects of arzanol (**1**) and **1e** on 5-LO inhibition in human whole blood.*

Heparinized whole blood was pre-incubated with arzanol, 1e or vehicle (DMSO) for 15 min at 37 °C and stimulated with A23187 (30 µM) for 10 min. Reaction was stopped on ice and 5-LO product formation was detected using RP-HPLC. Data are given as mean + S.E. n=2-3.

Together, arzanol (**1**) and its synthetic derivative **1e** are direct inhibitors of 5-LO. Both could be identified as redox active inhibitors with a reversible mechanism of action largely independent of the substrate supply. Interference with 5-LO regulation can be excluded. 5-LO inhibition in cell-based assay was comparable to the results from semi-purified 5-LO assay. In crude neutrophil homogenates and human whole blood inhibition of 5-LO product formation seem to be hampered by components present in the assays medium.

3.4.1.2   Arzanol (1) and 1e block mPGES-1 derived PGE$_2$ formation

As reported in **Table 3.6**, arzanol (**1**) and **1e** potently inhibited PGE$_2$ formation in microsomal preparations of IL-1ß stimulated A549 cells with IC$_{50}$ values of 3.1 and 1.2 µM, respectively. Alteration of PGH$_2$ to lower (1, 5 µM) or higher (50 µM) concentration caused only slight changes in the potency of **1e** (**Fig. 3.14A**), suggesting that mPGES-1 inhibition is largely independent of the substrate supply. Alteration to lower PGH$_2$ concentration (1 µM) shifted IC$_{50}$ value to 0.25 µM, whereas higher PGH$_2$ concentration (50 µM) did not change the inhibitory potential of arzanol (**1**), indicating a competitive mode of action. Washout experiments were carried out, to investigate whether inhibition of PGE$_2$ synthesis is reversible (**Fig. 3.14B**). A 10-fold dilution of the samples containing 1 µM arzanol (**1**) or **1e** restored mPGES-1 activity, implying a reversible mode of inhibition. Adding 10% FCS to the sample of **1e** reduced the potency (60% remaining activity at 10 µM), suggesting that plasma protein binding due to the lipophilic acid structure might occur. MK886 was used as standard inhibitor and blocked PGE$_2$ formation as expected (not shown).

A
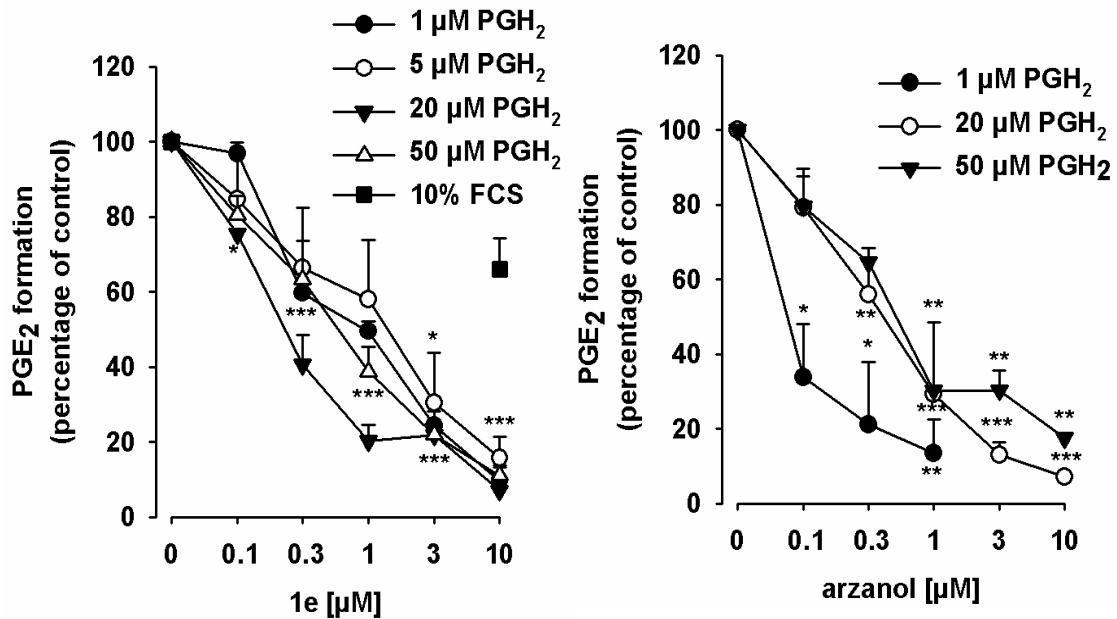
B
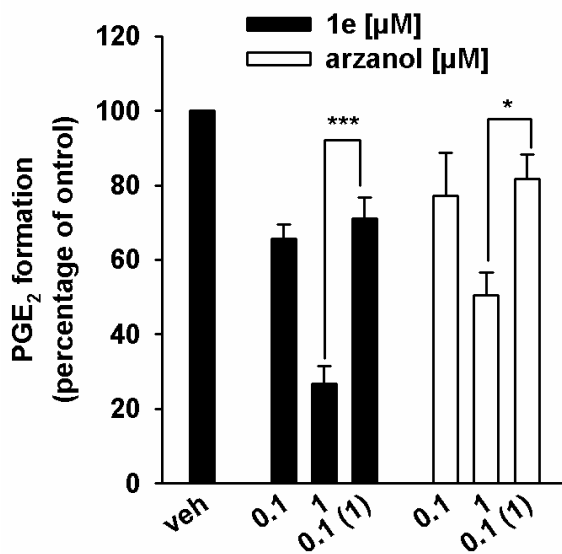
Fig. 3.14: Effects of arzanol[¶] (1) and 1e on mPGES-1 in cell-free assay.

(A) Concentration-response analysis of arzanol[¶] and 1e. Microsomal preparations of IL-1β-stimulated A549 cells were pre-incubated with arzanol, 1e or vehicle (DMSO) for 15 min at 4 °C and PGE_2 formation was induced by addition of variable PGH_2 concentrations (1, 5, 20 and 50 μM). The amount of PGE_2 was quantified for 1 and 5 μM PGH_2 by the use of a PGE_2 High Sensitivity EIA Kit according to the manufacturer's protocol and PGE_2 formation of samples with or w/o 10% FCS stimulated with 20 and 50 μM PGH_2 was analyzed by RP-HPLC. Data are given as mean + S.E., n=3, *p < 0.05, **p < 0.01 ***p < 0.001 vs. vehicle (DMSO) control, ANOVA + Tukey HSD post-hoc tests. (B) Reversibility of mPGES-1 inhibition. Microsomal preparations were pre-incubated for 15 min with 1 μM arzanol, 1e or vehicle (DMSO), and an aliquot was diluted 10-fold to

obtain an inhibitor concentration of 0.1 µM. Then, 20 µM PGH$_2$ was added and all samples were incubated for 1 min on ice, and PGE$_2$ formation was analyzed as described by RP-HPLC. Data are given as mean + S.E., n=3, *p < 0.05 or ***p < 0.001 vs. diluted sample, ANOVA + Tukey HSD post-hoc tests.

In summary, arzanol (**1**) and **1e** potently inhibit mPGES-1 derived PGE$_2$ formation under cell-free conditions. Both act in a reversible mode of action largely independent of the substrate supply. Lower concentrations of PGH$_2$ (1 µM) enhanced the inhibitory potential of arzanol (**1**) by 10-fold (IC$_{50}$= 0.25 µM), indicating a competitive mode of action.

3.4.1.3   Arzanol (1) and 1e interfere with the prostanoid synthesis

As mPGES-1 acts downstream of COX, arzanol (**1**) and **1e** were investigated for their ability to interfere with either COX-1 or -2. Therefore, arzanol (**1**) and **1e** were analyzed in test system of isolated ovine COX-1 and human recombinant COX-2. Indomethacin and celecoxib were used as reference inhibitors and blocked 12-HHT formation as expected (not shown). No inhibition of isolated COX-1 could be observed for arzanol (**1**) and **1e**. In contrast, COX-2 derived 12-HHT formation was moderately affected by **1e** (IC$_{50}$ > 10 µM), but not by arzanol (**1**).
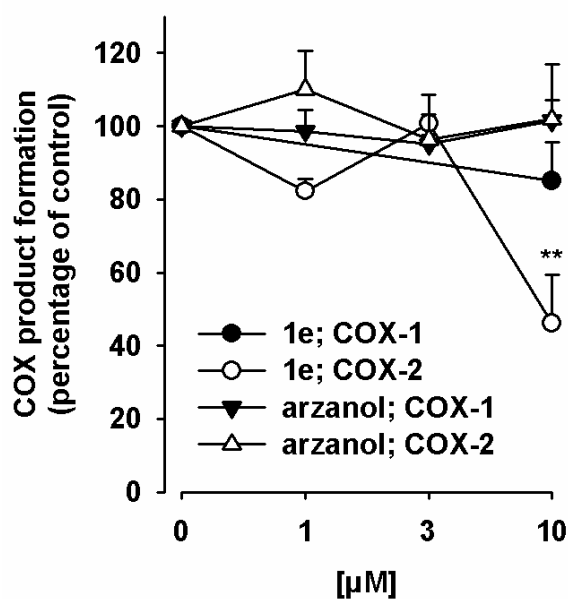
Fig. 3.15: Effects of arzanol[¶] (1) and 1e on isolated COX-1 and -2

Purified ovine COX-1 (50 units) or human recombinant COX-2 (20 units) were pre-incubated 5 min prior stimulation with AA (5 µM or 2 µM, respectively). 12-HHT in the samples was analyzed using RP-HPLC. Data are given as mean + S.E., n=2-3, **p < 0.01 vs. vehicle (DMSO) control, ANOVA + Tukey HSD post-hoc tests.

Using a cell-based test system for COX-1, intact human platelets were pre-incubated with arzanol (1) or 1e and the formation of 12-HHT and TXB_2 was measured after addition of AA (5 µM). The formation of 12-HHT (IC_{50} = 2.3 and 1.6 µM, respectively) and TXB_2 (IC_{50} = 2.9 and 2.2 µM, respectively) was concentration-dependently blocked by arzanol (1) and 1e (**Fig. 3.16**). The reference inhibitor indomethacin blocked COX-1 product formation as expected (not shown).

A   **B**
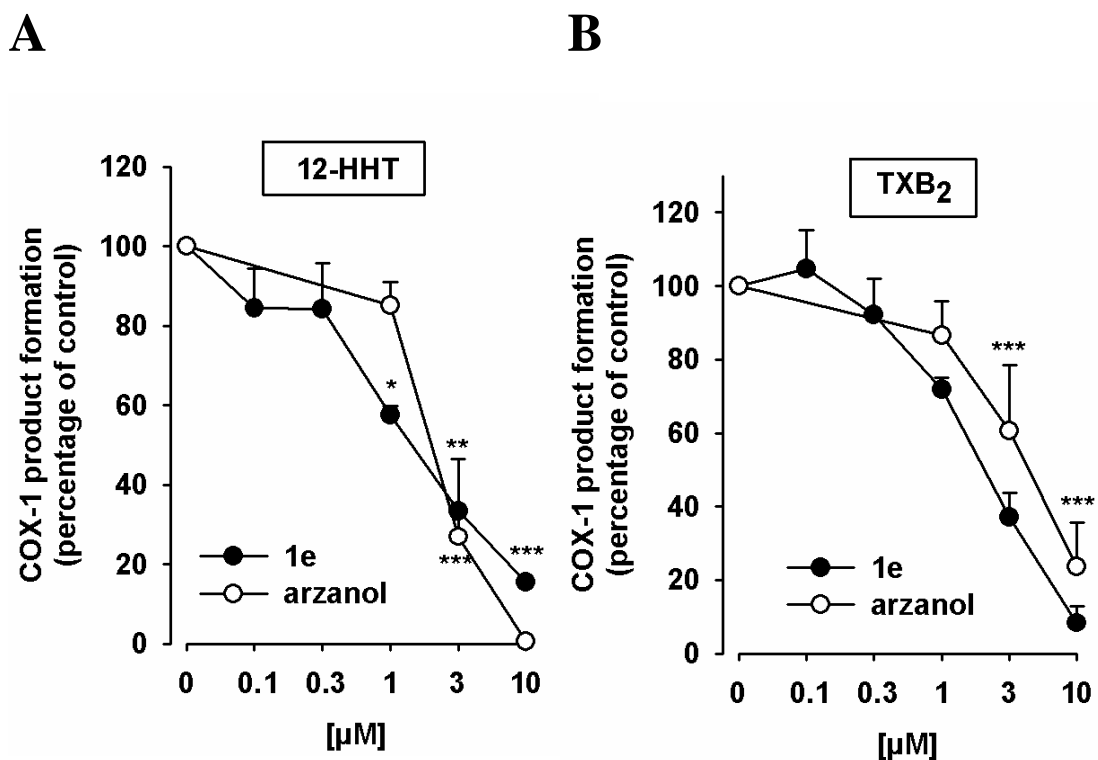
Fig. 3.16: Effects of arzanol[¶] (1) and 1e on human platelets

Platelets (10^8/ml PBS containing 1 mM $CaCl_2$) were pre-incubated for 5 min prior to stimulation with AA (5 μM). After another 5 min at 37 °C, the formation of (A) 12-HHT was determined by RP-HPLC (B) and formation of TXB_2 was determined using a TXB_2 High Sensitivity EIA Kit according to the manufacturer's protocol. Data are given as mean + S.E., n=3-5, *p < 0.05, **p < 0.01 ***p < 0.001 vs. vehicle (DMSO) control, ANOVA + Tukey HSD post-hoc tests.

Because direct inhibition of COX-1 can be excluded, the inhibitory effects observed in platelets may be due to thromboxane synthase (TXAS) inhibition. To check if TXAS is directly affected by arzanol (1) and 1e, freshly prepared platelet homogenates were pre-incubated with the compounds and stimulated with PGH_2 (20 μM) as substrate of TXAS. Both, arzanol (1) and 1e concentration-dependently blocked the formation of TXB_2 (as a biomarker for TXA_2) from PGH_2 with IC_{50} values of 2.7 and 2.5 μM, respectively, suggesting a direct inhibition of TXAS (**Fig. 3.17**). CV4151, used as selective inhibitor of TXAS suppressed TXB_2 formation as expected (not shown).
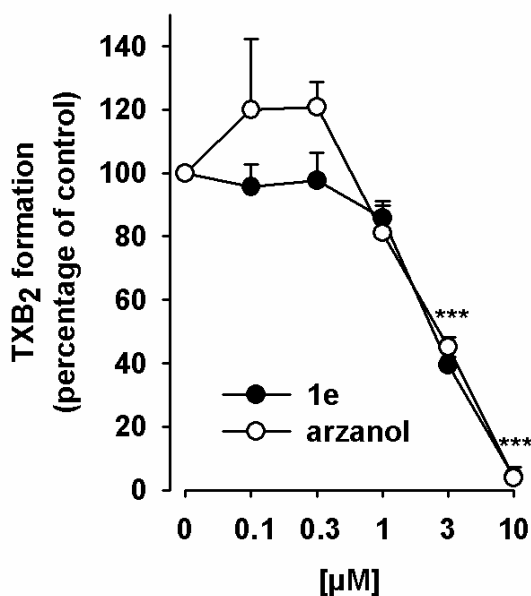
Fig. 3.17: Effects of arzanol (1) and 1e on TXAS

Thromboxane A_2 synthase (TXAS) activity was determined in platelet homogenates (10^8/ml PBS containing 1 mM $CaCl_2$, sonified 3 x 15 sec) pre-incubated for 15 min on ice and stimulated with 20 μM PGH_2 for 1 min. TXB_2 levels were detected in the supernatant using a TXB_2 High Sensitivity EIA Kit according to the manufacturer's protocol. Data are given as mean + S.E., n=3-4, ***p < 0.001 vs. vehicle (DMSO) control, ANOVA + Tukey HSD post-hoc tests.

In addition, intact human monocytes stimulated with LPS and arzanol (1) or 1e for 24 h were used as cell-based system for COX-2. As can be seen in **Fig. 3.18B/D** the reference inhibitor dexamethason completely blocked COX-2 and mPGES-1 expression comparable to the unstimulated sample. Arzanol (1) and 1e did not affect COX-2 expression. In addition, influence on mPGES-1 expression can be excluded for arzanol (1). 1e suppressed TXB_2 formation comparable to the levels detected in unstimulated monocytes. Also PGE_2 formation was affected by 1e, suggesting a synergistic effect of COX-2 and mPGES-1 inhibition. Arzanol (1) potently suppressed the formation PGE_2 and TXB_2 detected in the supernatant of intact human monoycte cultures after 24 h (**Fig. 3.18A**). Cytotoxic effects can be excluded as arzanol (1) suppressed prostanoid formation below the levels detected in the unstimulated cells. Therefore, a concentration-response analysis of arzanol (1) on cellular COX-2-derived PGE_2 formation in intact human monocytes primed with LPS for 20 h was conducted (**Fig. 3.18C**). Arzanol (1) significantly inhibited PGE_2 formation already at 3 μM

(IC_{50} = 9 µM). Indomethacin and MD-52, a selective mPGES-1 inhibitor, were used as controls.

A

B

LPS (1 µg/ml)	-	+	+	+	+
Dex (1 µM)	-	-	+	-	-
arzanol [µM]	-	-	-	10	-
1e [µM]	-	-	-	-	10

C

D

LPS	-	+	+	+	+
arzanol [µM]	-	-	3	10	-
Dex	-	-	-	-	+
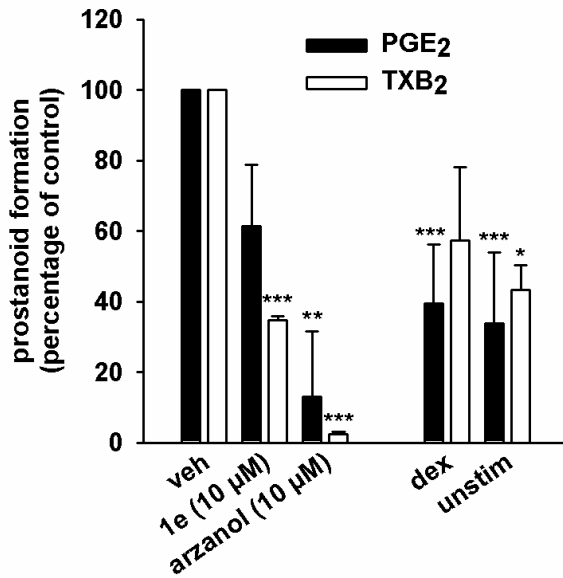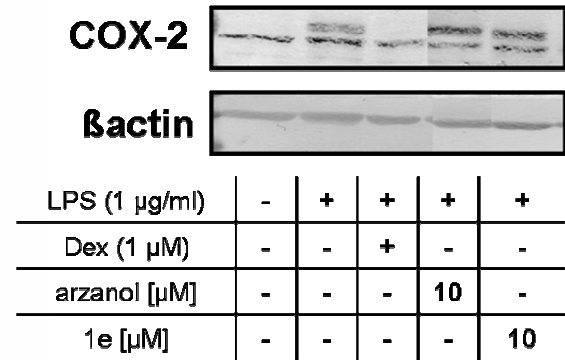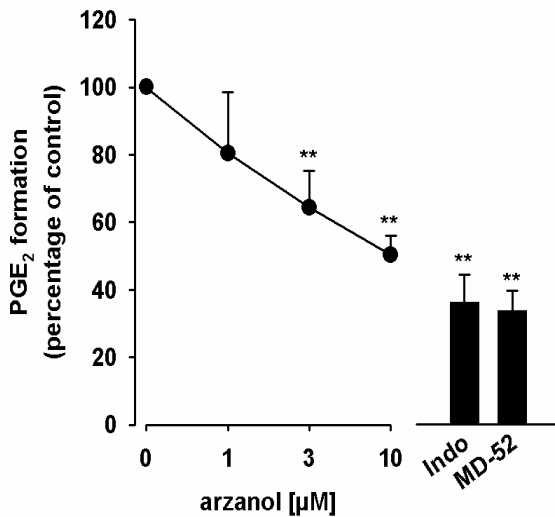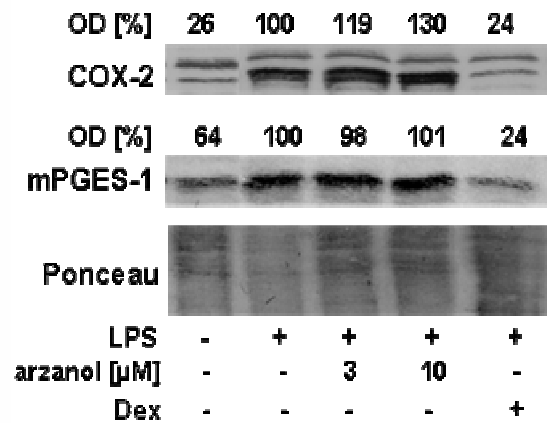
*Fig. 3.18: Effects of arzanol[¶] (**1**) and **1e** (10 µM) on intact human monocytes and A549 cells stimulated with LPS.*

(A) PGE₂ and TXB₂ levels of LPS stimulated monocytes. Intact human monocytes (5 x 10⁶/exp. in RPMI 1640 medium containing 0.5% FCS, P/S and 2 mM glutamine) were stimulated with 1 µg/ml LPS and arzanol, 1e (10 µM), dexamethason (1 µM) or vehicle

(DMSO) was added for 24 h at 37 °C. PGE$_2$ and TXB$_2$ levels were detected in the supernatant using a PGE$_2$ and TXB$_2$ High Sensitivity EIA Kit according to the manufacturer's protocol. Data are given as mean + S.E., n =2-4, *p < 0.05, **p < 0.01 ***p < 0.001 vs. vehicle (DMSO) control, ANOVA + Tukey HSD post-hoc tests. (B) COX-2 expression in LPS stimulated monocytes. Monocytes were stimulated as described above. After 24 h cells were detached and lysed (2 x SDS-b.). Samples were subjected to SDS-PAGE and WB using a specific antibody against COX-2. ßactin was used as loading control. Results are representative of 2-4 independent experiments. (C) PGE$_2$ formation as parameter of COX-2 activity. Monocytes were pre-treated with LPS (1 µg/ml) for 20 h, cells were washed, and pre incubated with arzanol¶, indomethacin (Indo, 10 µM), MD52 (2 µM) or vehicle (veh, DMSO) for 15 min. PGE$_2$ formation was initiated by addition of AA (1 µM), and after 30 min, PGE$_2$ in the supernatant was analyzed by ELISA. Data are given as mean + S.E., n = 2-4, **p < 0.01 vs. vehicle (DMSO) control, ANOVA + Tukey HSD post-hoc tests. (D) Expression of COX-2 and mPGES-1. Monocytes (2 x 10^6 cells/ml, RPMI plus 0.5% FCS) were incubated in the presence or absence of 10 µg/ml LPS together with arzanol, dexamethasone (1 µM) or vehicle (DMSO) for 20 h at 37 °C. Cells were harvested, lysed by addition of SDS/PAGE sample loading buffer and proteins were separated by SDS–PAGE and analyzed for COX-2 (upper panel) and mPGES-1 (lower panel) by WB. Ponceau S staining confirms equal loading of protein and transfer of proteins to the membrane. Data are given as mean + S.E., n=3–4.

Cytotoxic effects of arzanol (**1**) and **1e** were analyzed in the MTT assay using HL60 or A549 cells for 24 h or 48 h. At 50 µM arzanol (**1**) significantly impaired cell viability within 24 h. Therefore, higher concentrations of more than 30 µM were not investigated in a cell-based assay. **1e** slightly affected cell viability at 48 h but not 24 h (**Fig. 3.19**), implying that no unspecific cellular effects modulate prostanoid formation in cell-based assays up to 24 h. Staurosporin, used as positive control, significantly affected cell-viability as expected.
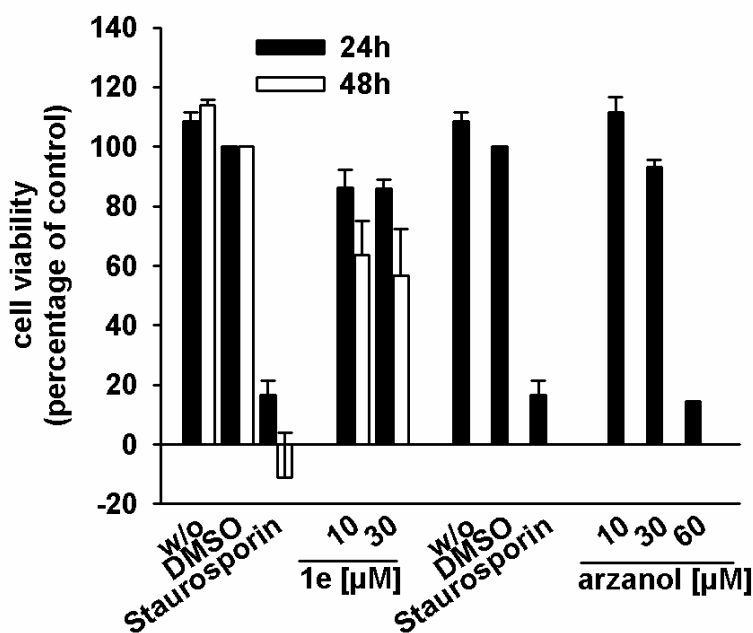
Fig. 3.19: cytotoxic properties of arzanol (1) and 1e.

A549 or HL60 cells (3 x 10^5/exp.) were incubated for 24 h and 48 h at 37 °C with arzanol, 1e or vehicle (DMSO). After 24 h or 48 h, MTT was added and samples were incubated for 4 h at 37 °C. Reaction was stopped and the absorption was measured at 570 nm. Data are given as mean + S.E. n=3. MTT in HL60 cells was performed by Dagmar Blaesius in the lab of Prof. Dr. O. Werz (University of Tübingen, Germany).

Along these lines, arzanol (1) concentration-dependently inhibited PGE_2 formation in human whole blood primed with LPS for 5 h (**Fig. 3.20**). In parallel, the accompanied COX-2-mediated biosynthesis of TXB_2 and 6-ketoPGF_{1a} were hardly affected by arzanol (1). 1e, in contrast, did not inhibit the formation of PGE_2, TXB_2 and 6-ketoPGF_{1a} in human whole blood experiments primed with LPS for 24 h (not shown). The selective mPGES-1 inhibitor MD52 showed a comparable inhibitory profile as arzanol (1) by reducing PGE_2 synthesis in LPS-treated whole blood for 5 h and hardly affected 6-ketoPGF_{1a} in the respective assays. In contrast, indomethacin blocked the formation of the analyzed prostanoids in all assays as expected.
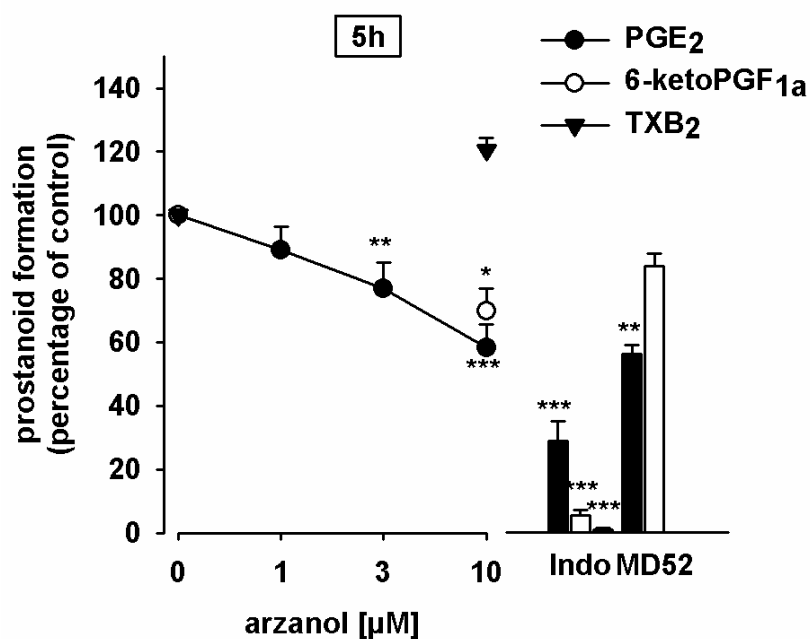
Fig. 3.20: Effects of arzanol[¶] (1) on prostanoid formation in human whole blood. PGE_2. Heparinized human blood, treated with 1 μM thromboxane synthase inhibitor and 50 μM aspirin, was pre-incubated with arzanol, indomethacin (Indo, 50 μM), MD52 (6 μM) or vehicle (DMSO) for 5 min at RT, and then, PGE_2 formation was induced by addition of 10 μg/ml LPS. After 5 h at 37 °C, PGE_2 was extracted from plasma and analyzed as described. TXB_2 Heparinized blood was pre-incubated with arzanol, indomethacin (Indo, 50 μM) or vehicle (DMSO) for 5 min, then 10 μg/ml LPS were added and TXB_2 was analyzed after 5 h at 37 °C in the plasma by ELISA. 6-keto PGF_{1a} Heparinized human blood, treated with 1 μM thromboxane synthase inhibitor, was pre-incubated with arzanol, indomethacin (Indo, 50 μM), MD52 (6 μM) or vehicle (DMSO) for 5 min at RT, prior to addition of 10 μg/ml LPS. After 5 h at 37 °C, 6-keto PGF1a was directly analyzed in plasma by ELISA. Data are given as mean ± S.E., n=3, **p < 0.01 or ***p < 0.001 vs. vehicle (0.1% DMSO) control, ANOVA + Tukey HSD post hoc tests.

Taken together, arzanol (1) and 1e inhibit TXAS derived TXB_2 formation in human platelets. No inhibition of COX enzymes for arzanol (1) and only moderate COX-2 inhibition (IC_{50} > 10 μM) by 1e was observed. Interference at the level of COX-2 and mPGES-1 expression can be excluded. For arzanol (1) effects on PGE_2 biosynthesis were also evident in human whole blood stimulated with LPS for 5 h. 1e did not markedly inhibit prostanoid biosynthesis in human whole blood. Cytotoxic effects on

intact cells up to 30 µM can be excluded for both compounds, since cell-viability was not affected within 24 h.

3.4.1.4   Arzanol (1) suppresses carrageenan-induced pleurisy in rats and inhibits eicosanoid biosynthesis *in vivo*

The anti-inflammatory effectiveness of arzanol (**1**) was also assessed *in vivo* using a model of carrageenan-induced pleurisy in rats. Injection of carrageenan into the pleural cavity of rats (DMSO 4% group) elicited an inflammatory response within 4 h, characterized by the accumulation of fluid that contained large numbers of inflammatory cells (**Table 3.13**). Arzanol (**1**) inhibited the inflammatory response as demonstrated by the significant attenuation of exudate formation (59%) and cell infiltration (48%). Indomethacin (5 mg/kg) reduced the exudate formation and cell infiltration by 75% and 65%, respectively (**Table 3.13**). In comparison with the corresponding exudates from DMSO treated rats, exudates of arzanol-treated animals exhibited decreased PGE_2 levels (47% inhibition), whereas indomethacin almost completely suppressed PGE_2 (95%) as well as 6-ketoPGF$_{1a}$ (94%) levels as expected. In agreement with the moderate inhibition of COX-2-derived 6-keto PGF$_{1a}$ formation in human whole blood (see above), arzanol (**1**) also slightly reduced the levels of 6-ketoPGF$_{1a}$ (27% inhibition). On the other hand, indomethacin failed to significantly reduce LTB$_4$ levels which were lowered by arzanol (**1**) (31% inhibition), seemingly due to direct inhibition of 5-LO.

*Table 3.13: Effect of arzanol (**1**) on carrageenan-induced pleurisy in rats.*

Thirty min before intrapleural injection of carrageenan, rats (n = 10 for each experimental group) were treated i.p. with 3.6 mg/kg arzanol, 5 mg/kg indomethacin or vehicle (DMSO 4%). Exudate volume, eicosanoids and inflammatory cell accumulation in the pleural cavity were assessed 4 h after carrageenan injection. Data are expressed as mean ± SEM. n=10, * p<0.05. *** p<0.01 vs. vehicle. Experiments were performed by Dr. Rossi and Prof. Sautebin, Univ. Naples, Italy.

Treatment	Volume exudate [ml]	Inflammatory cells x 10^6	PGE_2 (ng/rat)	LTB_4 (ng/rat)	6-ketoPGF$_{1a}$ (ng/rat)
Vehicle	0.41±0.019	46.5±6.0	4.26±0.67	1.22±0.26	10.72±1.43
arzanol (3.6 mg/kg)	0.17±0.05 *** (59%)	24.0±5.9 * (48%)	2.27±0.35 * (47%)	0.84±0.21 (31%)	7.79±0.72 (27%)
Indo-methacin (5 mg/kg)	0.10±0.03 *** (76%)	16.28±2.30 *** (65%)	0.21±0.024 *** (95%)	1.06±0.20 (13%)	0.64±0.09 *** (94%)

3.4.2 Pharmacological profile of CFA (**19**) within the AA-cascade

3.4.2.1   CFA (**19**) interferes with the prostaglandin biosynthetic pathway

CFA (**19**) was identified to potently inhibit the formation of PGE_2 (IC_{50}= 1.8 µM) in microsomal preparations of IL-1ß stimulated A549 cells as source of mPGES-1. Variation of the substrate (PGH_2) concentration for mPGES-1 did not markedly alter the potency of CFA (**19**) (IC_{50} = 1.8 - 3.7 µM; **Fig. 3.21A**). The reference inhibitor MK886 blocked PGE_2 formation as expected (data not shown). Wash out experiments demonstrate that the inhibitory effect on mPGES-1 is fully reversible (**Fig. 3.21B**). To check for plasma protein binding, 10% FCS was added to the sample. The inhibitory

potential shifted from 9.9% remaining activity at 10 μM to 61.6% remaining activity (**Fig. 3.21A**), indicating that CFA (**19**) binds to plasma proteins.
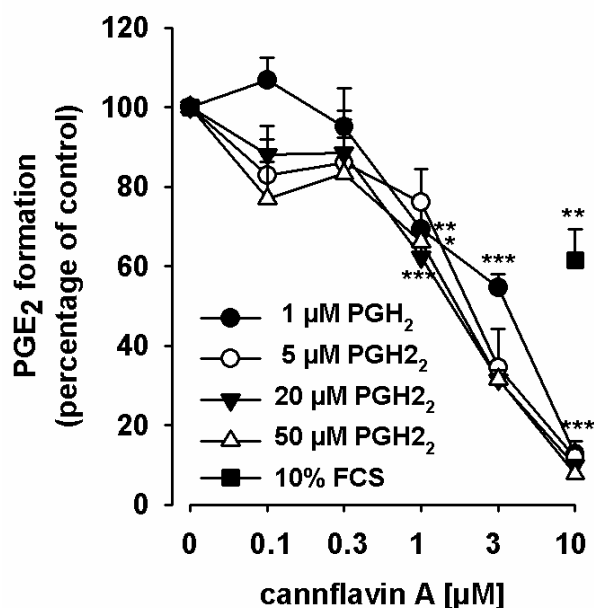
A   **B**
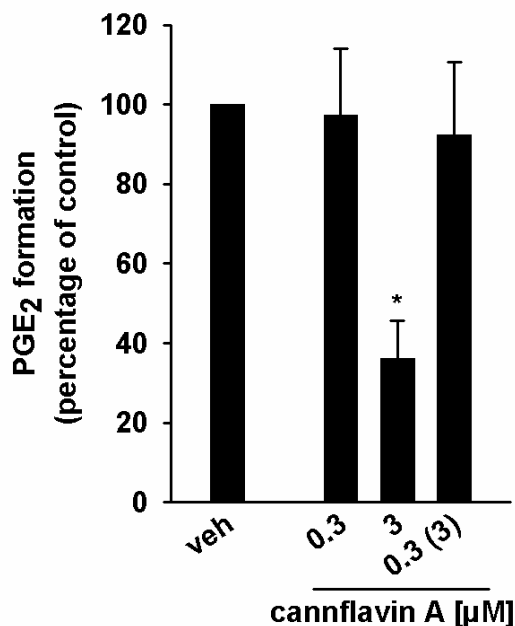
*Fig. 3.21: Effects of CFA (**19**) on mPGES-1 in cell-free assays.*

(A) Concentration-response analysis. Microsomal preparations of IL-1β-stimulated A549 cells were pre-incubated with CFA or vehicle (DMSO) for 15 min at 4 °C and PGE₂ formation was induced by addition of variable PGH₂ concentrations (1, 5, 20 and 50 μM). The amount of PGE₂ was quantified for 1 and 5 μM PGH₂ by the use of a PGE₂ High Sensitivity EIA Kit according to the manufacturer's protocol and PGE₂ formation of samples with or w/o 10% FCS stimulated with 20 and 50 μM PGH₂ was analyzed by RP-HPLC. Data are given as mean + S.E., n = 3, *p < 0.05, **p < 0.01 ***p < 0.001 vs. vehicle (DMSO) control, ANOVA + Tukey HSD post-hoc tests. (B) Reversibility of mPGES-1 inhibition. Microsomal preparations were pre-incubated for 15 min with 3 μM CFA or vehicle (DMSO), and an aliquot was diluted 10-fold to obtain an inhibitor concentration of 0.3 μM. Then, 20 μM PGH₂ was added and all samples were incubated for 1 min on ice, and PGE₂ formation was analyzed as described by RP-HPLC. Data are given as mean + S.E., n = 3, *p < 0.05 vs. vehicle (DMSO) control, ANOVA + Tukey HSD post-hoc tests.

For the biosynthesis of PGE_2 in the cell, AA must first be released by $cPLA_2$ which is further converted by COX-2 to PGH_2 that serves as substrate for mPGES-1 to form PGE_2. Interference in the PGE_2 biosynthesis at the level of AA supply can be excluded as CFA (**19**) barely inhibited the activity of human recombinant $cPLA_2$ at 10 µM (**Fig. 3.22**), whereas the $cPLA_2$ control inhibitor pyrrolidine-1 (1 µM) effectively blocked AA release from phospholipids as expected.
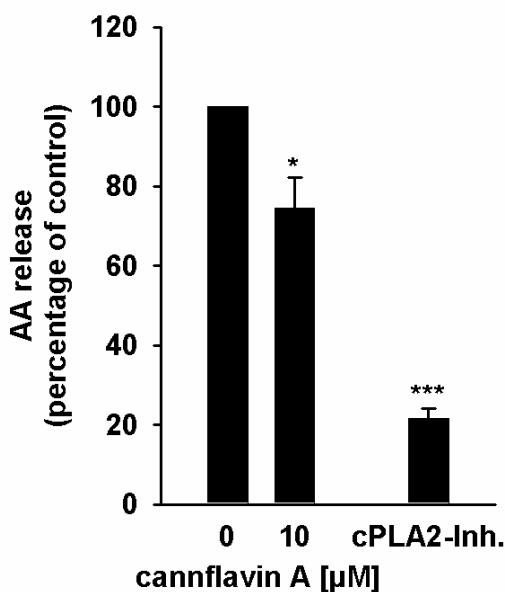
*Fig. 3.22: CFA (**19**) barely inhibits $cPLA_2$.*

Freshly prepared large unilamelar vesicles were incubated with $cPLA_2$ enzyme, 1 mM Ca^{2+} and the indicated compounds for 1 h at 37 °C. Reaction was stopped using methanol. Following derivatisation with p-anisidinium chloride, the resulting derivate was analyzed by RP-HPLC. Data are given as mean + S.E., n = 3, *p < 0.05, ***p < 0.001 vs. vehicle (DMSO) control, ANOVA + Tukey HSD post-hoc tests. Performed by Marius Melzer in the lab of Prof. Dr. O. Werz (University of Jena, Germany).

A potent suppressive effect of CFA (**19**) on PGE_2 biosynthesis in intact human rheumatoid synovial cells was already demonstrated [140] but no concrete point of attack could be identified. Potent suppression of PGE_2 biosynthesis could be confirmed in intact cells using LPS-stimulated human monocytes, where PGE_2 is essentially formed via the COX-2/mPGES-1 pathway (**Fig. 3.23A**) [100]. TXB_2 levels were completely blocked by CFA (**19**). Western blot experiments disclose that suppression of PGE_2 biosynthesis is also provoked by reduced levels of COX-2 (**Fig. 3.23B**), because CFA (**19**) blocked expression of COX-2 comparable to the control dexamethason.

A   **B**
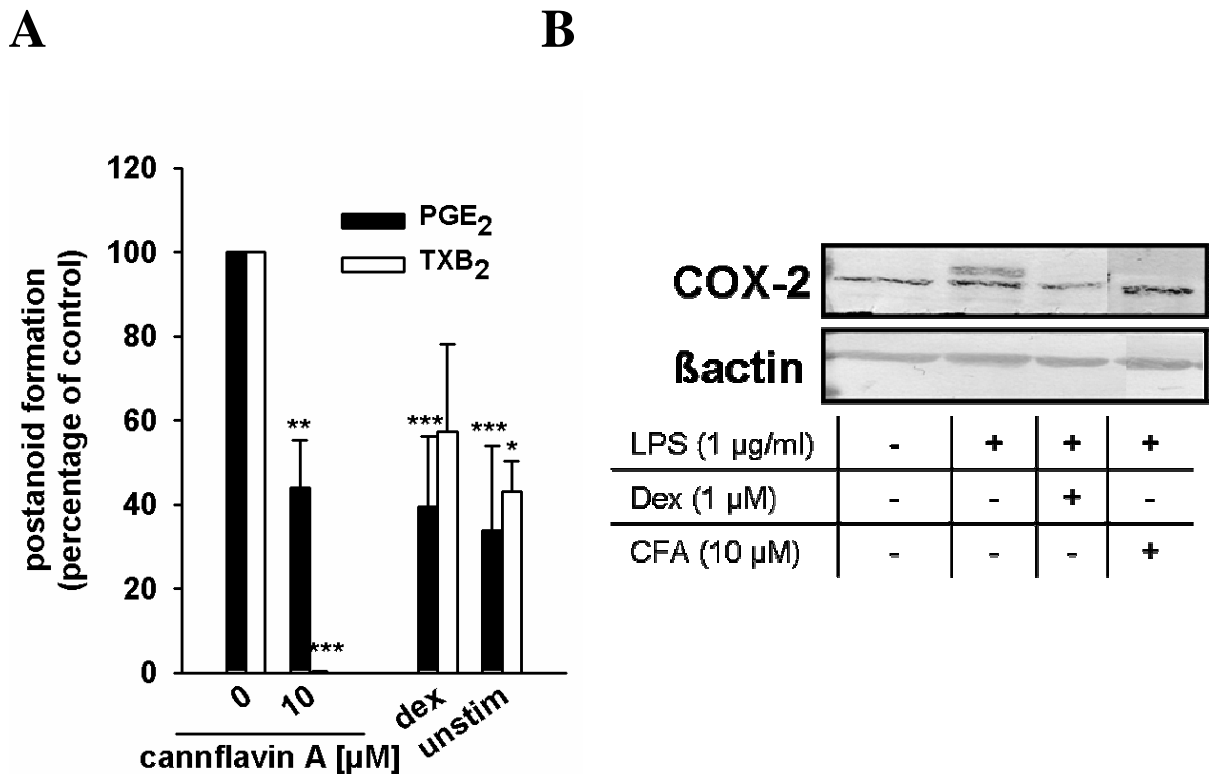
Fig. 3.23: Effects of CFA (**19**) (10 µM) on intact human monocytes stimulated with LPS. (A) PGE₂ and TXB₂ levels of LPS stimulated monocytes. Intact human monocytes (5 x 10⁶/exp. in RPMI 1640 medium containing 0.5% FCS, P/S and 2 mM glutamine) were stimulated with 1 µg/ml LPS and CFA (10 µM), dexamethasone (1 µM) or vehicle (DMSO) was added for 24 h at 37 °C. PGE₂ and TXB₂ levels were detected in the supernatant using a PGE₂ and TXB₂ High Sensitivity EIA Kit according to the manufacturer's protocol. Data are given as mean + S.E., n=2-4, *p < 0.05, **p < 0.01 ***p < 0.001 vs. vehicle (DMSO) control, ANOVA + Tukey HSD post-hoc tests. (B) COX-2 expression in LPS stimulated monocytes. Monocytes were stimulated as described above. After 24 h cells were detached and lysed (2 x SDS-b.). Samples were subjected to SDS-PAGE and WB using a specific antibody against COX-2. ßactin was used as loading control. Results are representative of 2-4 independent experiments.

Experiments in intact human platelets, which solely express COX-1, reveal a moderate inhibition of 12-HHT (IC₅₀ > 10 µM) and TXB₂ (IC₅₀= 6.8 µM) formation (**Fig. 3.24A**). The reference inhibitor indomethacin (10 µM) blocked the formation of 12-HHT and TXB₂ as expected (data not shown). 12-HHT (used as biomarker for COX activity) was hardly affected by CFA (**19**) with 30% inhibition at 10 µM (IC₅₀ > 10 µM). Because CFA (**19**)

blocked TXB_2 levels in intact human platelets as well as in human monocytes, platelet homogenates were stimulated with PGH_2 to form TXB_2 via the thromboxane A_2 synthase (TXAS). CFA (**19**) selectively blocked TXB_2 formation in intact platelets stimulated with AA (IC_{50}= 6.8 µM) and platelet homogenates stimulated with PGH_2 (IC_{50}= 2.3 µM), indicating TXAS as a direct target of CFA (**19**) (**Fig. 3.24A**). As 12-HHT in intact platelets was hardly affected, effects of CFA (**19**) on isolated COX enzymes were investigated, using ovine COX-1 and human recombinant COX-2. As shown in **Fig. 3.24B**, the activity of both enzymes is only moderately affected by CFA (**19**) comparable to the results in intact platelets with IC_{50} values > 10 µM, while the reference inhibitors indomethacin (10 µM) and celecoxib (5 µM) inhibited the enzyme activities efficiently (not shown).
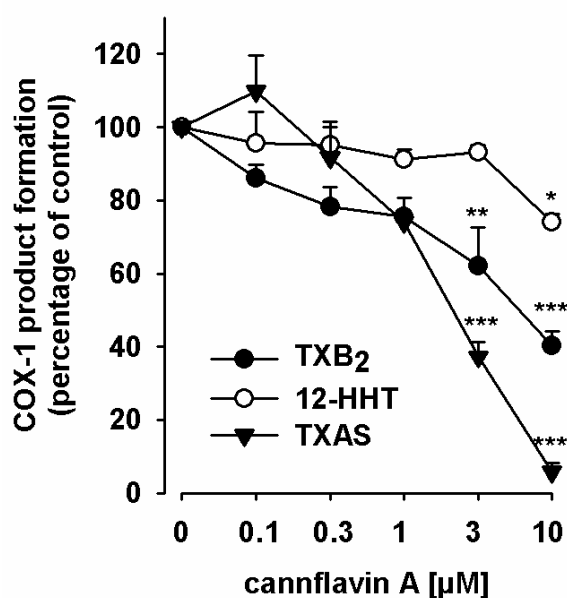
A   **B**
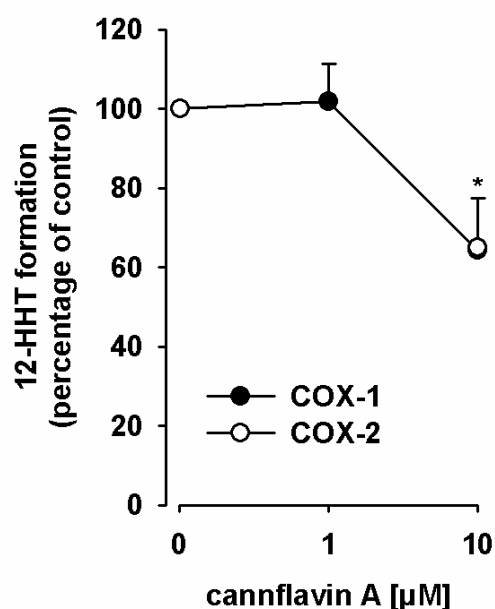
*Fig. 3.24: Effects of CFA (**19**) on human platelets and isolated COX-1 and -2*

(A) Effects in human platelets. Platelets (10^8/ml PBS containing 1 mM $CaCl_2$) were pre-incubated for 5 min prior to stimulation with AA (5 µM). After another 5 min at 37 °C, the formation of 12-HHT was determined by RP-HPLC as described and formation of TXB_2 was determined using a TXB_2 High Sensitivity EIA Kit according to the

manufacturer's protocol. TXAS activity was determined in platelet homogenates (10^8/ml PBS containing 1 mM $CaCl_2$, sonified 3 x 15 sec) pre-incubated for 15 min on ice and stimulated with 20 µM PGH_2 for 1 min. TXB_2 levels were detected in the supernatant using a TXB_2 High Sensitivity EIA Kit according to the manufacturer's protocol. Data are given as mean + S.E., n = 2-4, *p < 0.05, **p < 0.01 ***p < 0.001 vs. vehicle (DMSO) control, ANOVA + Tukey HSD post-hoc tests. (B) Isolated COX-1 and -2 inhibition. Purified ovine COX-1 (50 units) or human recombinant COX-2 (20 units) were pre-incubated 5 min prior stimulation with AA (5 µM or 2 µM, respectively). 12-HHT in the samples was analyzed using RP-HPLC. Data are given as mean + S.E., n = 2-3, *p < 0.05 vs. vehicle (DMSO) control, ANOVA + Tukey HSD post-hoc tests.

In studies using human whole blood CFA (**19**) failed to efficiently block the formation of the prostanoids 6-ketoPGF$_{1a}$ (the stable metabolite of PGI$_2$) and TXB$_2$. Indomethacin (50 µM), which was used as reference inhibitor of prostanoid biosynthesis blocked the formation of TXB$_2$ and 6-ketoPGF$_{1a}$ as expected (**Fig. 3.25**). Heparinized human whole blood was incubated with LPS (10 µg/ml) to induce COX-2/mPGES-1 expression and CFA (**19**), indomethacin (50 µM) or vehicle (DMSO) for 24h. After 24h reaction was stopped on ice and the formation of 6-ketoPGF$_{1a}$ was detected. For detection of TXB$_2$, as a source of the COX-1/TXAS pathway, citrated human whole blood was pre-incubated with CFA (**19**), indomethacin (50 µM) or vehicle (DMSO) for 15 min and reaction was initiated using thrombin 2 U/ml.
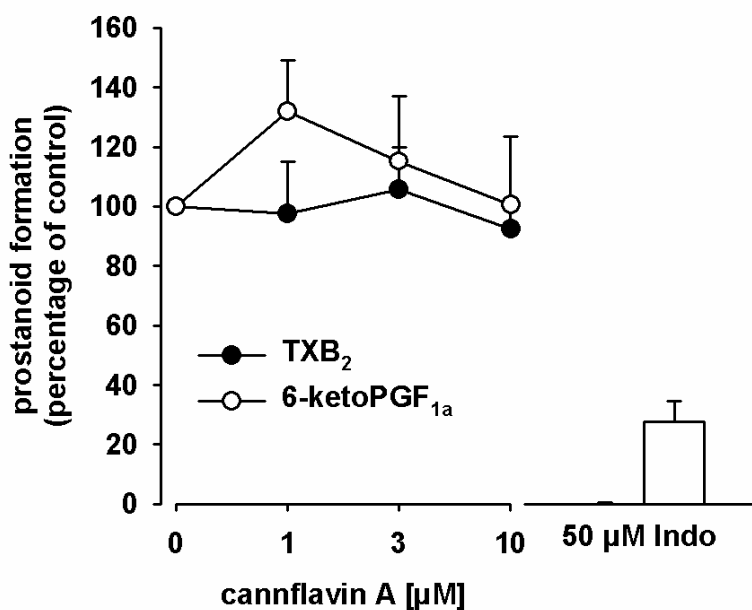
*Fig. 3.25: Effects of CFA (**19**) in whole blood experiments 6-ketoPGF$_{1a}$ detection in human whole blood. Heparinized human whole blood was incubated with LPS (10 µg/ml) and CFA, indomethacin (50 µM) or vehicle (DMSO) for 24 h at 37 °C. After 24 h the reaction was stopped on ice and the formation of 6-ketoPGF$_{1a}$ was detected in the supernatant using a 6-ketoPGF$_{1a}$ High Sensitivity EIA Kit according to the manufacturer's protocol. TXB$_2$ detection in human whole blood. Citrated human whole blood was pre-incubated with CFA, indomethacin (50 µM) or vehicle (DMSO) for 15 min at 37 °C and the reaction was initiated with thrombin 2 U/ml. After 10 min the reaction was stopped on ice and TXB$_2$ levels were detected in the supernatant using a TXB$_2$ High Sensitivity EIA Kit according to the manufacturer's protocol. Data are given as mean + S.E, n=3.*

Together, these findings propose mPGES-1 and TXAS as direct and potent molecular targets of CFA (**19**). 12-HHT formation in intact platelets and isolated COX enzymes was hardly affected (IC$_{50}$ > 10 µM). But plasma protein binding might impair effects in cell-based assay and human whole blood.

3.4.2.2   CFA (19) inhibits the 5-LO pathway

A concentration-response analysis of CFA (**19**) on 5-LO activity in cell-free assays is shown in **Fig. 3.26A**. CFA (**19**) was more efficient for semi-purified 5-LO (IC$_{50}$ = 0.9 µM) as compared to 5-LO inhibition in crude

neutrophil homogenates (IC_{50} = 5.4 µM) under the same experimental conditions, suggesting that cellular components present in the homogenates may hamper 5-LO inhibition. The 5-LO inhibitor BWA4C (0.3 µM) blocked 5-LO activity as expected (data not shown). Note, that inhibition of semi-purified 5-LO was only partially reversible, as demonstrated by wash-out experiments (**Fig. 3.26B**).
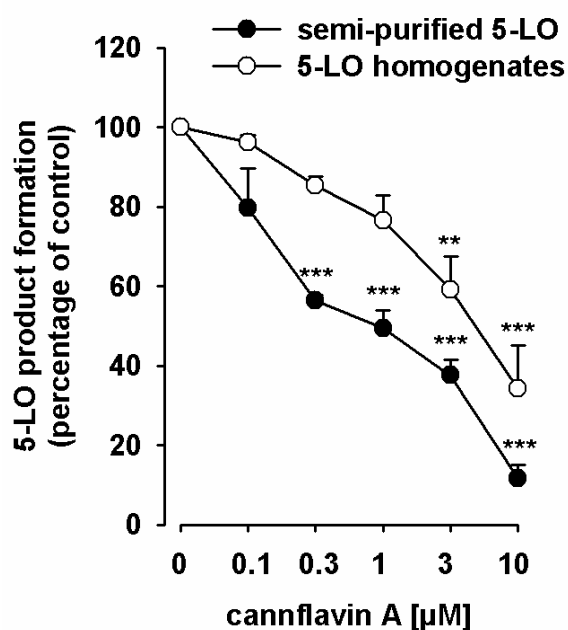
A   **B**
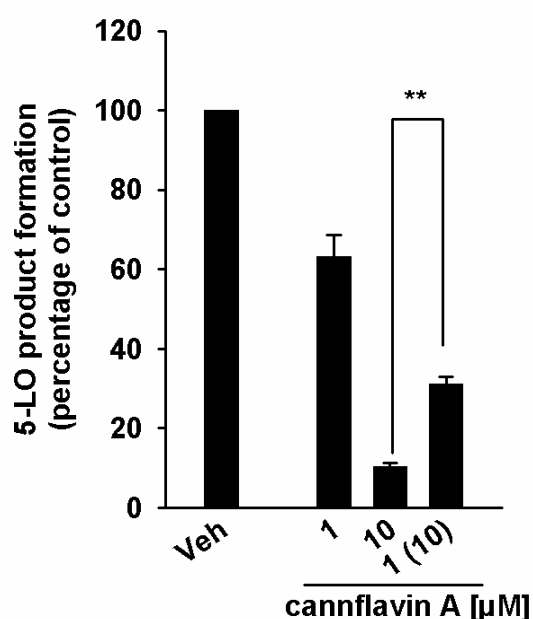
Fig. 3.26: effects of CFA (**19**) on isolated 5-LO

(A) Inhibition of isolated 5-LO. Semi purified, human recombinant 5-LO or neutrophil homogenates (5 x 10^6 cells/exp.) were pre-incubated with CFA, BWA4C (0.3 µM) or vehicle (DMSO) in the presence of 1 mM ATP for 10 min. 5-LO product formation was initiated by addition of 2 mM Ca^{2+} and 20 µM AA for 10 min at 37 °C. Reaction was stopped with methanol on ice and 5-LO products were analyzed by RP-HPLC. Data are given as mean + S.E., n = 2-3, **p < 0.01 and ***p < 0.001 vs. vehicle (DMSO) control, ANOVA + Tukey HSD post-hoc tests. (B) Reversibility of 5-LO inhibition. Semi purified, human recombinant 5-LO was pre-incubated in the presence of 2 mM Ca^{2+} and 1 mM ATP for 10 min and an aliquot was diluted 10-fold to obtain an inhibitor concentration of 1 µM. 5-LO product formation was initiated by addition of 20 µM AA for 10 min at 37 °C. Reaction was stopped with methanol on ice and 5-LO products

were analyzed by RP-HPLC. Data are given as mean + S.E., n =2, **p < 0.01; 10 µM
vs. diluted sample, ANOVA + Tukey HSD post-hoc tests.

The effects of CFA (**19**) on 5-LO inhibition in intact neutrophils stimulated
with A23187 was studied in the absence and presence of exogenous AA as
substrate for 5-LO product biosynthesis. CFA (**19**) suppressed 5-LO
product synthesis equally well, regardless of AA, with IC_{50} values of 1.6
µM (A23187 plus AA) and 2.4 µM (A23187) (**Fig. 3.27**). This implies that
(I) inhibition of 5-LO product synthesis is not related to block of substrate
supply, and (II) high AA concentrations do not impede interference of CFA
(**19**) with 5-LO. The reference inhibitor BWA4C suppressed 5-LO product
formation as expected (data not shown). CFA (**19**) failed to suppress 5-LO
product formation in intact PMNL stimulated with LPS/fMLP (**Fig. 3.27**).
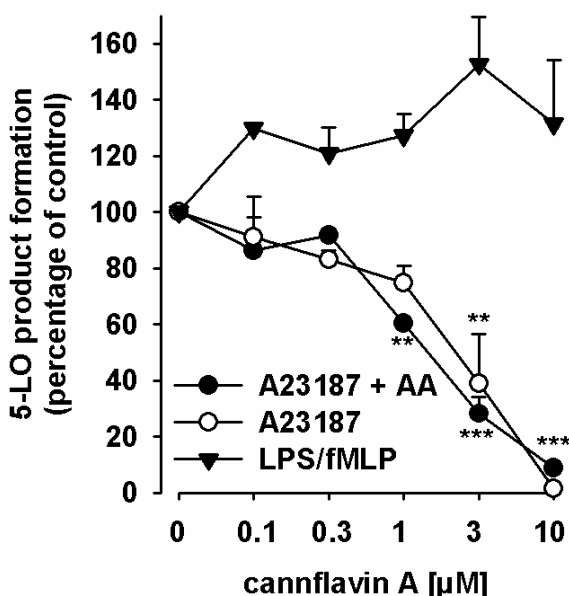
*Fig. 3.27: Effects of CFA (**19**) on 5-LO in intact PMNL.*

Isolated PMNL (5 x 10^6/ml) were pre-incubated with CFA or vehicle (DMSO) for 10 min at 37 °C and cells were stimulated with 2.5 µM A23187 or with 2.5 µM A23187 plus 20 µM AA. 5-LO products were determined by RP-HPLC. Alternatively, cells were primed LPS (1 µg/ml) for 30 min and formation of 5-LO products was initiated by addition of 1 µM fMLP. LTB_4 levels were detected using a TXB_2 High Sensitivity EIA Kit according to the manufacturer's protocol. Data are given as mean + S.E. n=3, **p < 0.01 and ***p < 0.001 vs. vehicle (DMSO) control, ANOVA + Tukey HSD post-hoc tests.

Studies of 5-LO inhibition in whole blood reveal that CFA (**19**) failed to
block 5-LO product formation, maybe due to plasma protein binding, i.e.

albumin, present in the whole blood samples (**Fig. 3.28**). Heparinized whole blood was therefore pre-incubated and stimulated with A23187 for 10 min. 5-LO product formation was detected in the supernatant.
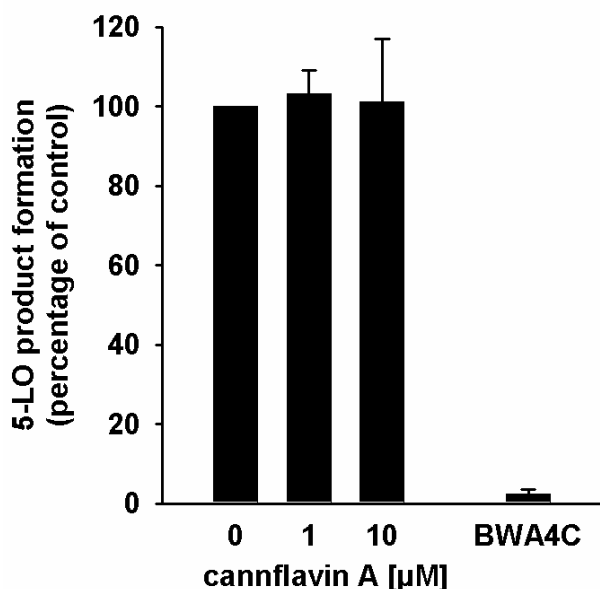
Fig. 3.28: Effects of CFA (19) on 5-LO inhibition in human whole blood.

Heparinized whole blood was pre-incubated with CFA or vehicle (DMSO) for 15 min at 37 °C and stimulated with A23187 (30 µM) for 10 min. Reaction was stopped on ice and 5-LO product formation was detected using RP-HPLC. Data are given as mean + S.E. n=2-3.

Mechanistic studies on 5-LO inhibition were performed to investigate the mechanism of action of CFA (**19**) on 5-LO. As 5-LO inhibitors often possess radical scavenger or antioxidant activities thereby uncoupling the redox cycle of the active site iron in 5-LO, CFA (**19**) was analyzed for its ability to reduce the stable DPPH radical. As shown in **Fig. 3.29A,** the antioxidants ascorbic acid and cysteine (used as positive controls) reduced the DPPH radical whereas CFA (**19**) failed in this respect, excluding radical scavenging features of CFA (**19**). Phosphorylation leads to strong upregulation of 5-LO and therefore CFA (**19**) was analyzed for its ability to interfere with ERK-1/2 and p38 MAPK phosphorylation. As can be seen in **Fig. 3.29B**, CFA (**19**) did not interfere with the ERK-1/2 or p38 MAPK signaling cascade, as it did not interrupt phosphorylation of ERK-1/2 and p38 MAPK. The reference inhibitor U0126 blocked phosphorylation of ERK-1/2 as expected.

A

B
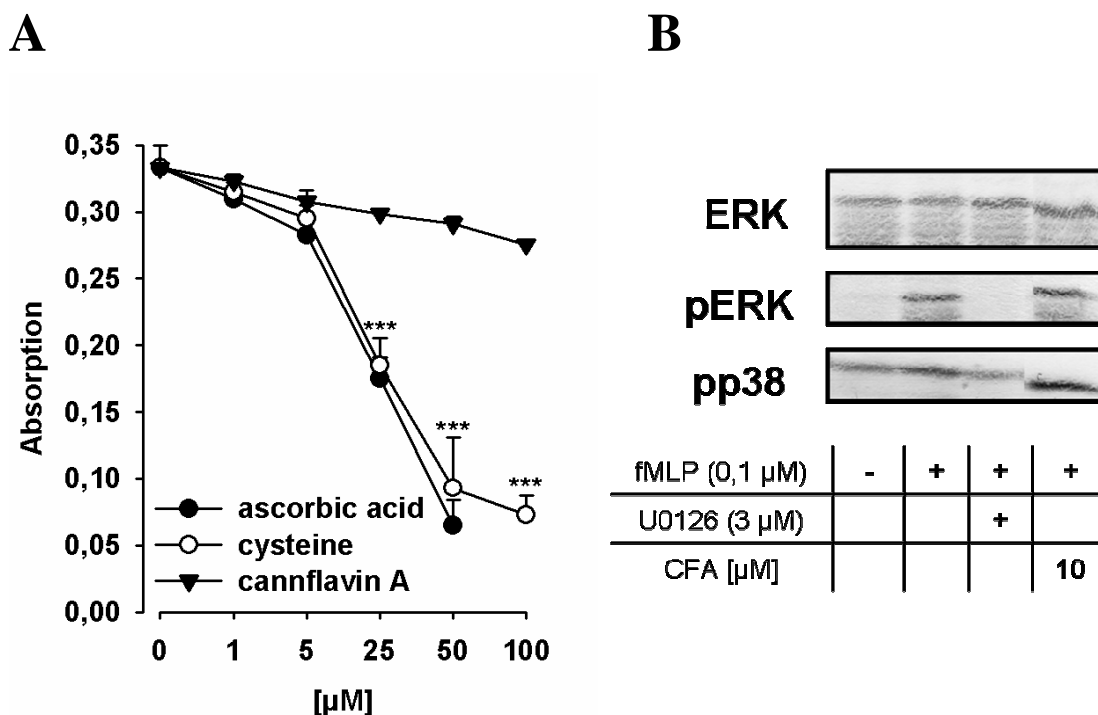
*Fig. 3.29: radical scavenger properties and effects on ERK or p38 MAPK pathway of CFA (**19**). (A) Radical scavenger capability. CFA, vehicle and controls were mixed with DPPH solution and incubated for 30 min in the dark. The absorbance was measured at 520 nm. Data are given as mean + S.E. n=3, ***p < 0.001 vs. vehicle, ANOVA + Tukey HSD post-hoc tests. (B) Neutrophils (10^7) were pre-warmed for 3 min at 37 °C and pre-incubated with CFA or vehicle (DMSO) at 37 °C for 15 min. The reaction was started by the addition of 0.1 µM fMLP, stopped after 1.5 min with SDS-b and heated for 6 min at 95 °C. Total cell lysates were analyzed for ERK1/2, phosphorylated ERK1/2 (Thr-202/Tyr-204) and phosphorylated p38 MAPK (Thr-180/Tyr-182) by SDS/PAGE and Western blotting. Results are representative of 2-3 independent experiments.*

Finally, it was assessed if CFA (**19**) may affect cell viability using human lung carcinoma A549 cells that were treated with 10 µM CFA (**19**) for 24 h and 48 h. Analysis by MTT assay revealed no cytotoxicity or detrimental effects on cell viability (**Fig. 3.30**) excluding unspecific influences in the cell-based assay. Similarly, neutrophils treated with 10 µM CFA (**19**) for 1 h still excluded the dye trypan blue, analyzed by light microscopy, implying cellular integrity (not shown).
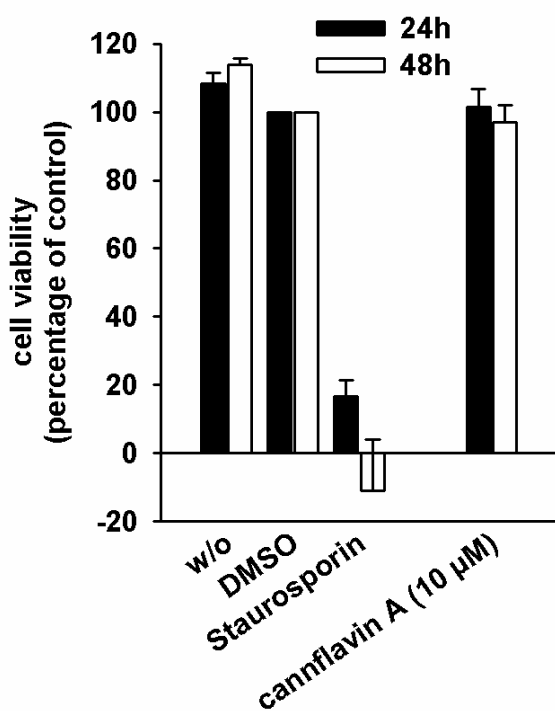
*Fig. 3.30: cytotoxic properties of CFA (**19**).*

Cells (3 x 10⁵) were incubated for 24 h and 48 h at 37 °C with CFA or vehicle (DMSO). After 24 h or 48 h, MTT was added and samples were incubated for 4 h at 37 °C. Reaction was stopped and the absorption was measured at 570 nm. Results are reported as percentage of viable cells as compared to vehicle control. Data are given as mean + S.E. n=3. Performed by Dr. Anja Schaible in the lab of Prof. Dr. O. Werz (University of Jena, Germany).

In summary, these findings indicate 5-LO as a direct target of CFA (**19**). The mechanism of action is apparently independent of redox actions, non competitive and only partially reversible. Inhibition of 5-LO in the cell-based assay was comparable to the effects observed under cell-free conditions. Studies in neutrophil homogenates and human whole blood indicate high protein binding of CFA (**19**), due to a reduced inhibitory potential.

3.4.3 Pharmacological profile of on eicosanoid biosynthesis pathway

3.4.3.1   Studies on the mode of action of perlatolic acid (30c) and physodic acid (29b) on mPGES-1

Perlatolic (**30c**) and physodic acid (**29b**) are potent inhibitors of mPGES-1 derived PGE_2 formation in microsomal preparations of IL-1ß stimulated A549 cells (IC_{50}= 0.4 and 0.43 µM, respectively). First it was investigated if alteration of the concentration of the substrate PGH_2 of mPGES-1 may change the potency of perlatolic (**30c**) and physodic acid (**29b**). As shown in **Fig. 3.31A**, inhibition of mPGES-1 derived PGE_2 formation by perlatolic acid (**30c**) and physodic acid (**29b**) at 1, 5, 20 and 50 µM PGH_2 led to similar concentration-response curves with largely consistent IC_{50} values in the range of 0.43 – 1.8 µM for perlatolic acid (**30c**) and 0.4 – 1.6 µM for physodic acid (**29b**). Addition of 10% FCS to the samples abolished the effect, suggesting a strong plasma protein-binding for both compounds. Washout experiments imply a reversible mode of action, as both compounds fail to efficiently block mPGES-1 derived PGE_2 formation after 10-fold dilution of the samples at 1 µM inhibitor (**Fig. 3.31B**). The reference inhibitor MK-886 (used as positive control) blocked mPGES-1 derived PGE_2 formation in all assays as expected (not shown).

A
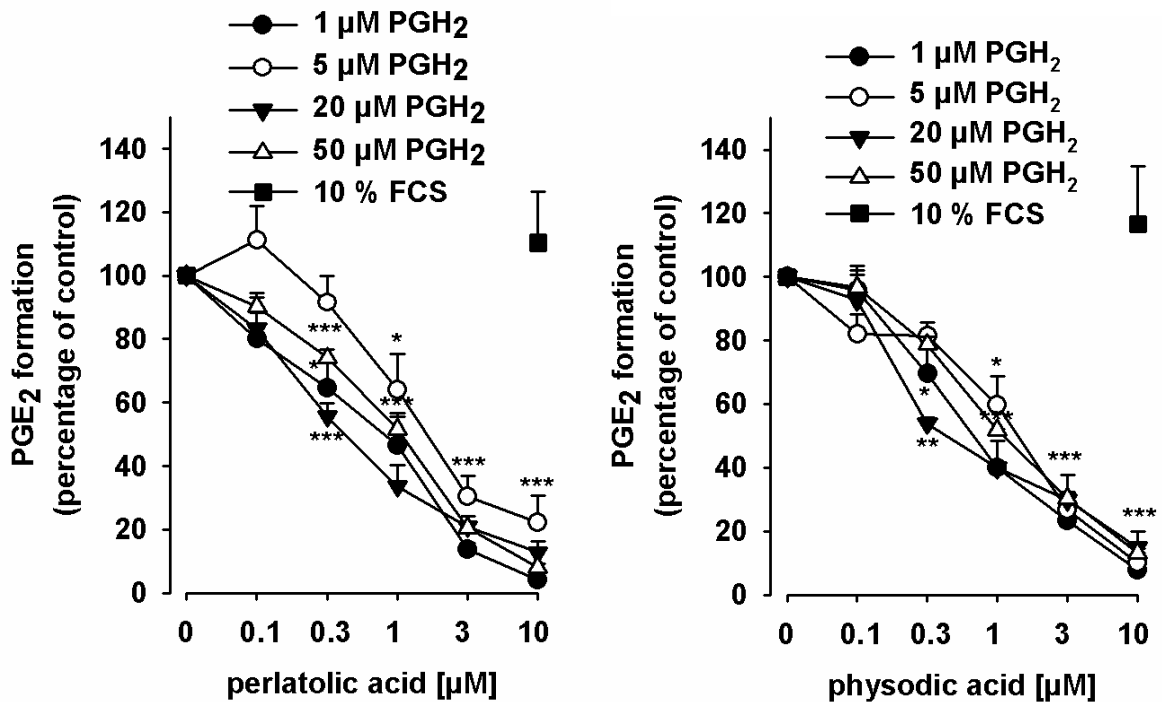
B
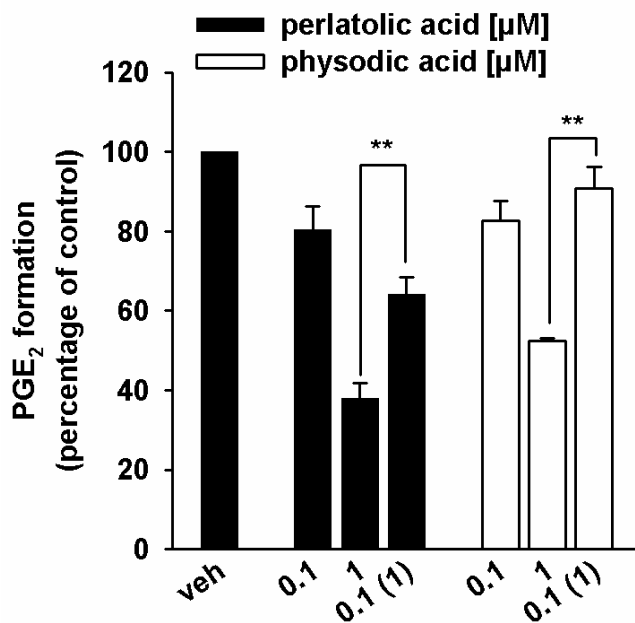
Fig. 3.31: Effects of perlatolic acid (**30c**) and physodic acid (**29b**) on mPGES-1.

(A) Concentration-response analysis. Microsomal preparations of IL-1β-stimulated A549 cells were pre-incubated for 15 min at 4 °C and PGE_2 formation was induced by addition of variable PGH_2 concentrations (1, 5, 20 and 50 µM). The amount of PGE_2 was quantified for 1 and 5 µM PGH_2 by the use of a PGE_2 High Sensitivity EIA Kit according to the manufacturer's protocol and PGE_2 formation of samples with or w/o 10% FCS stimulated with 20 and 50 µM PGH_2 was analyzed by RP-HPLC. Data are given as mean + S.E., n=2-3, *$p < 0.05$, **$p < 0.01$ ***$p < 0.001$ vs. vehicle (DMSO) control, ANOVA + Tukey HSD post-hoc tests (B) Reversibility of mPGES-1 inhibition.

Microsomal preparations were pre-incubated for 15 min with 1 µM perlatolic acid, physodic acid or vehicle (DMSO), and an aliquot was diluted 10-fold to obtain an inhibitor concentration of 0.1 µM. Then, 20 µM PGH_2 was added and all samples were incubated for 1 min on ice, and PGE_2 formation was analyzed as described by RP-HPLC. Data are given as mean + S.E., n=2-3, **p < 0.01 1 µM vs. diluted sample, ANOVA + Tukey HSD post-hoc tests.

3.4.3.2   Perlatolic acid (30c) and physodic acid (29b) affect prostanoid biosynthesis

To exclude interference of perlatolic acid (**30c**) or physodic acid (**29b**) at the level of AA supply, the effects on the enzymatic activity of human recombinant $cPLA_2$ were studied. The $cPLA_2$ control inhibitor pyrrolidine-1 (1 µM) effectively blocked AA release from phospholipids in a cell-free assay, whereas perlatolic (**30c**) and physodic acid (**29b**) did not influence AA release up to 10 µM (**Fig. 3.32**).
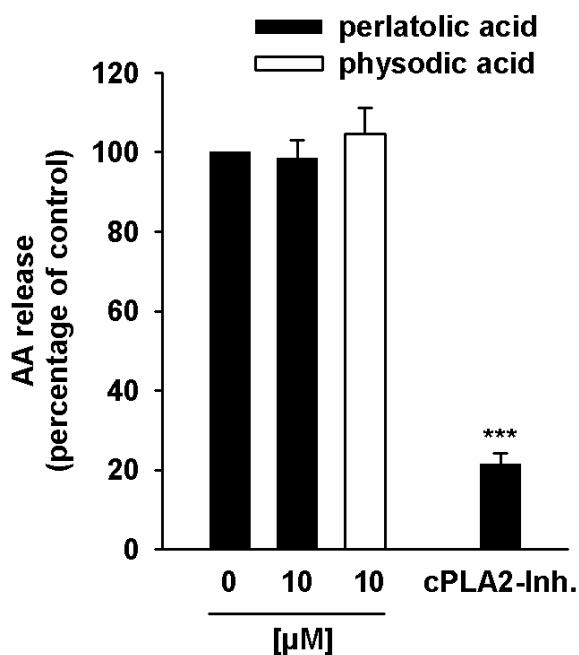
*Fig. 3.32: effects of perlatolic acid (**30c**) and physodic acid (**29b**) on $cPLA_2$ activity.*

Freshly prepared large unilamelar vesicles were incubated with $cPLA_2$ enzyme, 1 mM Ca^{2+} and the indicated compounds for 1 h at 37 °C. Reaction was stopped using methanol. Following derivatisation with p-anisidinium chloride, the resulting derivate was analyzed by RP-HPLC. Data are given as mean + S.E., n=3, ***p < 0.001 vs. vehicle (DMSO) control, ANOVA + Tukey HSD post-hoc tests. Performed by Marius Melzer in the lab of Prof. Dr. O. Werz (University of Jena, Germany).

Studies on the activity of isolated COX enzymes revealed that perlatolic acid (**30c**) only marginally inhibited isolated ovine COX-1 ($IC_{50} > 10$ µM) and did not affect COX-2 activity. In contrast, physodic acid (**29b**) did not interfere with the COX-1 or COX-2 derived 12-HHT formation up to 10 µM (**Fig. 3.33**). Indomethacin (10 µM) and the selective COX-2 inhibitor celecoxib (5 µM) clearly blocked the activities of COX-1 and -2 as expected (data not shown).
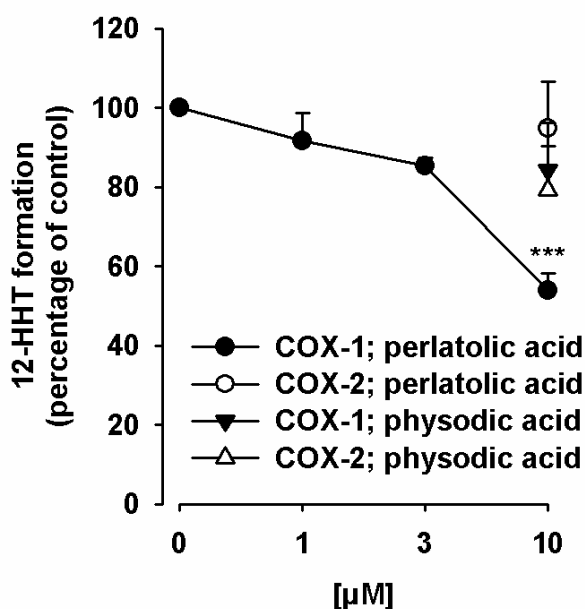
*Fig. 3.33: effects of perlatolic acid (**30c**) and physodic acid (**29b**) on isolated COX enzymes.*
Purified ovine COX-1 (50 units) or human recombinant COX-2 (20 units) were pre-incubated 5 min prior stimulation with AA (5 µM or 2 µM, respectively). 12-HHT in the samples was analyzed using RP-HPLC. Data are given as mean + S.E., n = 3, ***p < 0.001 vs. vehicle (DMSO) control, ANOVA + Tukey HSD post-hoc tests.

Next, the cell-based effects of perlatolic (**30c**) and physodic acid (**29b**) on the prostanoid synthesis were investigated. In line with previous findings by Bruno et al. [100], exposure of primary human monocytes to LPS for 24 h caused elevated expression of COX-2 and mPGES-1, accompanied by a three-fold increased release of PGE_2 but also by a two-fold increased release of TXB_2 (**Fig. 3.34**). Perlatolic acid (**30c**) (10 µM) completely blocked expression of COX-2, repressed PGE_2 biosynthesis to a minor extent and strongly blocked the formation of TXB_2. In contrast, physodic

acid (**29b**) showed only slight effects on COX-2 expression and unexpectedly rather increased PGE$_2$ formation but abolished TXB$_2$ release.
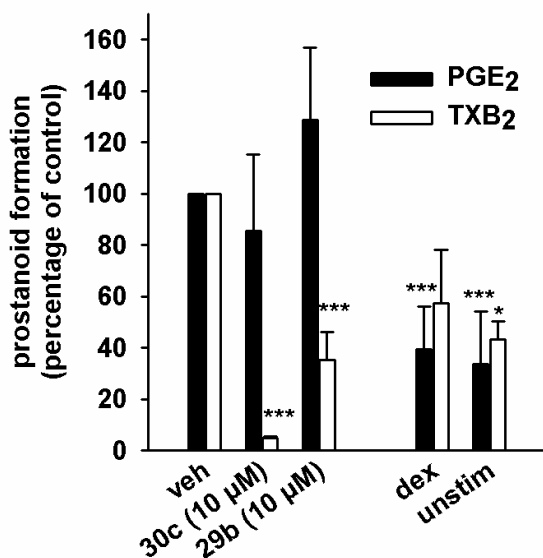
A   **B**
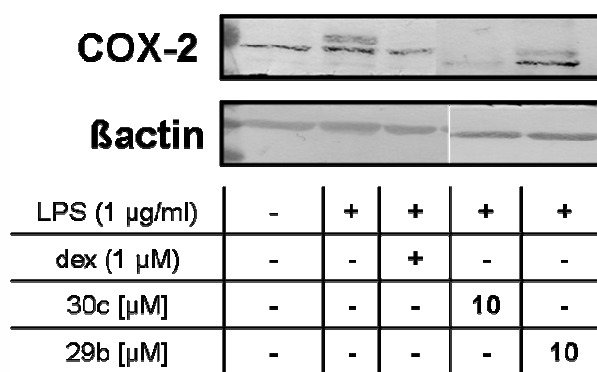
*Fig. 3.34: Effects of perlatolic (**30c**) and physodic acid (**29b**) on intact human monocytes stimulated with LPS.*

*(A) PGE$_2$ and TXB$_2$ levels of LPS stimulated monocytes. Intact human monocytes (5 x 10^6/exp. in RPMI 1640 medium containing 0.5% FCS, P/S and 2 mM glutamine) were stimulated with 1 µg/ml LPS and perlatolic acid and physodic acid (10 µM), dexathemason (dex 1 µM) or vehicle (DMSO) was added for 24 h at 37 °C. PGE$_2$ and TXB$_2$ levels were detected in the supernatant using a PGE$_2$ and TXB$_2$ High Sensitivity EIA Kit according to the manufacturer's protocol. Data are given as mean + S.E., n = 2-4, *p < 0.05 ***p < 0.001 vs. vehicle (DMSO) control, ANOVA + Tukey HSD post-hoc tests. (B) COX-2 expression in LPS stimulated monocytes. Monocytes were stimulated as described above. After 24 h cells were detached and lysed (2 x SDS-b.). Samples were subjected to SDS-PAGE and WB using a specific antibody against COX-2. ßactin was used as loading control. Results are representative of 2-4 independent experiments.*

Perlatolic acid (**30c**) and physodic acid (**29b**) did not or hardly inhibit COX-1/ -2 activity, but instead strongly blocked TXB$_2$ in intact human

monocytes. Therefore, perlatolic (**30c**) and physodic acid (**29b**) were analyzed in human washed platelets, stimulated with exogenous AA, as a source of 12-HHT and TXB_2 formed via the COX-1/TXAS pathway. Perlatolic acid (**30c**) potently inhibited the formation of 12-HHT and TXB_2 with IC_{50} values of 0.6 and 0.5 µM, respectively. Also physodic acid (**29b**) caused inhibition of 12-HHT and TXB_2 biosynthesis even though with lower potency (IC_{50}= 8.8 and 5.2 µM, respectively) as compared to perlatolic acid (**30c**) and the reference inhibitor indomethacin (20 µM) (**Fig. 3.35A**). To investigate whether perlatolic (**30c**) and physodic acid (**29b**) may act on TXAS, platelet homogenates were stimulated with 20 µM PGH_2 and substantial amounts of TXB_2 were detected in the supernatant. As reference inhibitor the selective TXAS inhibitor CV4151 (1 µM) was used, that blocked TXB_2 formation as expected. Pre-incubation of the platelet homogenates with perlatolic (**30c**) or physodic acid (**29b**) concentration-dependently blocked TXB_2 synthesis with IC_{50} values of 1.1 and 0.7 µM, respectively **Fig. 3.35B**.

A
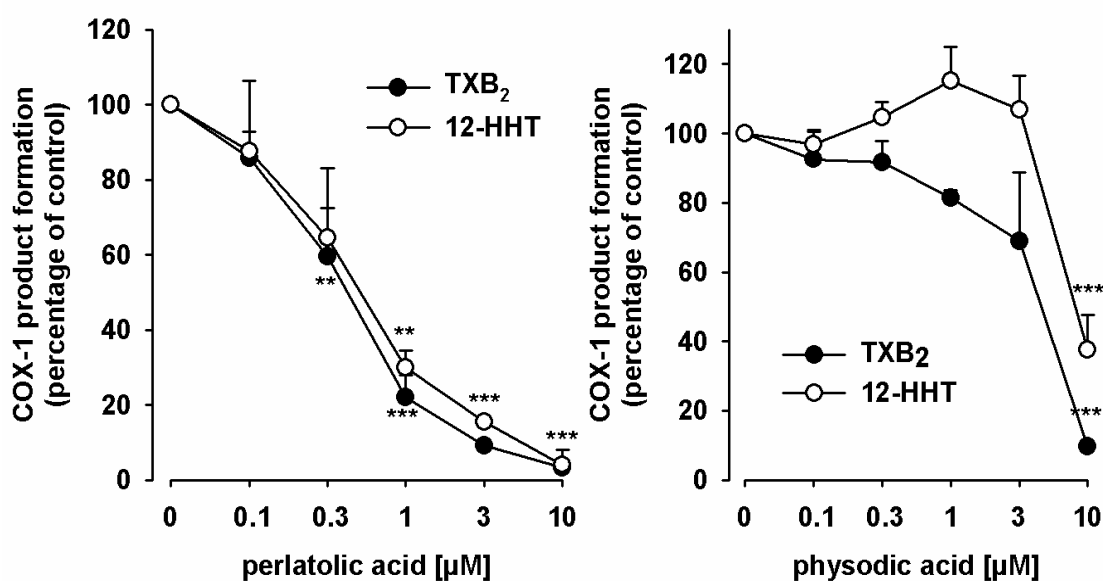
B
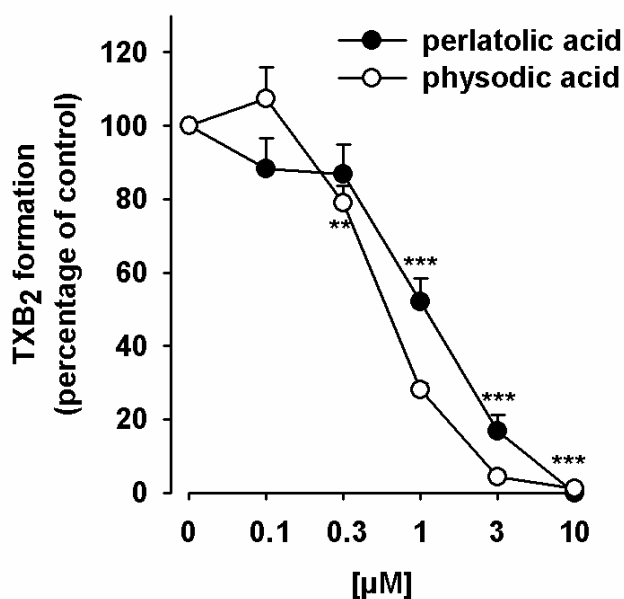
Fig. 3.35: Effects of perlatolic acid (**30c**) and physodic acid (**29b**) on human platelets and the activity of TXAS in a cell-free assay.

(A) TXB_2 and 12-HHT formation in human platelets. Platelets (10^8/ml PBS containing 1 mM $CaCl_2$) were pre-incubated for 5 min prior to stimulation with arachidonic acid (5 µM). After another 5 min at 37 °C, the formation of 12-HHT was determined by RP-HPLC as described and formation of TXB_2 was determined using a TXB_2 High Sensitivity EIA Kit according to the manufacturer's protocol. Data are given as mean + S.E., n=3-4, **p < 0.01, ***p < 0.001 vs. vehicle (DMSO) control, ANOVA + Tukey HSD post-hoc tests. (B) TXAS activity was determined in platelet homogenates (10^8/ml PBS containing 1 mM $CaCl_2$, sonified 3 x 15 sec) pre-incubated for 15 min on ice and stimulated with 20 µM PGH_2 for 1 min. TXB_2 levels were detected in the supernatant using a TXB_2 High Sensitivity EIA Kit according to the manufacturer's protocol. Data are given as mean + S.E., n =3-4, **p < 0.01, ***p < 0.001 vs. vehicle (DMSO) control, ANOVA + Tukey HSD post-hoc tests.

Studies on prostanoid formation in human whole blood were performed in citrated and heparinized whole blood. For investigation of 6-ketoPGF$_{1a}$ biosynthesis, heparinized human whole blood was incubated with LPS (10 µg/ml) to induce COX-2/mPGES-1 and perlatolic (**30c**) or physodic acid (**29b**) for 24 h at 37 °C and subsequent 6-ktoPGF$_{1a}$ level were detected as marker of COX-2. For detection of TXB_2, as a source of the COX-1/TXAS pathway, citrated human whole blood was pre-incubated with perlatolic acid (**30c**), physodic acid (**29b**) or vehicle (DMSO) for 15 min and

stimulated with thrombin (**Fig. 3.36**). The standard inhibitor indomethacin (50 µM) blocked prostanoid formation as expected (data not shown). Both failed to inhibit prostanoid formation in human whole blood, indicating a strong plasma protein binding.
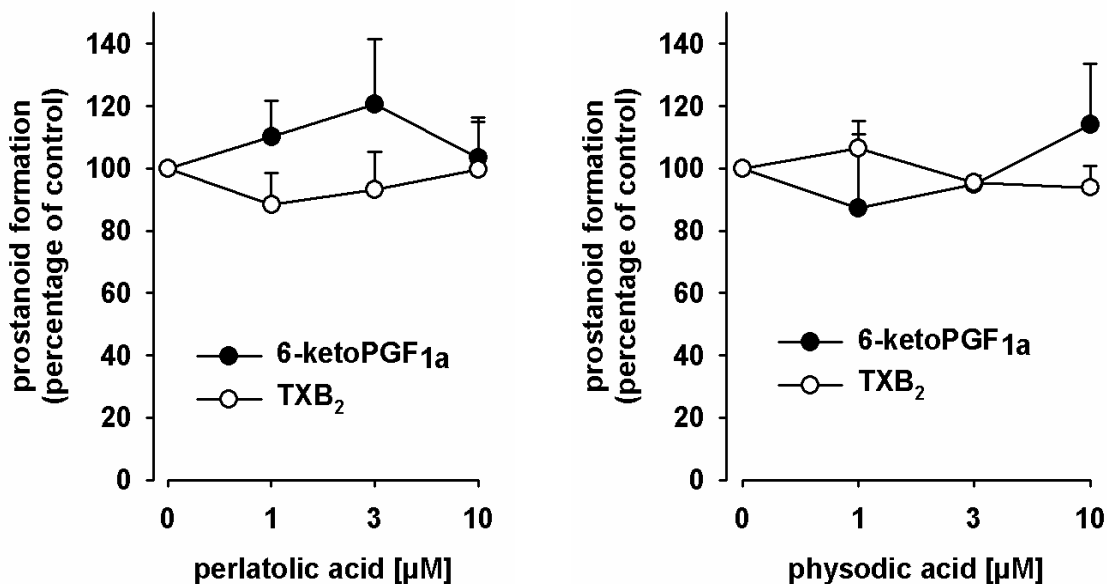
*Fig. 3.36: Effects of perlatolic acid (**30c**) and physodic acid (**29b**) in whole blood experiments.*

6-ketoPGF$_{1a}$ detection in human whole blood. Heparinized human whole blood was incubated with LPS (10 µg/ml) and perlatolic acid, physodic acid or vehicle (DMSO) for 24 h at 37 °C. After 24 h the reaction was stopped on ice and the formation of 6-ketoPGF$_{1a}$ was detected in the supernatant using a 6-ketoPGF$_{1a}$ High Sensitivity EIA Kit according to the manufacturer's protocol. TXB$_2$ detection in human whole blood. Citrated human whole blood was pre-incubated with perlatolic acid, physodic acid, indomethacin (50 µM) or vehicle (DMSO) for 15 min at 37 °C and the reaction was initiated with thrombin 2 U/ml. After 10 min the reaction was stopped on ice and TXB$_2$ levels were detected in the supernatant using a TXB$_2$ High Sensitivity EIA Kit according to the manufacturer's protocol. Data are given as mean + S.E. n=3.

Cytotoxic effects of perlatolic acid (**30c**) or physodic acid (**29b**) up to 30 µM can be excluded as no reduced viability of A549 cells occurred in the MTT assay during 24 h or 48 h, implying that no unspecific cytotoxic effects affected the modulation of prostanoid formation in cell-based assays

(**Fig. 3.37**). The control inhibitor staurosporin decreased cell viability as expected.
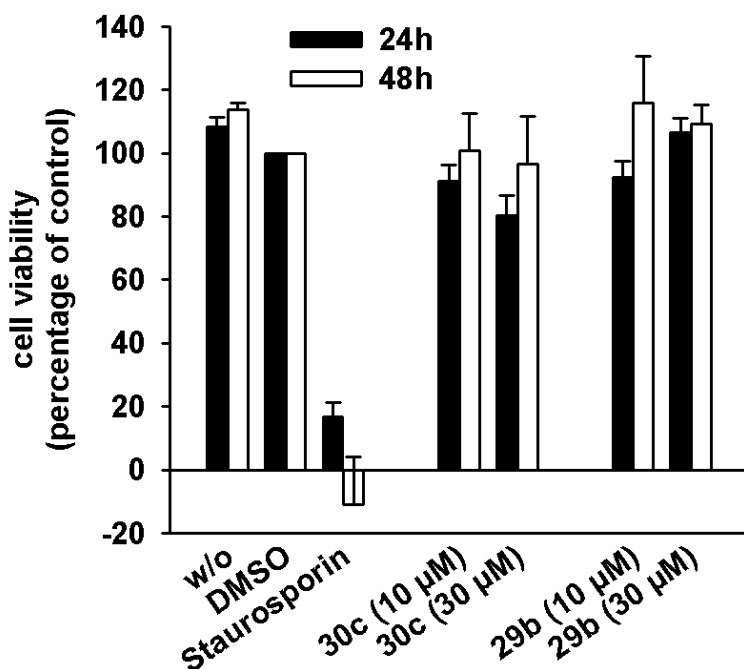
*Fig. 3.37: cytotoxic properties of perlatolic acid (**30c**) and physodic acid (**29b**). A549 cells (3 x 10^5) were incubated for 24 h and 48 h at 37 °C with perlatolic (30c), physodic acid (29b) or vehicle (DMSO). After 24 h or 48 h, MTT was added and samples were incubated for 4 h at 37 °C. Reaction was stopped and the absorption was measured at 570 nm. Results are reported as percentage of viable cells as compared to vehicle control. Data are given as mean + S.E. n=3.*

Taken together, mPGES-1 and TXAS could be identified as direct molecular targets of perlatolic acid (**30c**) and physodic acid (**29b**). Interference of physodic acid (**29b**) on upstream enzymes can be excluded as physodic acid (**29b**) failed to inhibit the activity of $cPLA_2$ and isolated COX-1 and -2. However, perlatolic acid (**30c**) moderately inhibited COX-1 derived 12-HHT formation and did not interfere with COX-2 and $cPLA_2$ activity. Efficiency was also evident *in vitro* in human platelets and monocytes. Inhibition of COX-2 expression was observed for perlatolic (**30c**) and physodic acid (**29b**) which might contribute to the inhibitory potential on pathophysiological PGE_2 synthesis. *In vivo* studies in human whole blood could however not confirm the results observed in cell-free and cell-based test systems.

3.4.3.3   Perlatolic acid (30c) and physodic acid (29b) interfere with the 5-LO pathway

Perlatolic acid (**30c**) and physodic acid (**29b**) inhibit the activity of isolated 5-LO in a concentration-dependent manner with IC_{50} values of 0.4 and 2.4 µM, respectively (**Fig. 3.38A**). Perlatolic acid (**30c**) lost its potency ($IC_{50} >$ 10 µM) when a cell-free 5-LO activity assay based on PMNL homogenates as 5-LO source was used while physodic acid (**29b**) showed only a marginal reduced potency in homogenates ($IC_{50} = 5.5$ µM) compared to isolated 5-LO, suggesting that cellular components present in the homogenates may hamper 5-LO inhibition by perlatolic acid (**30c**). BWA4C, used as reference 5-LO inhibitor, blocked the activity of 5-LO analogue in both test systems with same efficiency (data not shown). Washout experiments indicate a reversible inhibition of isolated 5-LO by perlatolic acid (**30c**) and physodic acid (**29b**) (**Fig. 3.38B**).

A
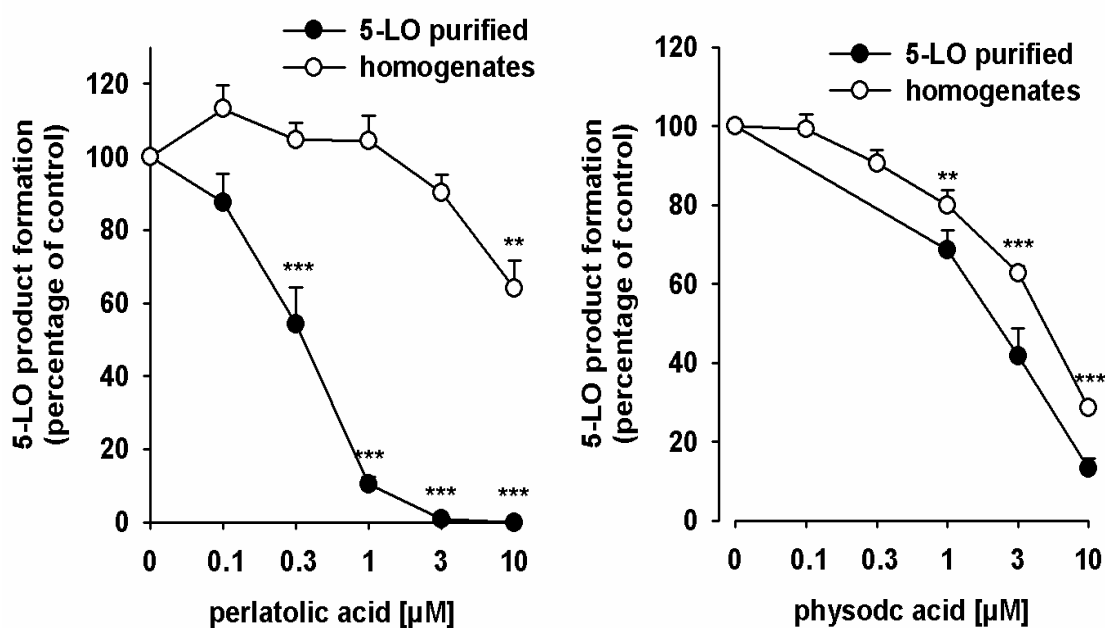
B
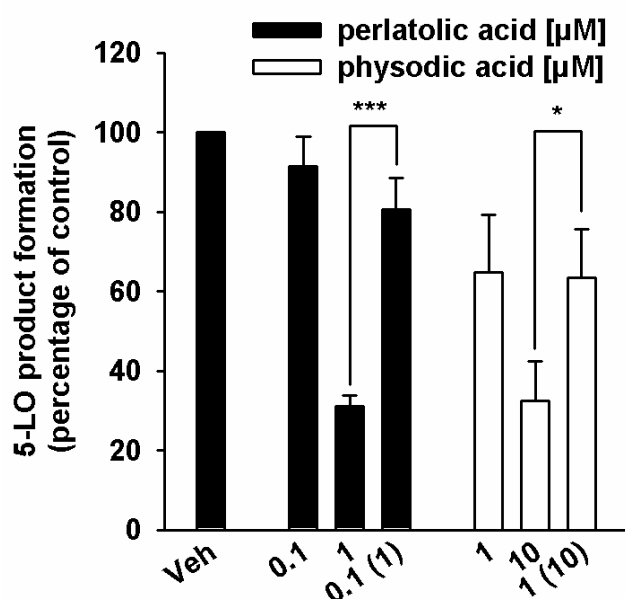
Fig. 3.38: effects of perlatolic acid (30c) and physodic acid (29b) on isolated 5-LO

(A) Inhibition of isolated 5-LO. Semi purified, human recombinant 5-LO or PMNL homogenates (5 x 10^6 cells/exp.) were pre-incubated with perlatolic acid, physodic acid, BWA4C (0.3 μM) or vehicle (DMSO) in the presence of 1 mM ATP for 10 min. 5-LO product formation was initiated by addition of 2 mM Ca^{2+} and 20 μM AA for 10 min at 37 °C. Reaction was stopped with methanol on ice and 5-LO products were analyzed by RP-HPLC. Data are given as mean + S.E., n = 2-3, **p < 0.01 and ***p < 0.001 vs. vehicle (DMSO) control, ANOVA + Tukey HSD post-hoc tests. (B) Reversibility of 5-LO inhibition. Semi purified, human recombinant 5-LO was pre-incubated in the presence of 1 mM ATP for 10 min and an aliquot was diluted 10-fold to obtain an inhibitor concentration of 1 or 10 μM. 5-LO product formation was initiated by addition of 2 mM Ca^{2+} and 20 μM AA for 10 min at 37 °C. Reaction was stopped with methanol on ice and 5-LO products were analyzed by RP-HPLC. Data are given as mean + S.E., n = 3-4, *p < 0.05 and ***p < 0.001; 1 or 10 μM vs. diluted sample, ANOVA + Tukey HSD post-hoc tests.

Due to the fact that several 5-LO inhibitors interrupt the catalytic redox cycle of 5-LO by reducing the active-site iron, antioxidant properties of perlatolic (**30c**) and physodic acid (**29b**) were analyzed. Radical scavenging activities of perlatolic (**30c**) and physodic acid (**29b**) were not evident, as both failed to reduce the stable DPPH radical up to 100 μM. the reference inhibitors ascorbic acid and cysteine reduced DPPH as expected **(Fig. 3.39)**.
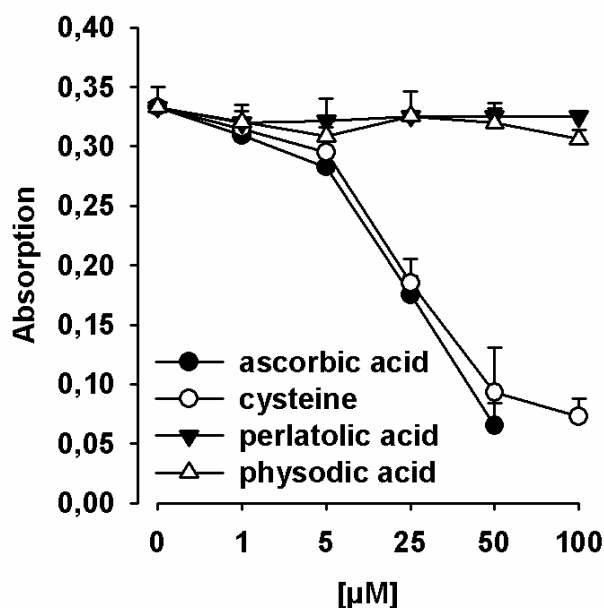
Fig. 3.39: radical scavenger properties of perlatolic acid (30c) and physodic acid (29b).
Perlatolic acid, physodic acid, vehicle and controls were mixed with DPPH solution and incubated for 30 min in the dark. The absorbance was measured at 520 nm. Data are given as mean + S.E. n=3.

Next, investigation on 5-LO inhibition in intact human neutrophils stimulated with A23187 in the presence and absence of exogenous AA were performed. Perlatolic acid (**30c**) blocked 5-LO product formation with $IC_{50} = 1.8$ µM (regardless of the presence of AA), and physodic acid (**29b**) inhibited 5-LO activity with IC_{50} values of 5.0 and 6.4 µM (without or with AA, respectively). Physodic acid (**29b**) was about 5-fold more potent in suppressing 5-LO product synthesis, when PMNL were primed with 1 µg/ml LPS and stimulated with 1 µM fMLP ($IC_{50} = 1.3$ µM). The potency of perlatolic acid (**30c**) was not improved in PMNL activated by LPS/fMLP ($IC_{50} = 8$ µM) (**Fig. 3.40A**). These stimuli-dependent inhibitory effects of physodic acid suggest that physodic acid (**29b**) might interfere with the 5-LO regulatory processes in the cell. Analysis on fMLP-induced ERK-1/2 activation in PMNL showed an increased phosphorylation of ERK-1/2 that was concentration-dependently repressed by physodic acid (**29b**), whereas perlatolic acid (**30c**) did not affect phosphorylation of ERK-1/2 or p38 MAPK (**Fig. 3.40B**).

A

B

fMLP (0,1 µM)	-	+	+	+	+	+	+
U0126 (3 µM)	-	-	+	-	-	-	-
30c [µM]	-	-	-	10	-	-	-
29b [µM]	-	-	-	-	1	3	10
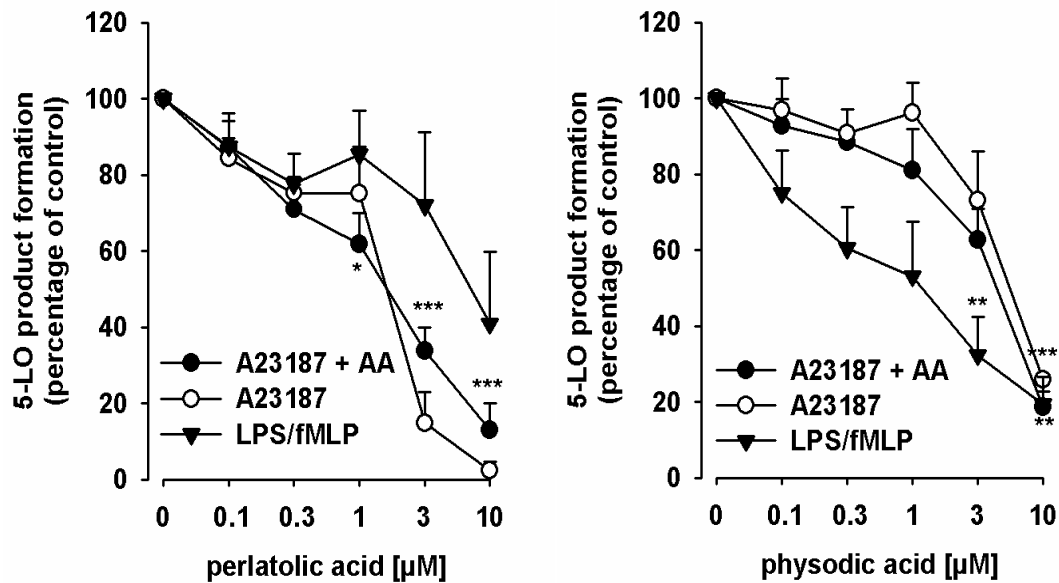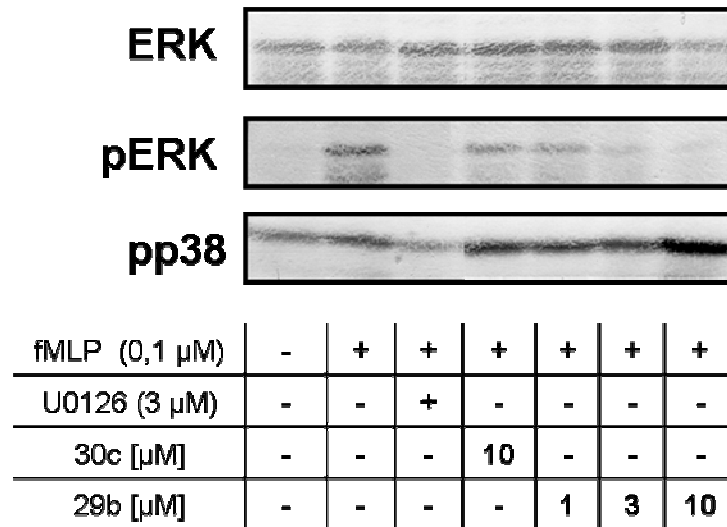
Fig. 3.40: Effects of perlatolic acid (30c) and physodic acid (29b) on 5-LO in intact PMNL.

(A) Isolated PMNL (5 x 10^6/ml) were pre-incubated with perlatolic acid, physodic acid or vehicle (DMSO) for 10 min at 37 °C and stimulated with 2.5 µM A23187 or 2.5 µM A23187 plus 20 µM AA. 5-LO products were determined by RP-HPLC. Alternatively, cells were primed with LPS (1 µg/ml) for 30 min and formation of 5-LO products was initiated by addition of 1 µM fMLP. LTB$_4$ levels were detected using a LTB4 High Sensitivity EIA Kit according to the manufacturer's protocol. Data are given as mean + S.E. n=3-5, *p < 0.05, **p < 0.01 and ***p < 0.001 vs. vehicle (DMSO) control,

*ANOVA + Tukey HSD post-hoc tests (B) Neutrophils (10^7) were pre-warmed for 3 min at 37 °C and pre-incubated with perlatolic acid (**30c**), phsysodic acid (**29b**) or vehicle (DMSO) at 37 °C for 15 min. The reaction was started by the addition of 0.1 µM fMLP, stopped after 1.5 min with SDS-b and heated for 6 min at 95 °C. Total cell lysates were analyzed for ERK1/2, phosphorylated ERK1/2 (Thr-202/Tyr-204), phosphorylated p38 MAPK (Thr-180/Tyr-182), by SDS/PAGE and western blotting. Results are representative of 2-3 independent experiments.*

Whole blood experiments reveal that perlatolic (**30c**) and physodic acid (**29b**) completely loose their 5-LO inhibitory potential (**Fig. 3.41**). This fact may be explained by plasma protein binding as already observed in mPGES-1 experiments when 10% FCS is present in the samples. For determination of 5-LO product formation in whole blood, perlatolic (**30c**) and physodic acid (**29b**) were pre-incubated and heparinized whole blood was stimulated with A23187 for 10 min. 5-LO product formation was detected in the supernatant. BWA4C was used as control inhibitor and suppressed 5-LO product formation as expected.
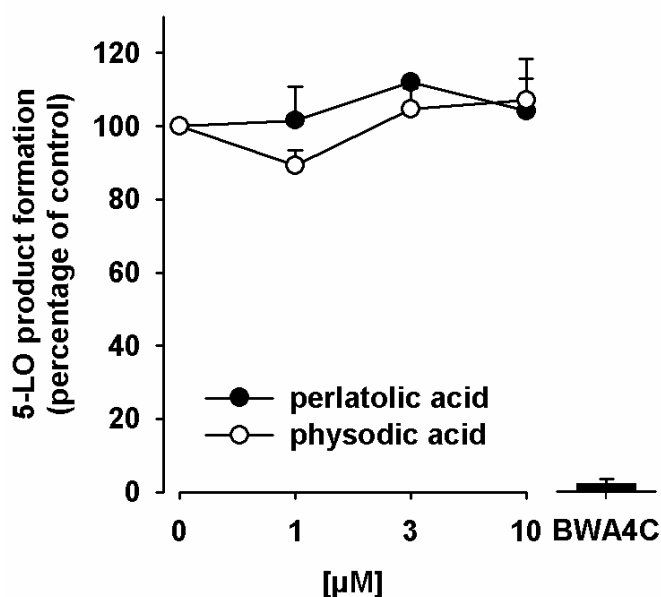
*Fig. 3.41: Effects of perlatolic acid (**30c**) and physodic acid (**29b**) on 5-LO inhibition in human whole blood.*

Heparinized whole blood was pre-incubated with perlatolic acid, physodic acid or vehicle (DMSO) for 15 min at 37 °C and stimulated with A23187 (30 µM) for 10 min. Reaction was stopped on ice and 5-LO product formation was detected using RP-HPLC. Data are given as mean + S.E. n=2-3.

Taken together, perlatolic (**30c**) and physodic acid (**29b**) inhibit 5-LO activity in a direct, non-redox and reversible manner. Physodic acid (**29b**) additionally prevents phosphorylation of ERK-1/2 which is responsible for upregulation of 5-LO activity, resulting in an increased potency of 5-LO inhibition. Both compounds failed to suppress 5-LO product formation *in vivo* in human whole blood.

3.4.3.4 Carrageenan-induced pleurisy in rats is inhibited by perlatolic acid (30c)

The activity of perlatolic acid (**30c**) was assessed *in vivo* using the carrageenan-induced pleurisy model in rats. These experiments were performed by Dr. Rossi and Prof. Sautebin, Univ. Naples, Italy. Injection of carrageenan into the pleural cavity of rats (DMSO 4% group) caused an inflammatory response within 4 h. Perlatolic acid (**30c**) (10 mg/kg, given i.p. 30 min prior the carrageenan injection) inhibited the inflammatory response by the decrease of PGE_2 levels (35% inhibition) (**Table 3.14**) in the exudates of the rats, whereas indomethacin (5 mg/kg, i.p.) completely suppressed PGE_2 levels as expected. Volume exudates and inflammatory cells in the pleural cavitiy were not affected by perlatolic acid (**30c**).

*Table 3.14: Effect of perlatolic acid (**30c**) on carrageenan-induced pleurisy in rats.*
Thirty min before intrapleural injection of carrageenan, rats (n=10 for each experimental group) were treated i.p. with 10 mg/kg perlatolic acid, 5 mg/kg indomethacin or vehicle (DMSO 4%). Exudate volume, PGE_2 and LTB_4 levels as well as inflammatory cell accumulation in pleural cavity were assessed 4 h after carrageenan injection. Data are expressed as mean ± S.E., n = 10. ANOVA + Tukey HSD post-hoc tests were performed, ***P < 0.01 vs vehicle (DMSO 4%). Experiments were performed by Dr. Rossi and Prof. Sautebin, Univ. Naples, Italy.

Treatment	Volume exudate [ml]	Inflammatory cells x 10^6	LTB$_4$ (ng/rat)	PGE$_2$ (ng/rat)
Vehicle	0.32 ± 0.06	99.63 ± 11.55	0.65 ± 0.19	0.93 ± 0.18
Perlatolic acid (10 mg/kg)	0.43 ± 0.09	158.86 ± 20.61	0.83 ± 0.24	0.61 ± 0.08 (35%)
Indomethacin (5 mg/kg)	0.08 ± 0.02 *** (75%)	35.67 ± 5.08 *** (64%)	0.56 ± 0.11 (14%)	0.05 ± 0.005 *** (95%)

3.4.4 Pharmacological profile of gingkolic acid (31) within the AA cascade

3.4.4.1 Mode of action on mPGES-1 derived PGE$_2$ inhibition

Ginkgolic acid (31) was identified to suppress mPGES-1 derived PGE$_2$ formation (IC$_{50}$= 0.7 µM) under cell-free conditions (see chapter 3.2.2). Studies demonstrate that alteration of the substrate concentration PGH$_2$ to lower (1 and 5 µM) or higher (50 µM) values lead to only slight changes in the potency (0.7 – 2.1 µM), suggesting that the mode of mPGES-1 inhibition is substrate independent (**Fig. 3.42A**). In addition, a reversible mechanism of action can be assumed, as ginkgolic acid (31) ailed to efficiently block mPGES-1 derived PGE$_2$ formation in washout experiments of a 10-fold dilution (**Fig. 3.42B**). Adding 10% FCS to the sample completely impaired the potency, indicating that ginkgolic acid (31) might bind to plasma proteins. MK-886 was used as control inhibitor and suppressed PGE$_2$ formation in all test systems as expected (not shown).

A **B**
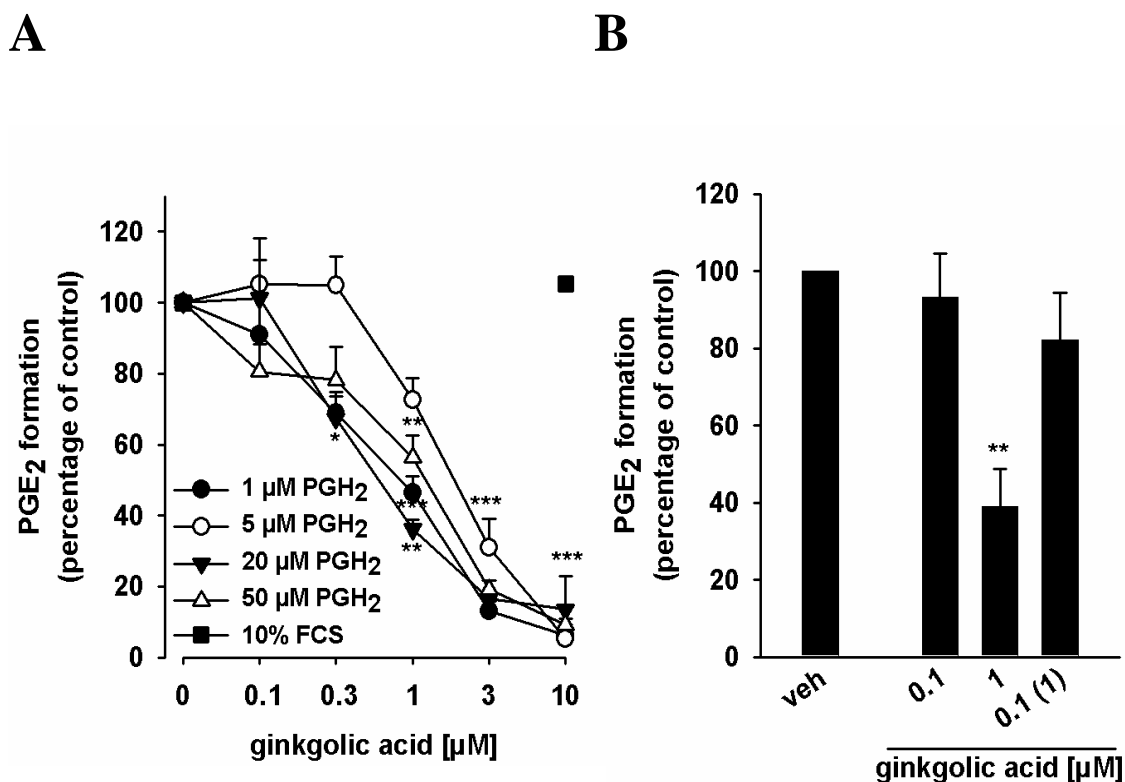
Fig. 3.42: Effects of ginkgolic acid (31) on mPGES-1.

(A) Concentration-response analysis. Microsomal preparations of IL-1β-stimulated A549 cells were pre-incubated for 15 min at 4 °C and PGE$_2$ formation was induced by addition of variable PGH$_2$ concentrations (1, 5, 20 and 50 μM). The amount of PGE$_2$ was quantified for 1 and 5 μM PGH$_2$ by the use of a PGE$_2$ High Sensitivity EIA Kit according to the manufacturer's protocol and PGE$_2$ formation of samples with or w/o 10% FCS stimulated with 20 and 50 μM PGH$_2$ was analyzed by RP-HPLC. Data are given as mean + S.E., n = 3, *p < 0.05, **p < 0.01 ***p < 0.001 vs. vehicle (DMSO) control, ANOVA + Tukey HSD post-hoc tests (B) Reversibility of mPGES-1 inhibition. Microsomal preparations were pre-incubated for 15 min with 1 μM ginkgolic acid or vehicle (DMSO), and an aliquot was diluted 10-fold to obtain an inhibitor concentration of 0.1 μM. Then, 20 μM PGH$_2$ was added and all samples were incubated for 1 min on ice, and PGE$_2$ formation was analyzed as described by RP-HPLC. Data are given as mean + S.E., n=3, **p < 0.01 1 μM vs. vehicle (DMSO), ANOVA + Tukey HSD post-hoc tests.

3.4.4.2 Ginkgolic acid (31) inhibits prostanoid formation *in vitro*

As COX enzymes are known to act upstream of mPGES-1, ginkgolic acid (**31**) was analyzed for its ability to interfere with COX-1 and -2. The formation of the COX-1 metabolites 12-HHT and TXB_2 was analyzed in human platelets, pre-incubated with ginkgolic acid (**31**) and stimulated with AA (3 µM) as substrate of COX-1 (**Fig. 3.43A**). Ginkgolic acid (**31**) concentration-dependently blocked 12-HHT and TXB_2 formation with similar IC_{50} values of 2.1 and 2.2 µM, respectively. To check whether this effect is due to a direct interference with COX, isolated ovine COX-1 and human recombinant COX-2 were pre-incubated with ginkgolic acid (**31**) and stimulated with AA for 5 min. Indomethacin, which was used as inhibitor in COX-1 test systems and celecoxib, as selective COX-2 inhibitor, completely blocked COX formation as expected (not shown). Ginkgolic acid (**31**) moderately inhibited 12-HHT formation of COX-1, but not COX-2, with $IC_{50} = 8.1$ µM (**Fig. 3.43B**). As TXB_2 formation in intact human platelets was affected with higher potency, the effects of ginkgolic acid (**31**) on TXAS in platelet homogenates stimulated with PGH_2 as substrate were analyzed. The TXAS inhibitor CV4151 was used as control and completely blocked TXB_2 formation as expected. Ginkgolic acid (**31**) could be identified as a moderate TXAS inhibitor ($IC_{50} = 5.2$ µM) (**Fig. 3.43B**).

A   **B**
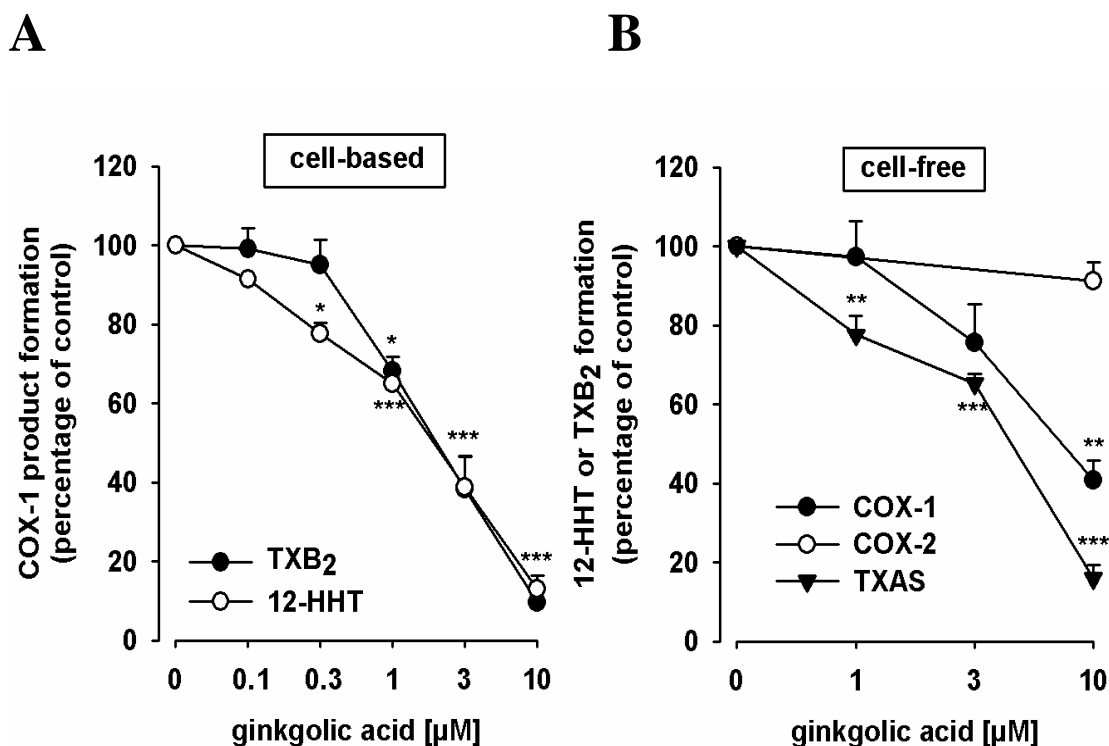
Fig. 3.43: Effects of ginkgolic acid (**31**) on human platelets, cell-free COX and TXAS
(A) Platelets (10^8/ml PBS containing 1 mM CaCl$_2$) were pre-incubated for 5 min prior
to stimulation with AA (5 μM). After another 5 min at 37 °C, the formation of 12-HHT
was determined by RP-HPLC as described and formation of TXB$_2$ was determined
using a TXB$_2$ High Sensitivity EIA Kit according to the manufacturer's protocol. Data
are given as mean + S.E., n = 3, *p < 0.05, ***p < 0.001 vs. vehicle (DMSO) control,
ANOVA + Tukey HSD post-hoc tests. (B) Purified ovine COX-1 (50 units) or human
recombinant COX-2 (20 units) were pre-incubated 5 min prior stimulation with AA (5
μM or 2 μM, respectively). 12-HHT in the samples was analyzed using RP-HPLC.
Thromboxane A$_2$ synthase (TXAS) activity was determined in platelet homogenates
(10^8/ml PBS containing 1 mM CaCl$_2$, sonified 3 x 15 sec) pre-incubated for 15 min on
ice and stimulated with 20 μM PGH$_2$ for 1 min. TXB$_2$ levels were detected in the
supernatant using a TXB$_2$ High Sensitivity EIA Kit according to the manufacturer's
protocol. Data are given as mean + S.E., n = 3-4, **p < 0.01, ***p < 0.001 vs. vehicle
(DMSO) control, ANOVA + Tukey HSD post-hoc tests.

In addition, studies of COX-2 expression in intact human monocytes
primed with LPS were performed. Dexamethason, used as control,
completely blocked COX-2 expression compared to the unstimulated
sample (**Fig. 3.44**). However, ginkgolic acid (**31**) only moderately blocked

the expression of COX-2, suggesting a slight synergistic effect on mPGES-1 activity and COX-2 expression to suppress PGE_2 formation.
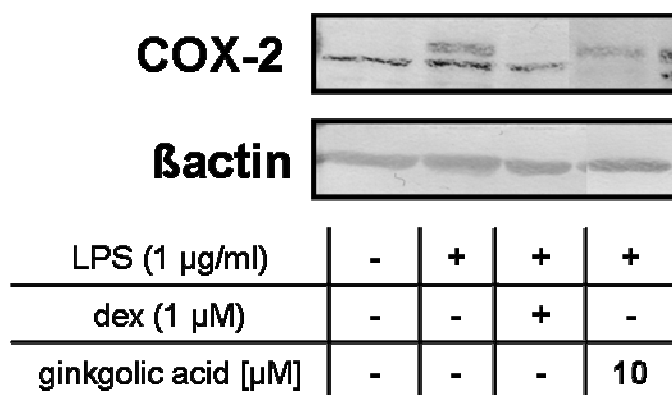
Fig. 3.44: Effects of ginkgolic acid (31) on intact human monocytes primed with LPS. Intact human monocytes (5 x 10^6/exp. in RPMI 1640 medium containing 0.5 % FCS, P/S and 2 mM glutamine) were stimulated with 1 µg/ml LPS and gingkolic acid (10 µM), dexathemason (1 µM) or vehicle (DMSO) was added for 24 h at 37 °C. After 24 h cells were detached and lysed (2 x SDS-b.). Samples were subjected to SDS-PAGE and WB using a specific antibody against COX-2. ßactin was used as loading control. Results are representative of 2-4 independent experiments.

To exclude interference of ginkgolic acid (**31**) at the level of AA supply, the effect on the enzymatic activity of human recombinant $cPLA_2$ was studied. Whereas the pyrrolidine inhibitor (1 µM) effectively blocked AA release from phospholipids, ginkgolic acid (**31**) did not affect $cPLA_2$ activity (**Fig. 3.45A**). Moreover, ginkgolic acid (**31**) showed only minimal cytotoxic effects after 24 h (80% cell viability) that could not be detected after 48h, implying that no unspecific cellular effects adulterate results for cell-based assays (**Fig. 3.45B**).
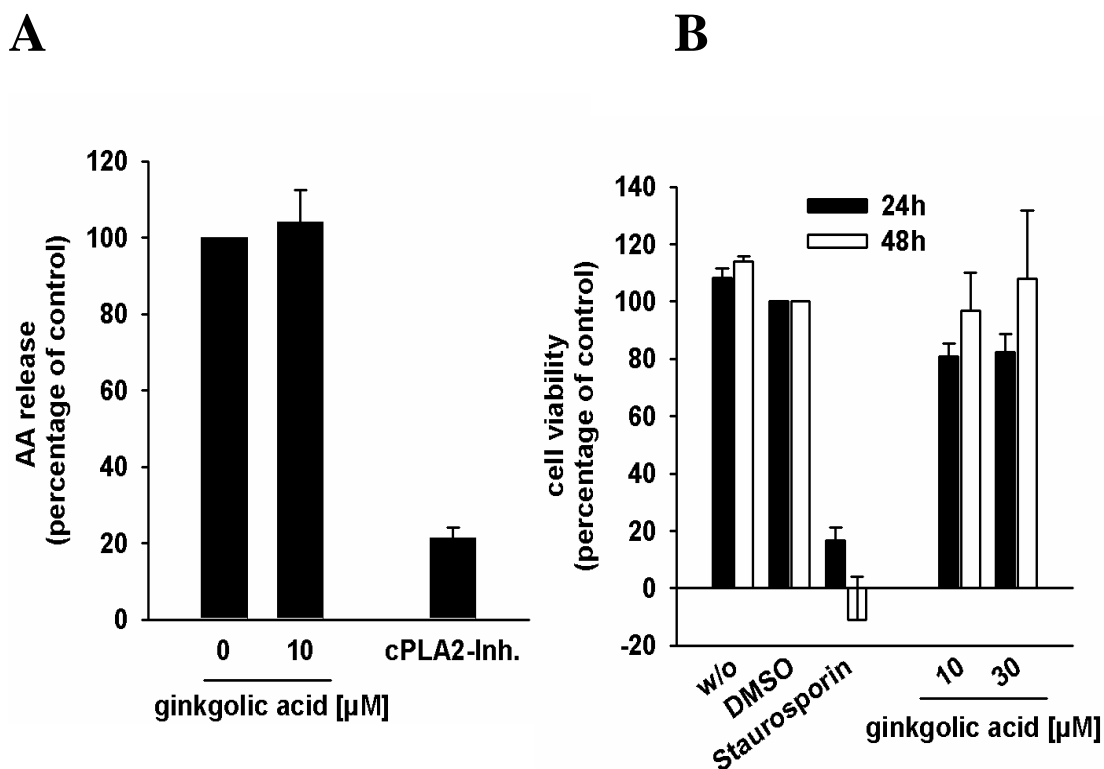
Fig. 3.45: effects of ginkgolic acid (31) on cPLA_2 activity and cytotoxic effects on A549 cells.

(A) Freshly prepared large unilamelar vesicles were incubated with cPLA_2 enzyme, 1 mM Ca^{2+} and the indicated compounds for 1 h at 37 °C. Reaction was stopped using methanol. Following derivatisation with p-anisidinium chloride, the resulting derivate was analyzed by RP-HPLC. Data are given as mean + S.E., n=3, ***p < 0.001 vs. vehicle (DMSO) control, ANOVA + Tukey HSD post-hoc tests. Performed by Marius Melzer in the lab of Prof. Dr. O. Werz (University of Jena, Germany). (B) Cytotoxicity in A549 cells. Cells (3 x 10^5) were incubated for 24 h and 48 h at 37 °C with Ginkgolic acid or vehicle (DMSO). After 24 h or 48 h, MTT was added and samples were incubated for 4 h at 37 °C. Reaction was stopped and the absorption was measured at 570 nm. Results are reported as percentage of viable cells as compared to vehicle control. Data are given as mean + S.E. n=3.

Studies using human whole blood could not confirm the potency of ginkgolic acid (31) demonstrated in the cell-free and cell-based experiments. Ginkgolic acid (31) did not interfere with prostanoid synthesis in vivo (Fig. 3.46). This might be due to plasma protein binding as has been demonstrated for mPGES-1 supplemented with 10% FCS (see Fig. 3.42).
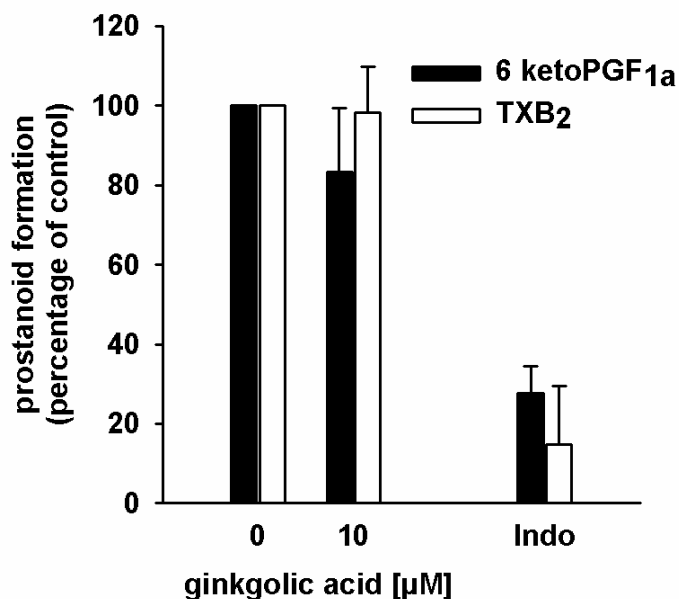
Fig. 3.46: Effects ginkgolic acid (31) in whole blood experiments

6-ketoPGF$_{1a}$ detection in human whole blood. Heparinized human whole blood was incubated with LPS (10 µg/ml) and ginkgolic acid or vehicle (DMSO) for 24 h at 37 °C. After 24 h the reaction was stopped on ice and the formation of 6-ketoPGF$_{1a}$ was detected in the supernatant using a 6-ketoPGF$_{1a}$ High Sensitivity EIA Kit according to the manufacturer's protocol. TXB$_2$ detection in human whole blood. Citrated human whole blood was pre-incubated with ginkgolic acid, indomethacin (50 µM) or vehicle (DMSO) for 15 min at 37 °C and the reaction was initiated with thrombin 2 U/ml. After 10 min the reaction was stopped on ice and TXB$_2$ levels were detected in the supernatant using a TXB$_2$ High Sensitivity EIA Kit according to the manufacturer's protocol. Data are given as mean + S.E. n=3.

In summary, ginkgolic acid (**31**) is a potent inhibitor of mPGES-1 with a substrate independent and reversible mode of action. Ginkgolic acid (**31**) did not affect COX-2 activity and moderately inhibited COX-2 expression in monocytes. In addition, COX-1 and TXAS could be identified as molecular targets.

3.4.4.3   Ginkgolic acid (31) interferes with the 5-LO pathway

Inhibition of semi-purified 5-LO turned out to be concentration dependent with IC$_{50}$ = 0.2 µM (**Fig. 3.47A**). However, when ginkgolic acid (**31**) was tested in a cell-free 5-LO activity assay based on crude neutrophil homogenates under the same experimental conditions, the potency clearly decreased (IC$_{50}$ > 10 µM), indicating that cellular components present in

the homogenates may hamper 5-LO inhibition. Washout experiments demonstrate that inhibition of 5-LO by ginkgolic acid (**31**) is fully reversible, as a 10-fold dilution of a potent concentration of 1 μM could counteract the inhibition (**Fig. 3.47B**). BWA4C was used as reference inhibitor and suppressed 5-LO product formation as expected (not shown).

A   **B**
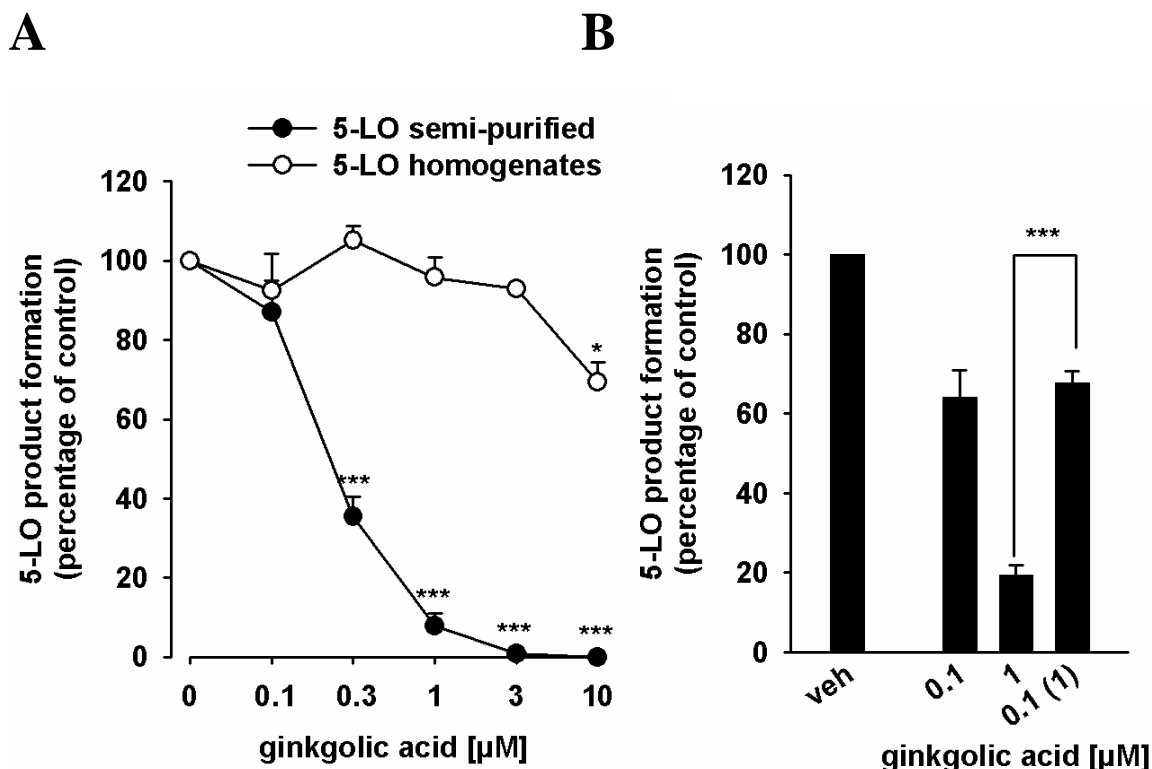
*Fig. 3.47: effects of ginkgolic acid (**31**) on isolated 5-LO*

(A) Inhibition of isolated 5-LO. Semi purified, human recombinant 5-LO or PMNL homogenates (5 x 10^6 cells/exp.) were pre-incubated with ginkgolic acid, BWA4C (0.3 μM) or vehicle (DMSO) in the presence of 1 mM ATP for 10 min. 5-LO product formation was initiated by addition of 2 mM Ca^{2+} and 20 μM AA for 10 min at 37 °C. Reaction was stopped with methanol on ice and 5-LO products were analyzed by RP-HPLC. Data are given as mean + S.E., n = 3, *p < 0.05 and ***p < 0.001 vs. vehicle (DMSO) control, ANOVA + Tukey HSD post-hoc tests. (B) Reversibility of 5-LO inhibition. Semi purified, human recombinant 5-LO was pre-incubated in the presence of 1 mM Ca^{2+} and 1 mM ATP for 10 min and an aliquot was diluted 10-fold to obtain an inhibitor concentration of 1 μM. 5-LO product formation was initiated by addition of 20 μM AA for 10 min at 37 °C. Reaction was stopped with methanol on ice and 5-LO products were analyzed by RP-HPLC. Data are given as mean + S.E., n = 3-4, ***p < 0.001; 1 μM vs. diluted sample, ANOVA + Tukey HSD post-hoc tests.

Further investigation on 5-LO inhibition were performed in a cell-based assay using intact human neutrophils, stimulated with A23187 in the presence and absence of exogenous AA as substrate for 5-LO. As can be seen in **Fig. 3.48**, ginkgolic acid (**31**) blocked 5-LO product formation independent of the substrate supply comparably well (IC_{50} = 3.8 and 2.9 µM, respectively), but was less potent in intact neutrophils primed with LPS and stimulated with fMLP (IC_{50} = 7.2 µM). BWA4C, used as reference inhibitor, suppressed 5-LO product formation in neutrophils as expected (not shown).
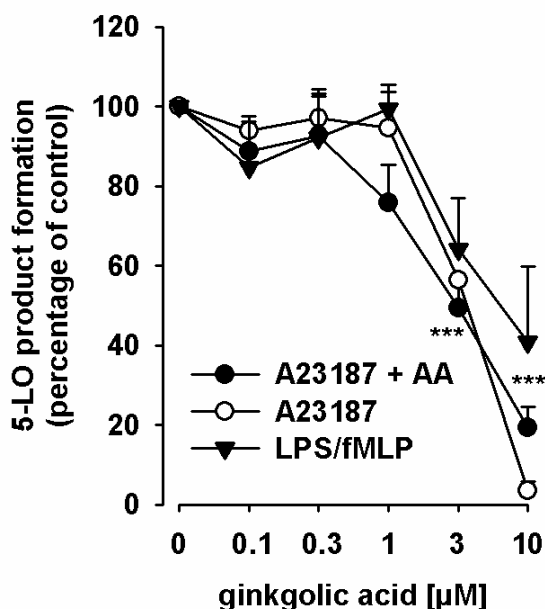
Fig. 3.48: Effects of ginkgolic acid (31) on 5-LO in intact PMNL.
Isolated PMNL (5 x 10^6/ml) were pre-incubated with ginkgolic acid or vehicle (DMSO) for 10 min at 37 °C and stimulated with 2.5 µM A23187 or 2.5 µM A23187 plus 20 µM AA. 5-LO products were determined by RP-HPLC. Alternatively, cells were primed with LPS (1 µg/ml) for 30 min and formation of 5-LO products was initiated by addition of 1 µM fMLP. LTB$_4$ levels were detected using a LTB4 High Sensitivity EIA Kit according to the manufacturer's protocol. Data are given as mean + S.E. n=3-5, ***p < 0.001 vs. vehicle (DMSO) control, ANOVA + Tukey HSD post-hoc tests

As 5-LO activity is strongly regulated in the cell, i.e. phosphorylation by ERK-1/2 or MAPK pathway, experiments with ginkgolic acid (**31**) on the phosphorylation status of ERK-1/2 and p38 MAPK in human neutrophils stimulated with fMLP were performed and revealed that phosphorylation is not affected by ginkgolic acid (**31**) (**Fig. 3.49A**). U0126 that was used as reference inhibitor of ERK-1/2 phosphorylation inhibited ERK-1/2 as

expected. Several 5-LO inhibitors act by uncoupling the catalytic cycle of 5-LO due to redox properties. Antioxidant properties can be excluded, since ginkgolic acid (**31**) failed to reduce the stable DPPH radical up to 100 µM, whereas the positive controls ascorbic acid and cysteine reduced DPPH as expected (**Fig. 3.49B**).

A   **B**
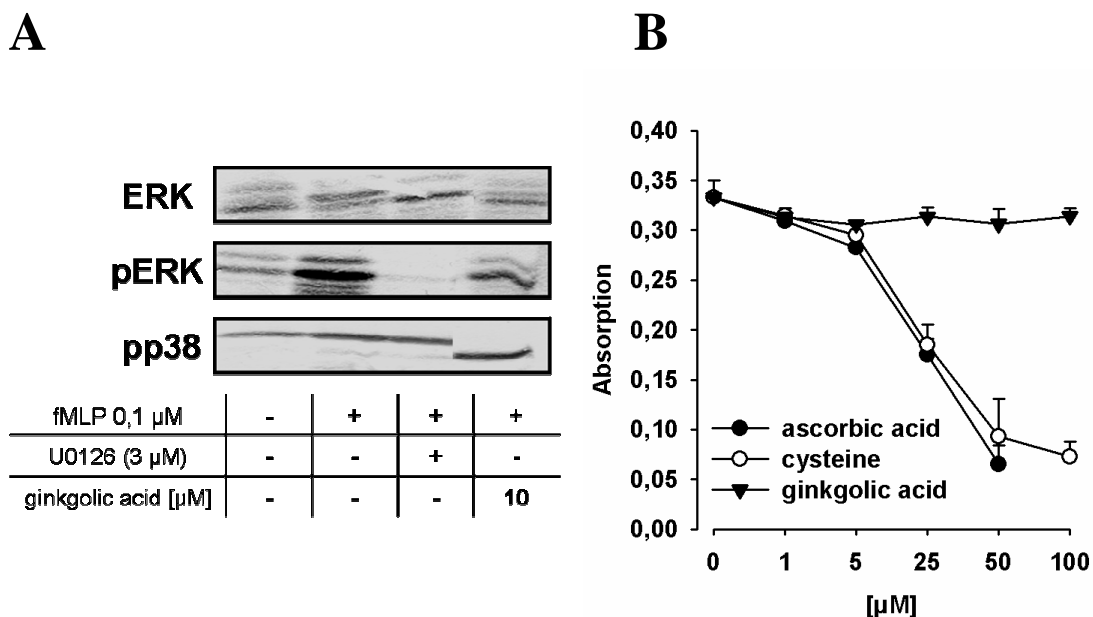
Fig. 3.49: Influence on MAPK signalling and radical scavenger properties of ginkgolic acid (31)

(A) Neutrophils (10^7) were pre-warmed for 3 min at 37 °C and pre-incubated with ginkgolic acid or vehicle (DMSO) at 37 °C for 15 min. The reaction was started by the addition of 0.1 µM fMLP, stopped after 1.5 min with SDS-b. and heated for 6 min at 95 °C. Total cell lysates were analyzed for ERK1/2, phosphorylated ERK1/2 (Thr-202/Tyr-204), phosphorylated p38 MAPK (Thr-180/Tyr-182), by SDS/PAGE and western blotting. Results are representative of 2-3 independent experiments (B) Radical scavenger capability. Ginkgolic acid, vehicle and controls were mixed with DPPH solution and incubated for 30 min in the dark. The absorbance was measured at 520 nm. Data are given as mean + S.E. n=3.

As has been demonstrated for prostanoid biosynthesis, ginkgolic acid (**31**) lost its inhibitory potential on 5-LO activity in human whole blood. BWA4C, which was used as standard inhibitor, reduced 5-LO product formation in human whole blood as expected.
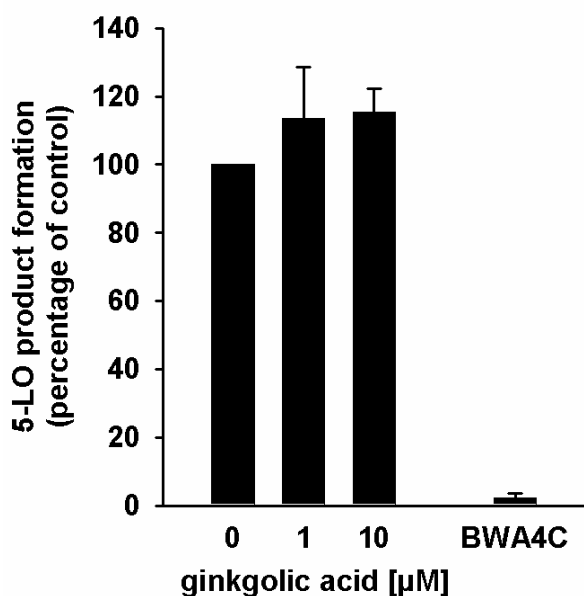
Fig. 3.50: Effects of ginkgolic acid (**31**) on 5-LO inhibition in human whole blood.
Heparinized whole blood was pre-incubated with ginkgolic acid or vehicle (DMSO) for 15 min at 37 °C and stimulated with A23187 (30 µM) for 10 min. Reaction was stopped on ice and 5-LO product formation was detected using RP-HPLC. Data are given as mean + S.E. n=2-3.

Together, ginkgolic acid (**31**) potently inhibited 5-LO product formation in cell-free and cell-based experiments. The mechanism of action was fully reversible and non redox active. Investigations in crude neutrophil homogenates and human whole blood indicate a high affinity to proteins present in the sample.

4   DISCUSSION

There is accumulating evidence that mPGES-1 might represent a druggable target in the therapy of inflammation and pain. mPGES-1 gene deletion studies and pharmacological approaches with selected mPGES-1 inhibitors support a role for mPGES-1 in inflammatory reactions, fever, pain, neurological disorders and cancer [20, 78, 194, 195]. In view of the considerable gastrointestinal, renal and cardiovascular side effects of COX inhibitors, the class of drugs widely used to treat inflammation, fever and pain, mPGES-1 inhibition might be a promising alternative strategy to NSAIDs. Accordingly, extensive efforts are underway to develop mPGES-1 inhibitors. However, only a few agents show sufficient efficacy in preclinical models of inflammation and pain so far and thus could potentially enter clinical trials [20, 78, 194].

Dual inhibition of 5-LO and mPGES-1 seems to be preferable since inhibition of COX and 5-LO was suggested to be superior over single NSAID administration related to an improved anti-inflammatory effectiveness associated with a lower risk of gastrointestinal and cardiovascular side effects [101, 196]. As PGE_2 is held the mainly responsible eicosanoid for inflammatory events, a dual inhibition of mPGES-1 and 5-LO is a promising strategy to avoid ordinary side effects of NSAIDs or coxibs and improve the safety of anti-inflammatory drugs [93].

4.1 The acylphloroglucinol arzanol from *Helichrysum italicum* is seemingly a responsible constituent for the anti-inflammatory potential of the plant

Arzanol was discovered as a bioactive ingredient from the Mediterranean curry plant (*Helichrysum italicum)*. With 0.05% of the dried plant weight, arzanol is one of its major active compounds. Extracts of the curry plant have been traditionally used in folk medicine to treat inflammatory disorders [197], but there are only few studies addressing the molecular targets. Interference at the level of pro-inflammatory cytokine and PGE_2 release from LPS stimulated human monocytes (IC_{50}= 5-22 µM), which is attributed to an impaired activation of the NFκB pathway (IC_{50}= 5 µM) [118, 129] could be monitored by the group of Appendino et al. in 2007. During my diploma thesis, mPGES-1 and 5-LO could be identified as molecular targets of arzanol [175, 198].

In this study the overall pharmacological profile within the eicosanoid biosynthesis was investigated and mechanistic studies were performed to identify the mode of action. Arzanol potently inhibits mPGES-1[¶] (IC_{50}= 0.3 µM), 5-LO[¶] (IC_{50}= 3.4 µM) and TXAS (IC_{50}= 2.7 µM) under cell-free conditions. A direct interference with the upstream signalling enzymes $cPLA_2$, COX-1[¶] and COX-2[¶] can be excluded, since arzanol failed to block AA release and 12-HHT product formation, which is non-enzymatically formed from PGH_2 [199], under cell-free conditions. Mechanistic studies reveal a reversible and competitive mode of action for mPGES-1 inhibition. Since arzanol was identified to protect linoleic acid against free radical attack in assays of autoxidation and EDTA-mediated oxidation, and inhibited TBH-induced oxidative stress in VERO cells [129], radical scavenger properties were assessed by DPPH assay. Thus, arzanol could be

identified as a redox-type inhibitor of 5-LO with a reversible mode of action.

The inhibitory potential of arzanol was also evident *in vitro* using cell-based test systems. As direct COX-2 inhibition can be excluded, PGE_2 suppression in human monocytes can be ascribed to an interference with mPGES-1 [200]. In addition, concomitant analysis of COX-2 and mPGES-1 protein in human monocytes revealed that arzanol does not interfere with their expression levels. 5-LO inhibition in intact neutrophils was selective and comparable to the results under cell-free conditions.

Many NSAIDs represent lipophilic acidic substances and hence suffer from high plasma protein binding in line with a loss of efficiency [201]. As arzanol is a lipophilic and weak vinylogue acid, plasma protein binding effects might play a role, but notably PGE_2 biosynthesis was efficiently blocked by arzanol in LPS-stimulated human whole blood, whereas the formation of other prostanoids such as 6-keto-PGF_{1a} and TXB_2 was hardly affected.

Extracts of *Helichrysum italicum* have already been shown to suppress 2-*O*tetradecanoylphorbol 13-acetate (TPA)-induced mouse ear edema formation in preclinical studies [117]. Thus, in a model of carrageenan-induced pleurisy in rats, arzanol was almost as effective as the NSAID indomethacin. Since PGE_2 is the primarily responsible mediator in the early phase of carrageenan-induced pleurisy [202], mPGES-1 inhibition might contribute to the anti-inflammatory efficacy of arzanol. Because 5-LO-derived metabolites cooperate with PGE_2 in the induction of pleurisy [203], synergistic anti-inflammatory effects of dual mPGES-1/5-LO have been observed [17, 93] that also might be responsible for an improved efficiency profile with less severe side effects.

In addition, other constituents from the genus *Helichrysum* have also been reported as anti-inflammatory agents [117, 126, 204]. Since their amount in curry plant extracts was found to be rather low, it is likely that they are not liable for the anti-inflammatory effects of the plant.

In summary, arzanol is a potent inhibitor of the key enzymes mPGES-1[¶], 5-LO[¶] and TXAS of the AA cascade. *In vivo* studies in human whole blood and carrageenan-induced pleurisy in rats could confirm the anti-inflammatory potential of arzanol and might explain the anti-inflammatory potential of *Helichrysum italicum*. As a dual mPGES-1/5-LO inhibitor of plant origin, arzanol might represent an innovative drug in the therapy of inflammation and cancer.

Current SAR studies demonstrate that the pharmacophore of arzanol can be improved towards its anti-inflammatory potential of mPGES-1 and 5-LO inhibition. As arzanol is a mixture of tautomers and atropoisomers [205], it is tempting to speculate that different forms of the compounds may target distinct biological end-points. Thus, it is known that heterodimeric phloroglucinyl pyrones co-occur with symmetric homodimeric alkyliden(bis) pyrones in many plants [205]. To these purposes, SAR studies were performed on the alkylidene linker and/or the pyrone moiety of homodimeric and heterodimeric analogues. Introduction of lipophilic elements to the alkylidene linker of (heterodimeric) acylphloroglucinols or (homodimeric) phloroacetophenon-derivatives yield potent inhibitors of mPGES-1 and semi-purified 5-LO with IC_{50} values in the submicromolar range. Most potent mPGES-1/5-LO inhibitor was achieved by introduction of an n-hexyl residue to the alkylidene linker of the heterodimeric scaffold (**1e**) [206].

In the present study **1e** was identified as a potent dual mPGES-1/5-LO inhibitor with an interesting pharmacological profile. In fact, detailed investigations on eicosanoid biosynthesis address mPGES-1 (IC_{50}= 0.2 µM), 5-LO (IC_{50}= 1.2 µM), COX-2 (IC_{50} > 10 µM) and TXAS (IC_{50}= 2.5 µM) as molecular targets of **1e,** whereas COX-1 and $cPLA_2$ activity were not affected. Importantly, COX-2 is only moderately inhibited by **1e** with an at least 100-fold higher selectivity for mPGES-1. Studies on the mechanistic properties of mPGES-1 and 5-LO inhibition identified **1e** as a direct and reversible inhibitor with redox-active and non-cytotoxic qualities. A loss of efficacy was observed in studies with human whole blood determined 5-LO product formations as well as TXB_2 and 6-$ketoPGF_{1a}$ formation. However, further investigations addressing *in vivo* effects and the bioavailability of **1e** will be necessary to assess the relevance as a potential anti-inflammatory drug.

4.2 Non-cannabinoids are involved in the anti-inflammatory actions of *cannabis sativa*

Cannabis sativa is one of the first plants that was used as herbal medicine. Up to date, several different phytocannabinoids and non-cannabinoids have been described, but only a few constituents were characterized for their biological activities. Pharmacological investigations on single cannabinoids, mostly THC, CBN and CBD, were first carried out in the early 1940s [207, 208]. Inhibition of PGE_1 biosynthesis in bull seminal vesicles (IC_{50}= 70 – 300 µM) by several cannabinoids was observed by Burstein et al. [209]. However, by now only few molecular targets of cannabis constituents involved in inflammation are known [141-143].

This thesis demonstrates that phytocannabinoids and non-cannabinoids inhibit mPGES-1 and 5-LO in cell-free conditions. CBG was the only one among the tested phytocannabinoids that could be identified as potent mPGES-1 inhibitor (IC_{50}= 0.9 µM). Notable, CBG is also present in *Helichrysum* species [134], implying that CBG might also contribute to the anti-inflammatory potential of *Helichrysum italicum*. Hence, further studies are necessary to verify the presence of CBG in *Helichrysum italicum*. Interestingly, THC inhibited mPGES-1 with a rather high IC_{50} value of 70 µM, suggesting that it is not the mainly responsible constituent of *Cannabis sativa* involved in anti-inflammatory events related to PGE_2. Among the non-cannabinoids, prenylated flavonoids (**19**, **20**) and the prenylated dihydrostilbene canniprene (**22**) could be identified as potent dual mPGES-1/5-LO inhibitors. Because 5-LO and mPGES-1 are key enzymes in the biosynthesis of lipid mediators involved in inflammation [25, 210] and CFA in line was already shown to inhibit TPA-induced PGE_2 release from cultured synovial cells [140], the overall pharmacological profile within the AA cascade was further investigated.

Studies on the prostanoid formation *in vitro* in human platelets and monocytes revealed a potent suppression of TXB_2 formation that could be identified as TXAS inhibition (IC_{50}= 6.8 µM). Notable, 12-HHT formation *in vitro* and in isolated COX-1 and -2 assays was hardly affected with IC_{50} values > 10 µM. CFA (10 µM) blocked PGE_2 formation in intact human monocytes comparable to the glucocorticoid dexamethasone. Since interference of CFA at the level of AA supply can be excluded, the observed effect might be due to synergistic (I) mPGES-1 inhibition and (II) blockage of COX-2 expression. Mechanistic investigations demonstrate a reversible mode of action that is independent of the substrate supply.

Also 5-LO could be identified as molecular target of CFA with a comparable potency of cell-free (IC_{50}= 0.9 µM) compared to cell-based (IC_{50}= 1.6 – 2.4 µM) assay. Indeed, studies in crude neutrophil homogenates resulted in a decreased potency (IC_{50}= 5.4 µM). A similar observation was made in microsomal preparations of A549 cells supplemented with 10% FCS, indicating that CFA suffers from plasma protein binding. This could also be shown *in vivo*, where CFA failed to inhibit 5-LO product formation in human whole blood. Mechanistic studies reveal that 5-LO inhibition is only partially reversible and not related to the substrate supply of AA. CFA was identified as a nonredox active inhibitor of 5-LO that does not interfere with the MAPK signaling pathway which is known to regulate 5-LO activity.

Plant *cannabis* extracts contain a complex mixture of phytocannabinoids and other non-cannabinoid compounds. In the 1970´s Sofia et al. [211-213] demonstrated potent anti-inflammatory effects of a crude marijuana extract and some single constituents (THC, CBD and CBN) in the carrageenan induced paw edema model of acute inflammation. Also CBCr was reported to possess anti-inflammatory potential in a carrageenan paw edema assay [214, 215]. More recently, CBD was shown to reduce joint inflammation in a murine model of collagen-induced arthritis [216]. Of interest, whole plant extracts of *cannabis sativa* seem to be superior over single administration of phytocannabinoids [217]. Hence, several animal models are reported on pytocannabinoids and only little is known about the effectiveness of non-cannabinoids in animal models of inflammation.

Taken together, CFA was identified as a potent dual mPGES-1/5-LO inhibitor in cell-free and cell-based test systems. In addition, TXAS could be identified as molecular target. Studies in human whole blood indicate high plasma protein binding due to its lipophilic character. Hence, further

in vivo studies are necessary to define the role of CFA in the treatment of inflammation.

4.3 Benzofurane derivatives are potential anti-inflammatory constituents of *Krameria lappacea*

The roots of *Krameria lappacea* (syn. rhatany) are used in the treatment of inflammation predominantly of the mouth and throat [187, 188]. Vegetable tannins, having astringent and antimicrobial properties, were considered as the active anti-inflammatory components [218], but previous studies indicate that lignan derivatives may act as potent anti-inflammatory agents [189, 190].

A topical anti-inflammatory potential of a CH_2Cl_2 rhatany extract and 11 isolated lignan derivatives could be revealed from animal studies, detected as antiedema activity in mice [176]. (Leukocyte infiltration and histological analysis were additionally performed). Attempts to clarify the mode of action were performed on the NFκB pathway and AA cascade that are involved in inflammation. Thus, interference with TNFa-induced NFκB signaling, COX-1 and -2, 5-LO and antioxidant properties could be demonstrated for several lignan derivatives, which may explain the promising anti-inflammatory activity of the CH_2Cl_2-soluble extract of *Krameria lappacea* roots on multiple targets *in vivo* and *in vitro* [176]. In this line mPGES-1 inhibition was suggested as a probable target for the anti-inflammatory effects.

This study addresses mPGES-1 as a direct target of several lignan derivatives in a cell-free assay (IC_{50} values 5.3 – 42 µM). In particular, substituted propenylbenzofurans (**9a** – **9e**) were most potent mPGES-1

inhibitors with IC_{50} values of 5.3 – 13.5 µM whereas 7,70-epoxy lignans showed no marked inhibition of mPGES-1 up to 50 µM. Taken together, these findings provide a strong evidence for the anti-inflammatory potential of rhatany by lignan derivatives, consistent with the anti-inflammatory targets that could already be addressed for several lignan derivatives.

4.4   Depsides and depsidones from *lichen spec.* dispose of a promising anti-inflammatory potential

Lichens are symbiotic associations between fungi (mycobionts) and algae and/or cyanobacteria (photobionts) [219]. Various extracts of *lichen species* have been used as remedies in folk medicine for the treatment of inflammatory disorders. By now, approximately 1,050 secondary metabolites from *lichens* have been identified [144]. Numerious pharmacological properties are reported for secondary metabolites, such as antibiotic, antimycobacterial, antifungal, antiviral, anticancer, antiproliferative, antioxidant, anti-inflammatory, analgesic, and antipyretic and cytotoxic effects [144, 148, 149, 220-225].
For the development of novel mPGES-1 inhibitors as promising anti-inflammatory agents, a pharmacophore model was generated by the group of Stuppner et al. (Innsbruck). *In silico* screening of the Chinese herbal medicine (CHM) database using this pharmacophore model revealed the group of depsides and depsidones as potential candidates [177]. To this purpose five depsides and five depsidones were investigated for their anti-inflammatory potential.

Among the selected depsides methylbetaorcinol carboxylate, evernic acid, perlatolic acid, olivetoric acid and atranorin only perlatolic acid (IC_{50} = 0.4

µM for mPGES-1 and 5-LO) and olivetoric acid (IC_{50} = 1.15 µM for mPGES-1 and 2.4 µM for 5-LO) could be identified as potent dual mPGES-1/5-LO inhibitors. Investigations on the selected depsidones fumarprotocetraric acid, physodic acid, salazinic acid, variolaric acid and scensidin revealed physodic acid as potent dual inhibitor of mPGES-1 and 5-LO (IC_{50}= 0.43 and 2.4 µM, respectively). In line with recent findings [82], lipophilic residues and abdication of the carboxylic group retained potent mPGES-1 inhibitors.

For the class of depsides and depsidones *in vitro* studies revealed antiviral [226, 227], antibacterial [228-231], antimicrobial [220, 232, 233], antifungal [230], anticancer [220, 234, 235] and antioxidant properties [220, 232, 233, 236-238] as well as inhibition of MAO-B [239], acetylcholinesterase [240, 241] and p12-LO [222]. Interference with PG biosynthesis in rabbit renal microsomes [146] as well as on the 5-LO signaling pathway in porcine leukocytes [242, 243] and inhibition of malondialdehyde (MDA) formation in rat and monkey liver microsomes [244] is known for both classes and might contribute to the anti-inflammatory potential of *lichens*. Hence, further studies adressing the molecular targets involved in inflammation are necessary.

This thesis demonstrates that the depside perlatolic acid and the depsidone physodic acid are potent inhibitors of mPGES-1 (IC_{50}= 0.4 and 0.43 µM, respectively), 5-LO (IC_{50}= 0.4 and 2.4 µM, respectively) and TXAS (IC_{50}= 1.1 and 0.7 µM, respectively) under cell-free conditions. Inhibition of NFkB (IC_{50}= 7.0 µM) [245] and COX-1 (IC_{50}> 10 µM) for perlatolic acid is also evident but to a lesser extent. Because mPGES-1 and 5-LO are key enzymes involved in inflammatory events [25, 210], their inhibition by

perlatolic acid and physodic acid might contribute to the anti-inflammatory potential of *lichens*.

Mechanistic studies on mPGES-1 and 5-LO inhibition reveal a concentration-dependent and reversible mode of action, which is largely independent of the substrate supply. Since radical scavenger properties can be excluded and no iron-chelating qualities are apparent for both, perlatolic acid and physodic acid can be structurally classed into non redox-type inhibitors of 5-LO.

Inhibitory effects were also evident in terms of cell-based assay systems. Interference at the level of AA supply can be excluded, as both failed to inhibit isolated $cPLA_2$ enzyme. PGE_2 biosynthesis is suppressed by synergistic effects *in vitro*. Perlatolic acid completely and physodic acid moderately blocked COX-2 expression in LPS stimulated human monocytes, which in turn with downstream mPGES-1 inhibition is responsible for suppression of pro-inflammatory PGE_2. Notable, inhibition of COX-2 activity could not be detected, what may contribute to an improved safety profile. 12-HHT and TXB_2 were potently blocked by perlatolic acid in human platelets, indicating synergistic effects of COX-1 and TXAS for blockade of TXB_2. Surprisingly, physodic acid potently blocked cell-free TXAS activity ($IC_{50}= 0.7$ µM), but the inhibitory potential decreased about 10 fold in intact human platelets, where the formation of 12-HHT and TXB_2 ($IC_{50}= 8.8$ and 5.2 µM, respectively) was detected.

5-LO inhibition in neutrophils was evident with similar efficacy, as both compounds have comparable IC_{50} values with exogenous supplemented AA (A23187 + 20 µM AA) and AA provided from endogenous sources (A23187). Of interest, stimulation with physiological occurring inflammatory mediators (LPS, fMLP) decreased the potency of perlatolic acid ($IC_{50}= 8.0$ µM in contrast to 1.8 µM with A23187 $\pm$ AA) in intact

human neutrophils, whereas the potency of physodic acid was increased (IC_{50}= 1.3 µM in contrast to 5.0 and 6.4 µM A23187 ± AA). 5-LO product formation is modulated by $cPLA_2$ (AA liberation) and regulation of 5-LO activity.

Recently p38 MAPK and ERK1/2 were identified to up-regulate 5-LO activity via phosphorylation [246]. However, regulation of 5-LO activity by phosphorylation could be identified as a further target of physodic acid. Phosphorylation of ERK1/2 was completely blocked in a concentration dependent manner, which is responsible for the increased potency of physodic acid in LPS/fMLP stimulated human neutrophils compared to the stimulation with A23187 ± AA.

Extracts of *Teloschistes flavicans* [247], *Cladonia clathrata* [248], *Cladonia rangiformis* [249] and *Peltigera rufescens* [250] have shown to suppress acute (carrageenan or formaldehyde induced) and/or chronic (cotton pellet granule) inflammation in mouse models of inflammation as well as acetic acid-induced abdominal writhes, but studies on isolated secondary metabolites are rare. Thus, perlatolic acid, which is a major ingredient of *lichens* [245], was shown to inhibit the inflammatory recruitment of leukocytes in a peritonitis mouse model *in vivo* [245] and blocked PGE_2 formation in a model of carrageenan-induced pleurisy in rats. Since PGE_2 is the primarily responsible mediator in the early phase of carrageenan-induced pleurisy [202], mPGES-1 inhibition might contribute to the anti-inflammatory potential of perlatolic acid.

In summary, perlatolic acid and physodic acid potently inhibit the biosynthesis of the pro-inflammatory mediators PGE_2, TXB_2 and LTB_4, implying synergistic anti-inflammatory effects [20, 103, 251] and therefore an improved pharmacological safety profile compared to NSAIDs and

coxibs. Thus, (pro-inflammatory) PGE_2 biosynthesis is selectively and reversibly blocked by the synergistic effect of (I) downstream mPGES-1 inhibition and (II) blockade of inducible COX-2 expression. Importantly, suppression of PGE_2 formation for perlatolic acid was also evident *in vivo* (physodic acid is not yet investigated). These findings offer broader perspectives and possibilities for the application of depsides and depsidones from *lichens*.

4.5 Ginkgolic acid contributes to the anti-inflammatory properties of *ginkgo biloba*

Ginkgo biloba is among the most widely used medicinal plants of the world. Its medicinal use goes back several centuries where it was first documented in the Chinese Materia Medica interalia for the treatment of cardiovascular and bronchial diseases, skin wounds and freckles [158, 159]. By now, ginkgo preparations, which have been mostly standardized for their amount of terpene trilactones and flavonol glycosides, are available by several manufacturers. Terpene trilactones and flavonol glycosides are deemed to be the pharmacological active constituents of *ginkgo biloba* [170]. The proposed anti-inflammatory potential of *Ginkgo biloba* is due to anti-PAF activity by terpene trilactones [252, 253], inhibition of COX and LO by flavonoids [166] and radical scavenger activities [254, 255]. However, since not all effects are clearly attributed to these constituents, effects of other components present in the extract can not be excluded [170].

To this purpose, the present study focused on ginkgolic acid, which is among the alkylphenols (ginkgolic acids) that are found in the fruit pods and in the leaves of *ginkgo biloba* [256]. Besides their antitumor,

antimicrobial and antiviral activities, allergenic effects are ascribed to alkylphenols [172, 256-258]. Ginkgolic acids are limited at 5 mg/g in commercial phytopreparations in the monograph of the Commission E of the former German Health Authority (Bundesgesundheitsamt, BGA) [259]. However, their allergenic potential has not been clearly verified, which in turn is why they were not yet in the main focus of inflammation research [173, 174, 260].

This thesis identified key enzymes involved in prostanoid and leukotriene biosynthesis as functional molecular targets of ginkgolic acid. Particularly, mPGES-1 (IC_{50}= 0.7 µM), 5-LO (IC_{50}= 0.3 µM), COX-1 (IC_{50}= 8.1 µM) and TXAS (IC_{50}= 5.2 µM) were affected by ginkgolic acid. Notable, inhibition of mPGES-1 and 5-LO is about 10 fold selective compared to COX-1 and TXAS. Studies on the mechanistic properties of mPGES-1 and 5-LO inhibition reveal a direct and reversible mode of action which is independent of the substrate supply. Interference at upstream signaling events such as AA release can be excluded since ginkgolic acid failed to block $cPLA_2$ activity. A moderate inhibition of COX-2 expression could be observed in human monocytes after 24 h, whereas COX-2 activity in cell-free conditions was not affected.

Efficiency of ginkgolic acid was also evident in cell-based assays of human platelets and neutrophils. 12-HHT and TXB_2 were concentration-dependently blocked by ginkgolic acid in human platelets equally well (IC_{50} values of 2.1 and 2.2. µM, respectively) indicating synergistic effects of COX-1 (IC_{50}= 8.1 µM) and TXAS (IC_{50}= 5.2 µM) inhibition. Investigations in human neutrophils reveal that 5-LO product formation is comparably blocked by ginkgolic acid where either substrate was provided from endogenous sources (stimulation with A23187 or LPS/fMLP) or supplemented exogenously (20 µM AA). Interference in 5-LO regulation

by phosphorylation can be excluded. Cytotoxic effects of alkylphenols (ginkgolic acids) are described in several human and animal cell-lines [261, 262]. Interestingly, in a recent study ginkgolic acid was demonstrated to show less cytotoxicity in 96 h cultured primary rat hepatocytes than in 20 h cultured primary rat hepatocytes and HepG2 cells [171]. These results could be confirmed by MTT assay using A549 cells, where ginkgolic acid showed minimal cytotoxic effects after 24 h (80% cell viability) that were not detectable after 48 h.

As ginkgolic acid is a lipophilic acidic agent, it suffers from high plasma protein binding. This could be demonstrated (I) in crude neutrophil homogenates, where ginkgolic acid lost its potency of 5-LO inhibition and (II) in microsomal preparations of A549 cells, where the potency of ginkgolic acid was impaired after addition of 10% FCS. Hence, *in vivo* studies in human whole blood resulted in a complete loss of efficacy.

Investigations with *Ginkgo biloba* extract (GBE) on endotoxin induced uveitis (EIU) in rats indicate that suppression of inflammation is due to blockade of iNOS expression and inhibition of PGE_2, TNFα and NO production [263]. Moreover, EGb 761 was shown to be beneficial in the prevention and treatment of mouse colitis by suppression of macrophage activation combined with a downregulation of several inflammatory markers (iNOS, COX-2 and TNFα) [264]. Since several GBEs are available standardized on different constituents with different amounts, the anti-inflammatory effects can not be explicit inferred. Notable, no adverse effects of Ginkgo homeopathic mother tinctures have been reported so far [170], although they contain 2.2% of ginkgolic acids which is about 22,000 ppm [265]. However, no studies in animal models of inflammation were performed for ginkgolic acid so far and nothing is known about its bioavailability.

Taken together, ginkgolic acid could be identified as potent dual inhibitor of mPGES-1 and 5-LO with weaker anti-COX-1 activity. High plasma protein binding probably due to its lipophilic character, lead to a loss of efficacy in human whole blood. However, *in vivo* studies of ginkgolic acid will be necessary to define its anti-inflammatory and allergenic potential and composition of *ginkgo biloba* extracts may need to be reconsidered then.

4.6   Synthetic-derivatives of acid-modified NSAIDs as mPGES-1 inhibitors

NSAID administration is considered as the "medication of choice" in the treatment of inflammatory diseases. In view of severe side effects particularly on long-term application, there is still a need for the development of "saver drugs" [266].

Structural modification of NSAIDs, like replacement of the carboxylic acid functionality by substituted sulphonamide moieties, has turned out to be a useful approach in the development of dual mPGES-1/5-LO inhibitors with impaired COX activity [82]. This has already been demonstrated by the example of the advanced dual 5-LO/COX inhibitor licofelone [82].

SAR studies with several NSAIDs (ibuprofen, ketoprofen, naproxen, indomethacin and lonazolac) yielded derivatives of lonazolac and indomethacin as new leads for dual mPGES-1/5-LO inhibitors with reduced COX-1 activity. The classical NSAIDs did not show any inhibition of mPGES-1 or 5-LO up to 10 µM. Introduction of lipophilic residues enhanced the inhibitory potential towards mPGES-1/5-LO inhibition. Most

potent inhibitor of mPGES-1/5-LO in this series was the chlorphenylsulfonamid and substituted phenylacetylene derivative **36g** (IC$_{50}$ values of 0.16 µM and 3.7 µM, respectively). The phenylacetylene substituted indomethacin derivative **35f** was most efficient with respect to 5-LO inhibition (IC$_{50}$ = 0.9 µM). Additionally, impaired COX activity could be demonstrated for all potent candidates.

Taken together, structural modifications of acidic NSAIDs by substituted sulphonamide residues have proved to yield (I) advanced mPGES-1 and 5-LO inhibitors with IC$_{50}$ values in the nanomolar to submicromolar range and (II) a reduced COX activity, which is attributed to an improved severe side effect profile [178].

5   SUMMARY

Prostaglandin (PG)E$_2$ is a bioactive lipid mediator derived from the cyclooxygenase (COX) pathway and exerts various physiological and pathological actions depending on the amount of PGE$_2$ and the subtype of receptor (EP1-4) available within the respective tissue. PGE$_2$ is deemed to play a key role in inflammatory events. Three terminal synthases that catalyze PGE$_2$ formation from COX-derived PGH$_2$ are known. The inducible microsomal PGE$_2$ synthase-1 (mPGES-1) is considered as the predominant isoform that is involved in pathophysiological PGE$_2$ formation. By now, multiple diverse structures of mPGES-1 inhibitors are described in literature, but no selective mPGES-1 inhibitor is available for clinical use.

Leukotrienes (LTs) are derived from arachidonic acid (AA) by the conversion of 5-Lipoxygenase (5-LO) and act through their corresponding receptors. LTs are known to be involved in several pathologies, including allergic and inflammatory diseases. Inhibition of 5-LO product biosynthesis can be achieved by direct inhibition of 5-LO or antagonism of FLAP and cPLA$_2$. By now, zileuton is the only 5-LO inhibitor that has entered the market.

Current research outcomes propose a dual inhibition of mPGES-1 and 5-LO as a promising strategy in the therapy of inflammation to avoid ordinary side effects of classical NSAIDs or coxibs and therefore improve the safety profile of anti-inflammatory drugs.

This study identified a number of natural compounds and synthetic derivatives that were identified as potent mPGES-1 and 5-LO inhibitors. Promising candidates were additionally characterized within the AA cascade.

Arzanol is a major bioactive constituent of the mediterranean curry plant (*Helichrysum italicum*), which possesses anti-inflammatory properties. Arzanol was reported to inhibit the release of PGE_2 from LPS stimulated human monocytes, but the underlying molecular mechanism have not been fully clarified. Inhibition of mPGES-1[¶] (IC_{50}= 0.3 µM) and 5-LO[¶] (IC_{50}= 3.4 µM) was identified in 2009 as a part of my diploma thesis. Here, the interference within the AA cascade was investigated additionally yielding TXAS (IC_{50}= 2.7 µM) as molecular target of arzanol. Inhibition of PGE_2, TXB_2 and LT biosynthesis was also evident *in vitro* and partially *in vivo*. In studies using LPS stimulated human whole blood, PGE_2[¶] was concentration-dependently inhibited by arzanol, whereas the formation of TXB_2, 6-ketoPGF_{1a} and LTs were not affected. In a model of carrageenan-induced pleurisy in rats intraperitoneal application of arzanol was almost as effective as the NSAID indomethacin. Thus, arzanol highly contributes to the anti-inflammatory potential of *Helichrysum italicum* and represents a promising candidate in the therapy of inflammation and cancer.

Structure activity relationship (SAR) studies were performed to improve the anti-inflammatory potency of arzanol. Introduction of a lipophilic n-hexyl residue to the alkylidene linker resulted in the derivative **1e** that inhibited mPGES-1 (IC_{50}= 0.2 µM), 5-LO (IC_{50}= 1.2 µM) and TXAS (IC_{50}= 2.5 µM) with higher potency. Additionally **1e** moderately affected isolated COX-2 activity (IC_{50} > 10 µM). The inhibitory potential of **1e** was also evident *in vitro*, but **1e** failed to suppress PG and LT formation *in vivo* using human whole blood.

Cannabis sativa possesses well known anti-inflammatory properties, which can not yet be clearly verified to its constituents. In this study, investigation of several phytocannabinoid and non-cannabinoid constituents identified CBG, CFA and CFB to block the conversion of PGH_2 to PGE_2 mediated by mPGES-1 (IC_{50}= 0.9, 1.8 and 3.7 µM, respectively). CFA was additionally investigated as potent inhibitor of semi-purified 5-LO (IC_{50}= 0.95 µM) and cell-free TXAS (IC_{50}= 6.8 µM), whereas 12-HHT formation in intact human platelets and isolated COX-1 and -2 was hardly affected (IC_{50} >10 µM). The effectiveness of CFA was also evident *in vitro*. In intact human monocytes TXB_2 and PGE_2 formation was suppressed after LPS stimulation by synergistic effects of mPGES-1 and TXAS inhibition and blockage of COX-2 expression. Inhibition of 5-LO product formation in intact neutrophils (IC_{50}= 1.6 – 2.4 µM) resulted in a slight decrease compared to the effects observed from semi-purified 5-LO. But no efficiency was observed on PG and LT formation *in vivo* using human whole blood probably due to the lipophilic properties of CFA. Together, CFA has a promising anti-inflammatory profile that requires further *in vivo* investigation.

Depsides and depsidones exclusively occur in *lichen* species that have been traditionally used for the treatment of inflammatory disorders. In this thesis, a dual inhibition of mPGES-1 derived PGE_2 formation and 5-LO product formation could be identified for the depsides perlatolic acid (IC_{50}= 0.4 µM, equal potency) and olivetoric acid (IC_{50}= 1.15 and 2.4 µM, respectively) as well as the depsidone physodic acid (IC_{50}= 0.43 and 2.4 µM, respectively). Further investigations revealed TXAS as molecular target of perlatolic and physodic acid (IC_{50}= 1.1 and 0.7 µM, respectively), whereas cell-free COX-1 and -2 and $cPLA_2$ activity was hardly (IC_{50} > 10 µM) or not affected. The mode of action is reversible and largely

independent of the substrate supply. In addition, effects on the expression of COX-2 could be identified to suppress pathophysiological PGE_2. Interference with leukotriene formation is mediated by (I) a direct inhibition of 5-LO (observed for perlatolic and physodic acid) and/or (II) a downregulation of 5-LO activity (observed for physodic acid via blockage of phosphorylation). A selective suppression of PGE_2 formation in a model of carrageenan induced pleurisy in rats is evident for perlatolic acid, whereby no inhibitory effects on LTB_4, TXB_2 and 6-ketoPGF_{1a} synthesis could be observed in *in vivo* studies with human whole blood. Thus, depsides and depsidones provide a rational basis for the anti-inflammatory effects of *lichen* species.

Ginkgo biloba is among the most widely used medicinal plants of the world and extracts are mostly standardized on terpene trilactones and flavonol glycosides that are deemed as the active constituents of the plant. Because the allergenic potential of alkylphenols is still disputed, ginkgolic acid was not yet investigated if it contributes to the anti-inflammatory potential of the plant. Notable, no adverse effects of Ginkgo homeopathic mother tinctures have been reported so far, although they contain 2.2% of ginkgolic acids which is about 22,000 ppm. This study identified mPGES-1 (IC_{50}= 0.7 µM), 5-LO (IC_{50}= 0.3 µM), COX-1 (IC_{50}= 8.1 µM) and TXAS (IC_{50}= 5.2 µM) as molecular targets of ginkgolic acid, whereby inhibition of mPGES-1 and 5-LO is about 10 fold selective compared to COX-1 and TXAS. Gingkolic acid suppressed the formation of PGE_2 and 5-LO products in a direct and reversible mode of action under cell-free conditions. Inhibition of PGE_2 synthesis in LPS stimulated intact monocytes could be demonstrated by synergistic inhibitory effects on mPGES-1 activity and COX-2 expression. Ginkgolic acid concentration-dependently blocked 12-HHT and TXB_2 formation equally well in intact

platelets due to its inhibitory effects on TXAS and COX-1 activity and investigations in intact human neutrophils reveal that 5-LO product formation is comparably blocked independent of the substrate supply. Minimal cytotoxic effects were observed after 24 h but not 48 h, which confirmed current findings described in literature. Likely because of its lipophilic character no inhibitory effects on PG and LT biosynthesis *in vivo* in human whole blood were observed for gingkolic acid. Therefore, further *in vivo* studies of ginkgolic acid will be necessary to define its anti-inflammatory role and allergenic potential.

6   ZUSAMMENFASSUNG

Prostaglandin (PG) E_2 ist ein biologisch aktiver, lipophiler Botenstoff der Cyclooxygenase (COX) Signalkaskade. Er ist an verschiedenen physiologischen und patho-physiologischen Vorgängen im Körper beteiligt. Die Wirkweise ist jeweils abhängig von der gebildeten PGE_2 Menge und dem Rezeptorsubtyp (EP1-4) am Gewebe. PGE_2 wird eine Schlüsselrolle im entzündlichen Geschehen zugesprochen. Drei terminale PGE_2 Synthasen sind bekannt, die PGE_2 aus dem COX Produkt PGH_2 katalysieren können. Dabei wird der induzierbaren mikrosomalen PGE_2 synthase-1 (mPGES-1) Isoform eine dominante Rolle im Entzündungsgeschehen zugesprochen. Mittlerweile sind diverse mPGES-1 Inhibitoren unterschiedlichster Strukturen in der Literatur beschrieben, allerdings steht noch kein selektiver mPGES-1 Hemmer für den klinischen Einsatz zur Verfügung.

Leukotriene (LTs) werden aus Arachidonsäure (AA) unter anderem durch die katalytische Aktivität der 5-Lipoxigenase (5-LO) gebildet und entfalten ihre Wirkung durch ihre entsprechenden Rezeptoren. LTs sind an verschiedenen pathogenen Vorgängen im Körper beteiligt, wie z.B. allergische und entzündliche Erkrankungen. Die Hemmung der 5-LO Produktbildung kann durch eine direkte Inhibition des Enzymes 5-LO oder durch einen Antagonismus an den Enzymen FLAP oder $cPLA_2$ erreicht werden. Bisher konnte nur der Wirkstoff Zileuton als direkter Hemmer der 5-LO auf den Markt gebracht werden.

Aktuellen Forschungsergebnissen zufolge handelt es sich bei der dualen Hemmung der Enzyme mPGES-1 und 5-LO um eine erfolgversprechende

Strategie in der antientzündlichen Therapie, da übliche Nebenwirkungen, die unter der Therapie mit klassischen NSAIDs oder Coxiben auftreten, hier vermieden werden können.

In dieser Doktorarbeit konnten mehrere Naturstoffe und/oder deren synthetische Derivate als potente mPGES-1/5-LO Inhibitoren identifiziert werden. Das Profil vielversprechender Kandidaten wurde zudem innerhalb der AA Kaskade umfassend charakterisiert.

Arzanol ist einer der Hauptinhaltsstoffe der mediterranen Curry Pflanze (*Helichrysum italicum*), die für ihre antientzündlichen Eigenschaften bekannt ist. In der Literatur ist bereits ein Einfluss auf die PGE_2 Freisetzung in LPS stimulierten Monozyten beschrieben, jedoch konnte der zugrunde liegende Mechanismus nicht abschließend geklärt werden. Eine direkte Hemmung der Enzyme mPGES-1[¶] ($IC_{50}= 0.3$ µM) und 5-LO[¶] ($IC_{50}= 3.4$ µM) konnte bereits 2009 als Teil meiner Diplomarbeit gezeigt werden. In dieser Arbeit wurde der Eingriff in die AA Kaskade näher untersucht, bei der zusätzlich TXAS ($IC_{50}= 2.7$ µM) als molekulares Target identifizieren konnte. Mechanistische Studien ergaben, dass es sich bei Arzanol um einen reversiblen Inhibitor der Enzyme mPGES-1 und 5-LO handelt, der zudem unabhängig von der Substratkonzentration ist. Die Hemmung der Biosynthese von PGE_2, TXB_2 und LTs konnte *in vitro* und teilweise *in vivo* bestätigt werden. Arzanol inhibierte die mPGES-1 vermittelte PGE_2 Bildung in intakten Monozyten und A549 Zellen[¶] sowie in LPS stimuliertem humanem Vollblut[¶]. Zudem konnte auch eine Hemmung der TXB_2 Bildung in intakten Thrombozyten ($IC_{50}= 2.9$ µM) und eine Hemmung der 5-LO Produktbildung in intakten neutrophilen Granulozyten ($IC_{50}= 2.4 - 2.9$ µM) nachgewiesen werden. Studien mit LPS stimuliertem humanem Vollblut zeigten eine konzentrationsabhängige

Hemmung der PGE_2 Bildung durch Arzanol, wohingegen die TXB_2, 6-ketoPGF$_{1a}$ und LT Bildung nicht beeinflusst wurde. Die intraperitoneale Applikation von Arzanol erwies sich im Tiermodell der Carrageen induzierten Brustfellentzündung in Ratten als nahezu ebenbürtig zu Indomethacin. Somit gilt Arzanol als vielversprechender Kandidat in der Entzündungs- und Krebstherapie.

Struktur-Wirkungs-Beziehungen wurden durchgeführt, um die Wirksamkeit von Arzanol noch zu steigern. Die Einführung einer n-hexyl-Seitenkette an der Alkylidenverbindung (Verbindung **1e**) zeigte ein deutlich verbessertes inhibtorisches Potential auf mPGES-1 (IC$_{50}$= 0.2 µM), 5-LO (IC$_{50}$= 1.2 µM) und TXAS (IC$_{50}$= 2.5 µM). Zusätzlich wurde für **1e** eine moderate Hemmung der isolierten COX-2 (IC$_{50}$ > 10 µM) nachgewiesen. **1e** erwies sich auch *in vitro* als wirksame Substanz, jedoch konnte in *in vivo* Untersuchungen mit humanem Vollblut keine Wirkung mehr auf die PG und LT Bildung nachgewiesen werden.

Cannabis sativa verfügt über bekannte antientzündliche Eigenschaften, die jedoch nicht eindeutig ihren Inhaltsstoffen zugeordnet werden können. In dieser Arbeit wurden verschiedene pflanzliche cannabinoide und nicht-cannabinoide Bestandteile auf ihre antientzündlichen Eigenschaften hin untersucht. Für CBG, CFA und CFB konnte eine Hemmung der mPGES-1 vermittelten PGE_2 Synthese in mikrosomalen Präparationen aus IL-1ß stimulierten A49 Zellen nachgewiesen werden mit entsprechenden IC$_{50}$ Werten von 0.9, 1.8 und 3.7 µM. Eine direkte Hemmung der aufgereinigten 5-LO (IC$_{50}$= 0.95 µM) und der zellfreien TXAS (IC$_{50}$= 6.8 µM) konnte zusätzlich für CFA gezeigt werden, wobei eine die Bildung von 12-HHT, als Marker der COX-1 und -2 Aktivität, in intakten Thrombozyten und am isolierten Enzym kaum beeinflusst wurde (IC$_{50}$ > 10 µM). Deutlich konnte die Wirksamkeit von CFA auch *in vitro* nachgewiesen werden. In intakten,

humanen Monozyten konnte die Hemmung der TXB_2 und PGE_2 Biosynthese nach pro-inflammatorischer Stimulation mit LPS durch synergistische Einflüsse auf die mPGES-1 und TXAS Aktivität sowie die COX-2 Expression nachgewiesen werden. In intakten neutrophilen Granulozyten wurde die Hemmung der 5-LO Produktsynthese durch CFA mit einem geringen Wirkverlust (IC_{50}= 1.6 – 2.4 µM) nachgewiesen verglichen mit den Effekten am isolierten Enzym. Allerdings konnte kein Effekt mehr auf die PG und LT Synthese *in vivo* in humanem Vollblut nachgewiesen werden. Wahrscheinlich gilt hierfür der lipophile Säurecharakter von CFA, der für eine ausgeprägte Plasmaproteinbindung verantwortlich sein kann. Zusammen genommen verfügt CFA über ein vielversprechendes antientzündliches Profil, welches jedoch noch weiterer *in vivo* Untersuchungen bedarf.

Depside und Depsidone kommen ausschließlich in Flechtenarten vor. Diese wurden bereits volksmedizinisch zur Behandlung entzündlicher Erkrankungen verwendet. In der vorliegenden Arbeit konnte eine duale Hemmung der mPGES-1 vermittelten PGE_2 Synthese und der 5-LO vermittelten Produktbildung für die Depside Perlatolsäure (IC_{50}= 0.4 µM, für beide Enzyme) und Olivetolsäure (IC_{50}= 1.15 bzw. 2.4 µM), sowie für das Depsidon Physodsäure (IC_{50}= 0.43 bzw. 2.4 µM) nachgewiesen werden. In weiteren Untersuchungen konnte TXAS als molekulare Zielstruktur von Perlatol- und Physodsäure (IC_{50}= 1.1 bzw. 0.7 µM) aufgeklärt werden. Ein direkter Einfluss auf die COX-1 oder -2 Aktivität sowie die $cPLA_2$ Aktivität konnte dagegen nicht oder nur kaum (IC_{50} > 10 µM) nachgewiesen werden. Die Wirkungsweise von Perlatol- und Physodsäure auf die Enzyme mPGES-1 und 5-LO ist reversibel weitestgehend unabhängig dem Substratangebot. Zudem konnte ein Einfluss auf die Expression der COX-2 nachgewiesen werden. Die

Hemmung der LT Bildung *in vitro* wird durch einen direkten Angriff am Enzym 5-LO (konnte für Perlatol- und Physodsäure beobachtet werden) und eine Herunterregulierung der 5-LO Aktivität (beobachtet für Physodsäure durch Eingriff in die Phosphorylierungskaskade) hervorgerufen. *In vivo* konnte eine selektive Hemmung der PGE_2 Biosynthese im Tiermodell der Carrageen-induzierten Brustfellentzündung in Ratten für Perlatolsäure nachgewiesen werden. Effekte auf die LTB_4, TXB_2 und 6-ketoPGF_{1a} Synthese konnten dagegen in humanem Vollblut nicht beobachtet werden. Somit lässt sich zusammenfassend sagen, dass Depside und Depsidone, vorallem Perlatol- und Physodsäure, sehr wahrscheinlich an der antientzündlichen Wirkung diverser Flechtenarten beteiligt sind.

Ginkgo biloba zählt zu den weltweit am häufigsten verwendeten Arzneipflanzen. Extrakte dieser Pflanze werden meist auf die für die Wirkung verantwortlich geltenden terpentrilaktonischen und flavonolglykosidischen Bestandteile standardisiert. Da ein allergenes Potential für Alklphenole noch immer umstritten ist, wurde Ginkgolsäure noch nicht auf mögliche antientzündliche Eigenschaften hin untersucht. Interessanterweise wurden für die homöopathische Ginkgo Urtinktur, welche große Mengen an Ginkgolsäuren enthält, bisher keine Nebenwirkungen gemeldet. In der vorliegenden Doktorarbeit konnten die Enzyme mPGES-1 ($IC_{50}= 0.7$ µM), 5-LO ($IC_{50}= 0.3$ µM), COX-1 ($IC_{50}= 8.1$ µM) und TXAS ($IC_{50}= 5.2$ µM) als molekulare Zielstrukturen der Ginkgolsäure identifiziert werden, wobei die duale mPGES-1/5-LO Inhibition etwa 10-fach potenter als die COX-1 und TXAS Hemmung auftrat. Ginkgolsäure ist ein direkter und reversibler Hemmer der PGE_2 und 5-LO Produktbildung. In LPS stimulierten Monozyten inhibierte Ginkgolsäure die PGE_2 Bildung durch synergistische Effekte auf die

mPGES-1 Aktivität und COX-2 Expression. Eine konzentrationsabhängige Unterdrückung der 12-HHT und TXB_2 Bildung in intakten Thrombozyten infolge der direkten COX-1 und TXAS Hemmung konnte beobachtet werden. Untersuchungen in intakten neutrophilen Granulozyten zeigen eine vergleichbare Hemmung der 5-LO Produktbildung unabhängig von der verfügbaren Substratkonzentration. Minimale zytotoxische Effekte auf die Zellvitalität nach 24 Stunden konnten beobachtet werden die jedoch nach 48 Stunden nicht mehr nachweisbar waren. Dieser Effekt wurde bereits in der Literatur beschrieben. Wahrscheinlich auf Grund der lipophilen Eigenschaften der Ginkgolsäure, konnten die beobachteten Effekte auf die PG und LT Biosynthese *in vivo* in humanem Vollblut nicht bestätigt werden. Somit sind weitere *in vivo* Untersuchungen notwendig, um das allergene Potential und eine mögliche antientzündliche Rolle im genau zu bestimmen.

7   REFERENCES

1.   Nathan, C., *Points of control in inflammation.* Nature, 2002. 420(6917): p. 846-52.

2.   Murakami, M., *Lipid mediators in life science.* Exp Anim, 2011. 60(1): p. 7-20.

3.   Ricciotti, E. and G.A. FitzGerald, *Prostaglandins and inflammation.* Arterioscler Thromb Vasc Biol, 2011. 31(5): p. 986-1000.

4.   Mantovani, A., et al., *Cancer-related inflammation.* Nature, 2008. 454(7203): p. 436-44.

5.   Coussens, L.M. and Z. Werb, *Inflammation and cancer.* Nature, 2002. 420(6917): p. 860-7.

6.   Coussens, L.M., et al., *MMP-9 supplied by bone marrow-derived cells contributes to skin carcinogenesis.* Cell, 2000. 103(3): p. 481-90.

7.   Lin, E.Y., et al., *Colony-stimulating factor 1 promotes progression of mammary tumors to malignancy.* J Exp Med, 2001. 193(6): p. 727-40.

8.   Mantovani, A., et al., *The origin and function of tumor-associated macrophages.* Immunol Today, 1992. 13(7): p. 265-70.

9.   Chan, A.T., et al., *A prospective study of aspirin use and the risk for colorectal adenoma.* Annals of Internal Medicine, 2004. 140(3): p. 157-166.

10.   Flossmann, E. and P.M. Rothwell, *Effect of aspirin on long-term risk of colorectal cancer: consistent evidence from randomised and observational studies.* Lancet, 2007. 369(9573): p. 1603-13.

11.   Koehne, C.H. and R.N. Dubois, *COX-2 inhibition and colorectal cancer.* Semin Oncol, 2004. 31(2 Suppl 7): p. 12-21.

12.   Porta, C., et al., *Cellular and molecular pathways linking inflammation and cancer.* Immunobiology, 2009. 214(9-10): p. 761-77.

13.   ;   Available   from:
http://www.nobelprize.org/nobel_prizes/medicine/laureates/1982/index.html.

14.   Funk, C.D., *Prostaglandins and leukotrienes: advances in eicosanoid biology.* Science, 2001. 294(5548): p. 1871-5.

15.   Legler, D.F., et al., *Prostaglandin E2 at new glance: novel insights in functional diversity offer therapeutic chances.* Int J Biochem Cell Biol, 2010. 42(2): p. 198-201.

16.   Nakanishi, M. and D.W. Rosenberg, *Multifaceted roles of PGE2 in inflammation and cancer.* Semin Immunopathol, 2013. 35(2): p. 123-37.

17.   Laufer, S., S. Gay, and K. Brune, *Inflammation and rheumatic diseases. The molecular basis of novel therapies*. 2003: Thieme Verlag.

18.   Powell, W.S., *COX and LOX pathway*, m. pathway, Editor.

19.   Vane, J.R. and R.M. Botting, *The mechanism of action of aspirin.* Thromb Res, 2003. 110(5-6): p. 255-8.

20.   Koeberle, A. and O. Werz, *Inhibitors of the microsomal prostaglandin E(2) synthase-1 as alternative to non steroidal anti-inflammatory drugs (NSAIDs)--a critical review.* Curr Med Chem, 2009. 16(32): p. 4274-96.

21.   Dey, I., M. Lejeune, and K. Chadee, *Prostaglandin E2 receptor distribution and function in the gastrointestinal tract.* Br J Pharmacol, 2006. 149(6): p. 611-23.

22.   Kobayashi, T. and S. Narumiya, *Function of prostanoid receptors: studies on knockout mice.* Prostaglandins Other Lipid Mediat, 2002. 68-69: p. 557-73.

23.   Park, J.Y., M.H. Pillinger, and S.B. Abramson, *Prostaglandin E2 synthesis and secretion: the role of PGE2 synthases.* Clin Immunol, 2006. 119(3): p. 229-40.

24.   Timmers, L., G. Pasterkamp, and D.P. de Kleijn, *Microsomal prostaglandin E2 synthase: a safer target than cyclooxygenases?* Mol Interv, 2007. 7(4): p. 195-9, 180.

25.   Samuelsson, B., R. Morgenstern, and P.J. Jakobsson, *Membrane prostaglandin E synthase-1: a novel therapeutic target.* Pharmacol Rev, 2007. 59(3): p. 207-24.

26.   Murakami, M., et al., *Cellular prostaglandin E2 production by membrane-bound prostaglandin E synthase-2 via both cyclooxygenases-1 and -2.* J Biol Chem, 2003. 278(39): p. 37937-47.

27.   Tanioka, T., et al., *Molecular identification of cytosolic prostaglandin E2 synthase that is functionally coupled with cyclooxygenase-1 in immediate prostaglandin E2 biosynthesis.* J Biol Chem, 2000. 275(42): p. 32775-82.

28.   Smith, W.L., Y. Urade, and P.J. Jakobsson, *Enzymes of the cyclooxygenase pathways of prostanoid biosynthesis.* Chem Rev, 2011. 111(10): p. 5821-65.

29.   Thoren, S., et al., *Human microsomal prostaglandin E synthase-1: purification, functional characterization, and projection structure determination.* J Biol Chem, 2003. 278(25): p. 22199-209.

30.   Jakobsson, P.J., et al., *Identification of human prostaglandin E synthase: a microsomal, glutathione-dependent, inducible enzyme, constituting a potential novel drug target.* Proc Natl Acad Sci U S A, 1999. 96(13): p. 7220-5.

31.   Sjogren, T., et al., *Crystal structure of microsomal prostaglandin E2 synthase provides insight into diversity in the MAPEG superfamily.* Proc Natl Acad Sci U S A, 2013. 110(10): p. 3806-11.

32.   Forsberg, L., et al., *Human glutathione dependent prostaglandin E synthase: gene structure and regulation.* FEBS Lett, 2000. 471(1): p. 78-82.

33.   Thoren, S. and P.J. Jakobsson, *Coordinate up- and down-regulation of glutathione-dependent prostaglandin E synthase and cyclooxygenase-2 in A549 cells. Inhibition by NS-398 and leukotriene C4.* Eur J Biochem, 2000. 267(21): p. 6428-34.

34.   Murakami, M., et al., *Regulation of prostaglandin E2 biosynthesis by inducible membrane-associated prostaglandin E2 synthase that acts in concert with cyclooxygenase-2.* J Biol Chem, 2000. 275(42): p. 32783-92.

35.   Uracz, W., et al., *Interleukin 1beta induces functional prostaglandin E synthase in cultured human umbilical vein endothelial cells.* J Physiol Pharmacol, 2002. 53(4 Pt 1): p. 643-54.

36.   Mancini, J.A., et al., *Cloning, expression, and up-regulation of inducible rat prostaglandin e synthase during lipopolysaccharide-induced pyresis and adjuvant-induced arthritis.* J Biol Chem, 2001. 276(6): p. 4469-75.

37.   Stichtenoth, D.O., et al., *Microsomal prostaglandin E synthase is regulated by proinflammatory cytokines and glucocorticoids in primary rheumatoid synovial cells.* J Immunol, 2001. 167(1): p. 469-74.

38.   Westman, M., et al., *Expression of microsomal prostaglandin E synthase 1 in rheumatoid arthritis synovium.* Arthritis Rheum, 2004. 50(6): p. 1774-80.

39.   Kojima, F., et al., *Coexpression of microsomal prostaglandin E synthase with cyclooxygenase-2 in human rheumatoid synovial cells.* J Rheumatol, 2002. 29(9): p. 1836-42.

40.   Kojima, F., et al., *Membrane-associated prostaglandin E synthase-1 is upregulated by proinflammatory cytokines in chondrocytes from patients with osteoarthritis.* Arthritis Res Ther, 2004. 6(4): p. R355-65.

41.   Masuko-Hongo, K., et al., *Up-regulation of microsomal prostaglandin E synthase 1 in osteoarthritic human cartilage: critical roles of the ERK-1/2 and p38 signaling pathways.* Arthritis Rheum, 2004. 50(9): p. 2829-38.

42.   Li, X., et al., *Expression and regulation of microsomal prostaglandin E synthase-1 in human osteoarthritic cartilage and chondrocytes.* J Rheumatol, 2005. 32(5): p. 887-95.

43.   Subbaramaiah, K., et al., *Microsomal prostaglandin E synthase-1 is overexpressed in inflammatory bowel disease. Evidence for involvement of the transcription factor Egr-1.* J Biol Chem, 2004. 279(13): p. 12647-58.

44. Cipollone, F., et al., *Overexpression of functionally coupled cyclooxygenase-2 and prostaglandin E synthase in symptomatic atherosclerotic plaques as a basis of prostaglandin E(2)-dependent plaque instability.* Circulation, 2001. 104(8): p. 921-7.

45. Cipollone, F., et al., *The receptor RAGE as a progression factor amplifying arachidonate-dependent inflammatory and proteolytic response in human atherosclerotic plaques: role of glycemic control.* Circulation, 2003. 108(9): p. 1070-7.

46. Gomez-Hernandez, A., et al., *Overexpression of COX-2, Prostaglandin E synthase-1 and prostaglandin E receptors in blood mononuclear cells and plaque of patients with carotid atherosclerosis: regulation by nuclear factor-kappaB.* Atherosclerosis, 2006. 187(1): p. 139-49.

47. Chaudhry, U.A., et al., *Elevated microsomal prostaglandin-E synthase-1 in Alzheimer's disease.* Alzheimers Dement, 2008. 4(1): p. 6-13.

48. Korotkova, M., et al., *Effects of immunosuppressive treatment on microsomal prostaglandin E synthase 1 and cyclooxygenases expression in muscle tissue of patients with polymyositis or dermatomyositis.* Ann Rheum Dis, 2008. 67(11): p. 1596-602.

49. Bage, T., et al., *Expression of prostaglandin E synthases in periodontitis immunolocalization and cellular regulation.* Am J Pathol, 2011. 178(4): p. 1676-88.

50. Kihara, Y., et al., *Targeted lipidomics reveals mPGES-1-PGE2 as a therapeutic target for multiple sclerosis.* Proc Natl Acad Sci U S A, 2009. 106(51): p. 21807-12.

51. Nakanishi, M., et al., *mPGES-1 as a target for cancer suppression: A comprehensive invited review "Phospholipase A2 and lipid mediators".* Biochimie, 2010. 92(6): p. 660-4.

52.   Sampey, A.V., S. Monrad, and L.J. Crofford, *Microsomal prostaglandin E synthase-1: the inducible synthase for prostaglandin E2.* Arthritis Res Ther, 2005. 7(3): p. 114-7.

53.   Boulet, L., et al., *Deletion of microsomal prostaglandin E2 (PGE2) synthase-1 reduces inducible and basal PGE2 production and alters the gastric prostanoid profile.* J Biol Chem, 2004. 279(22): p. 23229-37.

54.   Kamei, D., et al., *Reduced pain hypersensitivity and inflammation in mice lacking microsomal prostaglandin e synthase-1.* J Biol Chem, 2004. 279(32): p. 33684-95.

55.   Guay, J., et al., *Carrageenan-induced paw edema in rat elicits a predominant prostaglandin E2 (PGE2) response in the central nervous system associated with the induction of microsomal PGE2 synthase-1.* J Biol Chem, 2004. 279(23): p. 24866-72.

56.   Claveau, D., et al., *Microsomal prostaglandin E synthase-1 is a major terminal synthase that is selectively up-regulated during cyclooxygenase-2-dependent prostaglandin E2 production in the rat adjuvant-induced arthritis model.* J Immunol, 2003. 170(9): p. 4738-44.

57.   Trebino, C.E., et al., *Impaired inflammatory and pain responses in mice lacking an inducible prostaglandin E synthase.* Proc Natl Acad Sci U S A, 2003. 100(15): p. 9044-9.

58.   Uematsu, S., et al., *Lipopolysaccharide-dependent prostaglandin E(2) production is regulated by the glutathione-dependent prostaglandin E(2) synthase gene induced by the Toll-like receptor 4/MyD88/NF-IL6 pathway.* J Immunol, 2002. 168(11): p. 5811-6.

59.   Wang, M., et al., *Deletion of microsomal prostaglandin E synthase-1 augments prostacyclin and retards atherogenesis.* Proc Natl Acad Sci U S A, 2006. 103(39): p. 14507-12.

60.   Engblom, D., et al., *Microsomal prostaglandin E synthase-1 is the central switch during immune-induced pyresis.* Nat Neurosci, 2003. 6(11): p. 1137-8.

61.   Hofstetter, A.O., et al., *The induced prostaglandin E2 pathway is a key regulator of the respiratory response to infection and hypoxia in neonates.* Proc Natl Acad Sci U S A, 2007. 104(23): p. 9894-9.

62.   Akitake, Y., et al., *Microsomal prostaglandin E synthase-1 is induced in alzheimer's disease and its deletion mitigates alzheimer's disease-like pathology in a mouse model.* J Neurosci Res, 2013. 91(7): p. 909-19.

63.   Kamei, D., et al., *Microsomal prostaglandin E synthase-1 in both cancer cells and hosts contributes to tumour growth, invasion and metastasis.* Biochem J, 2010. 425(2): p. 361-71.

64.   Nakanishi, M., et al., *Genetic deletion of mPGES-1 suppresses intestinal tumorigenesis.* Cancer Res, 2008. 68(9): p. 3251-9.

65.   Sugimoto, Y. and S. Narumiya, *Prostaglandin E receptors.* J Biol Chem, 2007. 282(16): p. 11613-7.

66.   Moriyama, T., et al., *Sensitization of TRPV1 by EP1 and IP reveals peripheral nociceptive mechanism of prostaglandins.* Mol Pain, 2005. 1: p. 3.

67.   Stock, J.L., et al., *The prostaglandin E2 EP1 receptor mediates pain perception and regulates blood pressure.* J Clin Invest, 2001. 107(3): p. 325-31.

68.   Yuhki, K., et al., *Prostaglandin receptors EP2, EP3, and IP mediate exudate formation in carrageenin-induced mouse pleurisy.* J Pharmacol Exp Ther, 2004. 311(3): p. 1218-24.

69.   Honda, T., et al., *Prostacyclin-IP signaling and prostaglandin E2-EP2/EP4 signaling both mediate joint inflammation in mouse collagen-induced arthritis.* J Exp Med, 2006. 203(2): p. 325-35.

70.   Portanova, J.P., et al., *Selective neutralization of prostaglandin E2 blocks inflammation, hyperalgesia, and interleukin 6 production in vivo.* J Exp Med, 1996. 184(3): p. 883-91.

71.   Yang, L., et al., *Cancer-associated immunodeficiency and dendritic cell abnormalities mediated by the prostaglandin EP2 receptor.* J Clin Invest, 2003. 111(5): p. 727-35.

72.   Aronoff, D.M., C. Canetti, and M. Peters-Golden, *Prostaglandin E2 inhibits alveolar macrophage phagocytosis through an E-prostanoid 2 receptor-mediated increase in intracellular cyclic AMP.* J Immunol, 2004. 173(1): p. 559-65.

73.   Kunikata, T., et al., *Suppression of allergic inflammation by the prostaglandin E receptor subtype EP3.* Nat Immunol, 2005. 6(5): p. 524-31.

74.   Yamane, H., et al., *Prostaglandin E(2) receptors, EP2 and EP4, differentially modulate TNF-alpha and IL-6 production induced by lipopolysaccharide in mouse peritoneal neutrophils.* Biochem Biophys Res Commun, 2000. 278(1): p. 224-8.

75.   Fennekohl, A., et al., *Contribution of the two Gs-coupled PGE2-receptors EP2-receptor and EP4-receptor to the inhibition by PGE2 of the LPS-induced TNFalpha-formation in Kupffer cells from EP2-or EP4-receptor-deficient mice. Pivotal role for the EP4-receptor in wild type Kupffer cells.* J Hepatol, 2002. 36(3): p. 328-34.

76.   Wu, D., et al., *The effects of microsomal prostaglandin E synthase-1 deletion in acute cardiac ischemia in mice.* Prostaglandins Leukot Essent Fatty Acids, 2009. 81(1): p. 31-3.

77.   Degousee, N., et al., *Microsomal prostaglandin E2 synthase-1 deletion leads to adverse left ventricular remodeling after myocardial infarction.* Circulation, 2008. 117(13): p. 1701-10.

78.   Chang, H.H. and E.J. Meuillet, *Identification and development of mPGES-1 inhibitors: where we are at?* Future Med Chem, 2011. 3(15): p. 1909-34.

79.   Bannenberg, G., et al., *Leukotriene C4 is a tight-binding inhibitor of microsomal glutathione transferase-1. Effects of leukotriene pathway modifiers.* J Biol Chem, 1999. 274(4): p. 1994-9.

80.   Quraishi, O., J.A. Mancini, and D. Riendeau, *Inhibition of inducible prostaglandin E(2) synthase by 15-deoxy-Delta(12,14)-prostaglandin J(2) and polyunsaturated fatty acids.* Biochem Pharmacol, 2002. 63(6): p. 1183-9.

81.   Wobst, I., et al., *Dimethylcelecoxib inhibits prostaglandin E2 production.* Biochem Pharmacol, 2008. 76(1): p. 62-9.

82.   Koeberle, A., et al., *Licofelone suppresses prostaglandin E2 formation by interference with the inducible microsomal prostaglandin E2 synthase-1.* J Pharmacol Exp Ther, 2008. 326(3): p. 975-82.

83.   Koeberle, A., H. Northoff, and O. Werz, *Curcumin blocks prostaglandin E2 biosynthesis through direct inhibition of the microsomal prostaglandin E2 synthase-1.* Mol Cancer Ther, 2009. 8(8): p. 2348-55.

84.   Koeberle, A., et al., *Green tea epigallocatechin-3-gallate inhibits microsomal prostaglandin E(2) synthase-1.* Biochem Biophys Res Commun, 2009. 388(2): p. 350-4.

85.   Koeberle, A., H. Northoff, and O. Werz, *Identification of 5-lipoxygenase and microsomal prostaglandin E2 synthase-1 as functional targets of the anti-inflammatory and anti-carcinogenic garcinol.* Biochem Pharmacol, 2009. 77(9): p. 1513-21.

86.   Koeberle, A., et al., *Myrtucommulone, a natural acylphloroglucinol, inhibits microsomal prostaglandin E(2) synthase-1.* Br J Pharmacol, 2009. 156(6): p. 952-61.

87.   Siemoneit, U., et al., *Inhibition of microsomal prostaglandin E2 synthase-1 as a molecular basis for the anti-inflammatory actions of boswellic acids from frankincense.* Br J Pharmacol, 2011. 162(1): p. 147-62.

88.   Koeberle, A., et al., *Hyperforin, an Anti-Inflammatory Constituent from St. John's Wort, Inhibits Microsomal Prostaglandin E(2) Synthase-1 and Suppresses Prostaglandin E(2) Formation in vivo.* Front Pharmacol, 2011. 2: p. 7.

89.   Korotkova, M. and P.J. Jakobsson, *Characterization of mPGES-1 Inhibitors.* Basic Clin Pharmacol Toxicol, 2013.

90. Riendeau, D., et al., *Inhibitors of the inducible microsomal prostaglandin E2 synthase (mPGES-1) derived from MK-886.* Bioorg Med Chem Lett, 2005. 15(14): p. 3352-5.

91. Cote, B., et al., *Substituted phenanthrene imidazoles as potent, selective, and orally active mPGES-1 inhibitors.* Bioorg Med Chem Lett, 2007. 17(24): p. 6816-20.

92. Wu, T.Y., et al., *Biarylimidazoles as inhibitors of microsomal prostaglandin E2 synthase-1.* Bioorg Med Chem Lett, 2010. 20(23): p. 6978-82.

93. Koeberle, A., et al., *Pirinixic acid derivatives as novel dual inhibitors of microsomal prostaglandin E2 synthase-1 and 5-lipoxygenase.* J Med Chem, 2008. 51(24): p. 8068-76.

94. Greiner, C., et al., *Identification of 2-mercaptohexanoic acids as dual inhibitors of 5-lipoxygenase and microsomal prostaglandin E(2) synthase-1.* Bioorg Med Chem, 2011. 19(11): p. 3394-401.

95. Liedtke, A.J., et al., *Arylpyrrolizines as inhibitors of microsomal prostaglandin E2 synthase-1 (mPGES-1) or as dual inhibitors of mPGES-1 and 5-lipoxygenase (5-LOX).* J Med Chem, 2009. 52(15): p. 4968-72.

96. Karg, E.M., et al., *Structural optimization and biological evaluation of 2-substituted 5-hydroxyindole-3-carboxylates as potent inhibitors of human 5-lipoxygenase.* J Med Chem, 2009. 52(11): p. 3474-83.

97. Wang, J., et al., *Selective inducible microsomal prostaglandin E(2) synthase-1 (mPGES-1) inhibitors derived from an oxicam template.* Bioorg Med Chem Lett, 2010. 20(5): p. 1604-9.

98. Mbalaviele, G., et al., *Distinction of microsomal prostaglandin E synthase-1 (mPGES-1) inhibition from cyclooxygenase-2 inhibition in cells using a novel, selective mPGES-1 inhibitor.* Biochem Pharmacol, 2010. 79(10): p. 1445-54.

99. Chiasson, J.F., et al., *Trisubstituted ureas as potent and selective mPGES-1 inhibitors.* Bioorg Med Chem Lett, 2011. 21(5): p. 1488-92.

100. Bruno, A., et al., *Effects of AF3442 [N-(9-ethyl-9H-carbazol-3-yl)-2-(trifluoromethyl)benzamide], a novel inhibitor of human microsomal prostaglandin E synthase-1, on prostanoid biosynthesis in human monocytes in vitro.* Biochem Pharmacol, 2010. 79(7): p. 974-81.

101. Nickerson-Nutter, C.L. and E.D. Medvedeff, *The effect of leukotriene synthesis inhibitors in models of acute and chronic inflammation.* Arthritis Rheum, 1996. 39(3): p. 515-21.

102. Martel-Pelletier, J., et al., *Therapeutic role of dual inhibitors of 5-LOX and COX, selective and non-selective non-steroidal anti-inflammatory drugs.* Ann Rheum Dis, 2003. 62(6): p. 501-9.

103. Kulkarni, S.K. and V.P. Singh, *Positioning dual inhibitors in the treatment of pain and inflammatory disorders.* Inflammopharmacology, 2008. 16(1): p. 1-15.

104. Warner, T.D. and J.A. Mitchell, *Cyclooxygenases: new forms, new inhibitors, and lessons from the clinic.* FASEB J, 2004. 18(7): p. 790-804.

105. Bombardier, C., et al., *Comparison of upper gastrointestinal toxicity of rofecoxib and naproxen in patients with rheumatoid arthritis. VIGOR Study Group.* N Engl J Med, 2000. 343(21): p. 1520-8, 2 p following 1528.

106. Kuhn, H. and B.J. Thiele, *The diversity of the lipoxygenase family. Many sequence data but little information on biological significance.* FEBS Lett, 1999. 449(1): p. 7-11.

107. Pergola, C. and O. Werz, *5-Lipoxygenase inhibitors: a review of recent developments and patents.* Expert Opin Ther Pat, 2010. 20(3): p. 355-75.

108. Peters-Golden, M. and W.R. Henderson, Jr., *Leukotrienes.* N Engl J Med, 2007. 357(18): p. 1841-54.

109. Radmark, O., et al., *5-Lipoxygenase: regulation of expression and enzyme activity.* Trends Biochem Sci, 2007. 32(7): p. 332-41.

110.   Ochi, K., et al., *Arachidonate 5-lipoxygenase of guinea pig peritoneal polymorphonuclear leukocytes. Activation by adenosine 5'-triphosphate.* J Biol Chem, 1983. 258(9): p. 5754-8.

111.   Werz, O., et al., *5-lipoxygenase is phosphorylated by p38 kinase-dependent MAPKAP kinases.* Proc Natl Acad Sci U S A, 2000. 97(10): p. 5261-6.

112.   Werz, O., et al., *Extracellular signal-regulated kinases phosphorylate 5-lipoxygenase and stimulate 5-lipoxygenase product formation in leukocytes.* FASEB J, 2002. 16(11): p. 1441-3.

113.   Werz, O., et al., *Arachidonic acid promotes phosphorylation of 5-lipoxygenase at Ser-271 by MAPK-activated protein kinase 2 (MK2).* J Biol Chem, 2002. 277(17): p. 14793-800.

114.   Rouzer, C.A. and B. Samuelsson, *The importance of hydroperoxide activation for the detection and assay of mammalian 5-lipoxygenase.* FEBS Lett, 1986. 204(2): p. 293-6.

115.   Grant, G.E., J. Rokach, and W.S. Powell, *5-Oxo-ETE and the OXE receptor.* Prostaglandins Other Lipid Mediat, 2009. 89(3-4): p. 98-104.

116.   Chen, X.S., et al., *Role of leukotrienes revealed by targeted disruption of the 5-lipoxygenase gene.* Nature, 1994. 372(6502): p. 179-82.

117.   Sala, A., et al., *Anti-inflammatory and antioxidant properties of Helichrysum italicum.* J Pharm Pharmacol, 2002. 54(3): p. 365-71.

118.   Appendino, G., et al., *Arzanol, an anti-inflammatory and anti-HIV-1 phloroglucinol alpha-Pyrone from Helichrysum italicum ssp. microphyllum.* J Nat Prod, 2007. 70(4): p. 608-12.

119.   Mastelic, J., O. Politeo, and I. Jerkovic, *Contribution to the analysis of the essential oil of Helichrysum italicum (Roth) G. Don. Determination of ester bonded acids and phenols.* Molecules, 2008. 13(4): p. 795-803.

120.   Nostro, A., et al., *Effects of Helichrysum italicum extract on growth and enzymatic activity of Staphylococcus aureus.* Int J Antimicrob Agents, 2001. 17(6): p. 517-20.

121.   Angioni, A., et al., *Chemical composition, plant genetic differences, and antifungal activity of the essential oil of Helichrysum italicum G. Don ssp. microphyllum (Willd) Nym.* J Agric Food Chem, 2003. 51(4): p. 1030-4.

122.   Nostro, A., et al., *Evaluation of antiherpesvirus-1 and genotoxic activities of Helichrysum italicum extract.* New Microbiol, 2003. 26(1): p. 125-8.

123.   Orzalesi, G., T. Mezzetti, and V. Bellavita, *[A new natural triterpenic lactone, alpha-amyrin and uvaol from Helichrysum italicum (G. Don)].* Boll Chim Farm, 1969. 108(9): p. 540-5.

124.   Casinovi, C.G., et al., *[New beta-diketones from Helichrysum italicum G. Don].* Ann Ist Super Sanita, 1968. 4(3): p. 186-98.

125.   Facino, R.M., et al., *Phytochemical characterization and radical scavenger activity of flavonoids from Helichrysum italicum G. Don (Compositae).* Pharmacol Res, 1990. 22(6): p. 709-21.

126.   Sala, A., et al., *Assessment of the anti-inflammatory activity and free radical scavenger activity of tiliroside.* Eur J Pharmacol, 2003. 461(1): p. 53-61.

127.   Bianchini, A., et al., *Eudesm-5-en-11-ol from Helichrysum italicum essential oil.* Magn Reson Chem, 2004. 42(11): p. 983-4.

128.   Mancini, E., et al., *Chemical composition and possible in vitro phytotoxic activity of Helichrsyum italicum (Roth) Don ssp. italicum.* Molecules, 2011. 16(9): p. 7725-35.

129.   Rosa, A., et al., *Evaluation of the antioxidant and cytotoxic activity of arzanol, a prenylated alpha-pyrone-phloroglucinol etherodimer from Helichrysum italicum subsp.microphyllum.* Chem Biol Interact, 2007. 165(2): p. 117-26.

130. Minassi, A., et al., *A Multicomponent Carba-Betti Strategy to Alkylidene Heterodimers - Total Synthesis and Structure-Activity Relationships of Arzanol.* European Journal of Organic Chemistry, 2012(4): p. 772-779.

131. Bauer, J., et al., *Arzanol, a prenylated heterodimeric phloroglucinyl pyrone, inhibits eicosanoid biosynthesis and exhibits anti-inflammatory efficacy in vivo.* Biochem Pharmacol, 2011. 81(2): p. 259-68.

132. Zias, J., et al., *Early medical use of cannabis.* Nature, 1993. 363(6426): p. 215.

133. Kogan, N.M. and R. Mechoulam, *Cannabinoids in health and disease.* Dialogues Clin Neurosci, 2007. 9(4): p. 413-30.

134. Bohlmann, F. and E. Hoffmann, *Naturally Occurring Terpene Derivatives .208. Compounds from Helichrysum-Umbraculigerum Related to Cannabigerol.* Phytochemistry, 1979. 18(8): p. 1371-1374.

135. Appendino, G., G. Chianese, and O. Taglialatela-Scafati, *Cannabinoids: occurrence and medicinal chemistry.* Curr Med Chem, 2011. 18(7): p. 1085-99.

136. Buchweitz, J.P., et al., *Targeted deletion of cannabinoid receptors CB1 and CB2 produced enhanced inflammatory responses to influenza A/PR/8/34 in the absence and presence of Delta9-tetrahydrocannabinol.* J Leukoc Biol, 2008. 83(3): p. 785-96.

137. Fimiani, C., et al., *Opiate, cannabinoid, and eicosanoid signaling converges on common intracellular pathways nitric oxide coupling.* Prostaglandins Other Lipid Mediat, 1999. 57(1): p. 23-34.

138. Sumariwalla, P.F., et al., *A novel synthetic, nonpsychoactive cannabinoid acid (HU-320) with antiinflammatory properties in murine collagen-induced arthritis.* Arthritis Rheum, 2004. 50(3): p. 985-98.

139. Costa, B., et al., *Oral anti-inflammatory activity of cannabidiol, a non-psychoactive constituent of cannabis, in acute carrageenan-induced inflammation in the rat paw.* Naunyn Schmiedebergs Arch Pharmacol, 2004. 369(3): p. 294-9.

140.   Barrett, M.L., D. Gordon, and F.J. Evans, *Isolation from Cannabis sativa L. of cannflavin--a novel inhibitor of prostaglandin production.* Biochem Pharmacol, 1985. 34(11): p. 2019-24.

141.   Ruhaak, L.R., et al., *Evaluation of the cyclooxygenase inhibiting effects of six major cannabinoids isolated from Cannabis sativa.* Biol Pharm Bull, 2011. 34(5): p. 774-8.

142.   Takeda, S., et al., *Cannabidiolic acid as a selective cyclooxygenase-2 inhibitory component in cannabis.* Drug Metab Dispos, 2008. 36(9): p. 1917-21.

143.   Takeda, S., et al., *Delta9-tetrahydrocannabinol and its major metabolite Delta9-tetrahydrocannabinol-11-oic acid as 15-lipoxygenase inhibitors.* J Pharm Sci, 2011. 100(3): p. 1206-11.

144.   Muller, K., *Pharmaceutically relevant metabolites from lichens.* Appl Microbiol Biotechnol, 2001. 56(1-2): p. 9-16.

145.   Huneck, S., *The significance of lichens and their metabolites.* Naturwissenschaften, 1999. 86(12): p. 559-70.

146.   Sankawa, U., et al., *Depside as potent inhibitor of prostaglandin biosynthesis: a new active site model for fatty acid cyclooxygenase.* Prostaglandins, 1982. 24(1): p. 21-34.

147.   Kumar, K.S. and K. Muller, *Depsides as non-redox inhibitors of leukotriene B(4) biosynthesis and HaCaT cell growth, 2. Novel analogues of obtusatic acid.* Eur J Med Chem, 2000. 35(4): p. 405-11.

148.   Kumar, K.C. and K. Muller, *Lichen metabolites. 1. Inhibitory action against leukotriene B4 biosynthesis by a non-redox mechanism.* J Nat Prod, 1999. 62(6): p. 817-20.

149.   Okuyama, E., et al., *Usnic acid and diffractaic acid as analgesic and antipyretic components of Usnea diffracta.* Planta Med, 1995. 61(2): p. 113-5.

150.   Gissurarson, S.R., et al., *Effect of lobaric acid on cysteinyl-leukotriene formation and contractile activity of guinea pig taenia coli.* J Pharmacol Exp Ther, 1997. 280(2): p. 770-3.

151. CO, W., *Textbook of organic medicinal and pharmaceutical chemistry*. 1998.

152. Molnar, K. and E. Farkas, *Current results on biological activities of lichen secondary metabolites: a review*. Z Naturforsch C, 2010. 65(3-4): p. 157-73.

153. Russo, A., et al., *Lichen metabolites prevent UV light and nitric oxide-mediated plasmid DNA damage and induce apoptosis in human melanoma cells*. Life Sci, 2008. 83(13-14): p. 468-74.

154. Kumar, K.C. and K. Muller, *Lichen metabolites. 2. Antiproliferative and cytotoxic activity of gyrophoric, usnic, and diffractaic acid on human keratinocyte growth*. J Nat Prod, 1999. 62(6): p. 821-3.

155. Mahady, G.B., *Ginkgo biloba for the prevention and treatment of cardiovascular disease: a review of the literature*. J Cardiovasc Nurs, 2002. 16(4): p. 21-32.

156. Smith, J.V. and Y. Luo, *Studies on molecular mechanisms of Ginkgo biloba extract*. Appl Microbiol Biotechnol, 2004. 64(4): p. 465-72.

157. Mahadevan, S. and Y. Park, *Multifaceted therapeutic benefits of Ginkgo biloba L.: chemistry, efficacy, safety, and uses*. J Food Sci, 2008. 73(1): p. R14-9.

158. Chavez, M.L. and P.I. Chavez, *Ginkgo (part 1): history, use, and pharmacologic properties. .* Hosp. Pharm. , 1998. 33: p. 658-672.

159. Bilia, A.R., *Ginkgo biloba L.* Fitoterapia, 2002. 73(3): p. 276-9.

160. Ramassamy, C., F. Longpre, and Y. Christen, *Ginkgo biloba extract (EGb 761) in Alzheimer's disease: is there any evidence?* Curr Alzheimer Res, 2007. 4(3): p. 253-62.

161. Sticher, O., *Quality of Ginkgo preparations*. Planta Med, 1993. 59(1): p. 2-11.

162. McKenna, D.J., K. Jones, and K. Hughes, *Efficacy, safety, and use of ginkgo biloba in clinical and preclinical applications*. Altern Ther Health Med, 2001. 7(5): p. 70-86, 88-90.

163.   Braquet, P., *The Ginkgolides: Potent platelet-activating factor antagonists isolated from Ginkgo bilobaL.: Chemistry, pharmacology and clinical applications.* Drugs of the Future, 1987. 12(7): p. 643-699.

164.   Braquet, P. and D. Hosford, *Ethnopharmacology and the development of natural PAF antagonists as therapeutic agents.* J Ethnopharmacol, 1991. 32(1-3): p. 135-9.

165.   Lee, S.J., et al., *Suppression of mouse lymphocyte proliferation in vitro by naturally-occurring biflavonoids.* Life Sci, 1995. 57(6): p. 551-8.

166.   Houghton, P., *Herbal products. 2. Ginkgo.* The Pharmaceutical Jour. , 1994. 253: p. 122-124.

167.   Gardes-Albert M, A.S., Ferradini C, Droy-Lefaix M., *Egb 761 scavenger effect against OH and O2- radicals. A gamma pulse radiolysis study.* Fre Radic. Biol. Med., 1990. 9(Suppl. 1): p. 190.

168.   Scholtyssek, H., et al., *Antioxidative activity of ginkgolides against superoxide in an aprotic environment.* Chem Biol Interact, 1997. 106(3): p. 183-90.

169.   Atzori, C., et al., *Activity of bilobalide, a sesquiterpene from Ginkgo biloba, on Pneumocystis carinii.* Antimicrob Agents Chemother, 1993. 37(7): p. 1492-6.

170.   van Beek, T.A., *Chemical analysis of Ginkgo biloba leaves and extracts.* J Chromatogr A, 2002. 967(1): p. 21-55.

171.   Liu, Z.H. and S. Zeng, *Cytotoxicity of ginkgolic acid in HepG2 cells and primary rat hepatocytes.* Toxicol Lett, 2009. 187(3): p. 131-6.

172.   Jaggy, H. and E. Koch, *Chemistry and biology of alkylphenols from Ginkgo biloba L.* Pharmazie, 1997. 52(10): p. 735-8.

173.   Satyan, K.S., et al., *Anxiolytic activity of ginkgolic acid conjugates from Indian Ginkgo biloba.* Psychopharmacology (Berl), 1998. 136(2): p. 148-52.

174.   Ghosal, S., et al., *The chemistry and action of 6-alkylsalicylates of Indian Ginkgo biloba.* Indian Journal of Chemistry Section B-Organic Chemistry Including Medicinal Chemistry, 1997. 36(3): p. 257-263.

175.   Koeberle, A., *Identification and Characterization of Microsomal Prostaglandin E2 Synthase-1 Inhibitors.* 2009, University of Tuebingen.

176.   Baumgartner, L., et al., *Lignan derivatives from Krameria lappacea roots inhibit acute inflammation in vivo and pro-inflammatory mediators in vitro.* J Nat Prod, 2011. 74(8): p. 1779-86.

177.   Bauer, J., et al., *Discovery of depsides and depsidones from lichen as potent inhibitors of microsomal prostaglandin E2 synthase-1 using pharmacophore models.* ChemMedChem, 2012. 7(12): p. 2077-81.

178.   Elkady M, N.R., Schaible AM, Bauer J, Luderer S, Ambrosi G, Werz O, Laufer SA., *Modified Acidic Nonsteroidal Anti-Inflammatory Drugs as Dual Inhibitors of mPGES-1 and 5-LOX.* J Med Chem., 2012. [Epub ahead of print].

179.   Pergola, C., et al., *ERK-mediated regulation of leukotriene biosynthesis by androgens: a molecular basis for gender differences in inflammation and asthma.* Proc Natl Acad Sci U S A, 2008. 105(50): p. 19881-6.

180.   Fischer, L., et al., *Phosphorylation- and stimulus-dependent inhibition of cellular 5-lipoxygenase activity by nonredox-type inhibitors.* FASEB J, 2003. 17(8): p. 949-51.

181.   Werz, O., et al., *Activation of 5-lipoxygenase by cell stress is calcium independent in human polymorphonuclear leukocytes.* Blood, 2002. 99(3): p. 1044-52.

182.   Albert, D., et al., *Hyperforin is a dual inhibitor of cyclooxygenase-1 and 5-lipoxygenase.* Biochem Pharmacol, 2002. 64(12): p. 1767-75.

183.   Hoffmann, M., et al., *Hyperforin induces Ca(2+)-independent arachidonic acid release in human platelets by facilitating cytosolic phospholipase A(2) activation through select phospholipid interactions.* Biochim Biophys Acta, 2010. 1801(4): p. 462-72.

184.   Tateson, J.E., et al., *Selective inhibition of arachidonate 5-lipoxygenase by novel acetohydroxamic acids: biochemical assessment in vitro and ex vivo.* Br J Pharmacol, 1988. 94(2): p. 528-39.

185.   Carini, M., et al., *Antioxidant and photoprotective activity of a lipophilic extract containing neolignans from Krameria triandra roots.* Planta Med, 2002. 68(3): p. 193-7.

186.   ESCOP, *Monographs Supplement 2009.* 2009, Georg Thieme Verlag: Stuttgart. p. 213 - 216.

187.   Simpson, B., *Krameriaceae.* Flora Neotropica, 1989. 49: p. 1-108.

188.   Simpson, B.B., *The Past and Present Uses of Rhatany (Krameria, Krameriaceae).* Economic Botany, 1991. 45(3): p. 397-409.

189.   Schuhly, W., et al., *Design and synthesis of ten biphenyl-neolignan derivatives and their in vitro inhibitory potency against cyclooxygenase-1/2 activity and 5-lipoxygenase-mediated LTB4-formation.* Bioorg Med Chem, 2009. 17(13): p. 4459-65.

190.   Saleem, M., et al., *An update on bioactive plant lignans.* Nat Prod Rep, 2005. 22(6): p. 696-716.

191.   Waltenberger, B., et al., *Pharmacophore modeling and virtual screening for novel acidic inhibitors of microsomal prostaglandin E(2) synthase-1 (mPGES-1).* J Med Chem, 2011. 54(9): p. 3163-74.

192.   Fakhrudin, N., et al., *Computer-aided discovery, validation, and mechanistic characterization of novel neolignan activators of peroxisome proliferator-activated receptor gamma.* Mol Pharmacol, 2010. 77(4): p. 559-66.

193.   Werz, O., *Inhibition of 5-lipoxygenase product synthesis by natural compounds of plant origin.* Planta Med, 2007. 73(13): p. 1331-57.

194.   Radmark, O. and B. Samuelsson, *Microsomal prostaglandin E synthase-1 and 5-lipoxygenase: potential drug targets in cancer.* J Intern Med, 2010. 268(1): p. 5-14.

195. Hara, S., et al., *Prostaglandin E synthases: Understanding their pathophysiological roles through mouse genetic models.* Biochimie, 2010. 92(6): p. 651-9.

196. Fiorucci, S., et al., *Dual inhibitors of cyclooxygenase and 5-lipoxygenase. A new avenue in anti-inflammatory therapy?* Biochem Pharmacol, 2001. 62(11): p. 1433-8.

197. Elder, P.t., in *Naturalis Historia*. XXI. p. 168-169.

198. Bauer, J., *Identifizierung und Charakterisierung anti-inflammatorischer Naturstoffe als duale mPGES-1/5-LO Inhibitoren.* 2008, Universitiy of Tuebingen.

199. Capdevila, J.H., et al., *The catalytic outcomes of the constitutive and the mitogen inducible isoforms of prostaglandin H2 synthase are markedly affected by glutathione and glutathione peroxidase(s).* Biochemistry, 1995. 34(10): p. 3325-37.

200. McQuay, H.J. and R.A. Moore, *Dose-response in direct comparisons of different doses of aspirin, ibuprofen and paracetamol (acetaminophen) in analgesic studies.* Br J Clin Pharmacol, 2007. 63(3): p. 271-8.

201. Kato, M., et al., *Cyclooxygenase-1 and cyclooxygenase-2 selectivity of non-steroidal anti-inflammatory drugs: investigation using human peripheral monocytes.* J Pharm Pharmacol, 2001. 53(12): p. 1679-85.

202. Kawamura, M., et al., *Are the anti-inflammatory effects of dexamethasone responsible for inhibition of the induction of enzymes involved in prostanoid formation in rat carrageenin-induced pleurisy?* Eur J Pharmacol, 2000. 400(1): p. 127-35.

203. Cuzzocrea, S., et al., *5-Lipoxygenase knockout mice exhibit a resistance to pleurisy and lung injury caused by carrageenan.* J Leukoc Biol, 2003. 73(6): p. 739-46.

204.   Sala, A., et al., *New acetophenone glucosides isolated from extracts of Helichrysum italicum with antiinflammatory activity.* J Nat Prod, 2001. 64(10): p. 1360-2.

205.   Jachak, S.M., *Cyclooxygenase inhibitory natural products: current status.* Curr Med Chem, 2006. 13(6): p. 659-78.

206.   Alberto Minassi, L.C., Andreas Koeberle, Julia Bauer, Stefan Laufer, Oliver Werz and Giovanni Appendino, *A Multicomponent Carba-Betti Strategy to Alkylidene Heterodimers – Total Synthesis and Structure–Activity Relationships of Arzanol.* European Journal of Organic Chemistry, 2012. 2012(4): p. 772–779

207.   Pertwee, R.G., *Cannabinoid pharmacology: the first 66 years.* Br J Pharmacol, 2006. 147 Suppl 1: p. S163-71.

208.   Mechoulam, R. and L. Hanus, *A historical overview of chemical research on cannabinoids.* Chem Phys Lipids, 2000. 108(1-2): p. 1-13.

209.   Burstein, S., E. Levin, and C. Varanelli, *Prostaglandins and cannabis. II. Inhibition of biosynthesis by the naturally occurring cannabinoids.* Biochem Pharmacol, 1973. 22(22): p. 2905-10.

210.   Werz, O. and D. Steinhilber, *Therapeutic options for 5-lipoxygenase inhibitors.* Pharmacol Ther, 2006. 112(3): p. 701-18.

211.   Sofia, R.D., L.C. Knobloch, and H.B. Vassar, *The anti-edema activity of various naturally occurring cannabinoids.* Res Commun Chem Pathol Pharmacol, 1973. 6(3): p. 909-18.

212.   Sofia, R.D., et al., *Anti-edema and analgesic properties of delta9-tetrahydrocannabinol (THC).* J Pharmacol Exp Ther, 1973. 186(3): p. 646-55.

213.   Sofia, R.D., et al., *Comparative anti-phlogistic activity of delta 9-tetrahydrocannabinol, hydrocortisone and aspirin in various rat paw edema models.* Life Sci, 1974. 15(2): p. 251-60.

214.   Wirth, P.W., et al., *Anti-inflammatory properties of cannabichromene.* Life Sci, 1980. 26(23): p. 1991-5.

215.   Turner, C.E. and M.A. Elsohly, *Biological activity of cannabichromene, its homologs and isomers.* J Clin Pharmacol, 1981. 21(8-9 Suppl): p. 283S-291S.

216.   Malfait, A.M., et al., *The nonpsychoactive cannabis constituent cannabidiol is an oral anti-arthritic therapeutic in murine collagen-induced arthritis.* Proc Natl Acad Sci U S A, 2000. 97(17): p. 9561-6.

217.   Russo, E. and G.W. Guy, *A tale of two cannabinoids: the therapeutic rationale for combining tetrahydrocannabinol and cannabidiol.* Med Hypotheses, 2006. 66(2): p. 234-46.

218.   Scholz, E. and H. Rimpler, *Proanthocyanidins from Krameria triandra root.* Planta Med, 1989. 55(4): p. 379-84.

219.   Ingolfsdottir, K., *Usnic acid.* Phytochemistry, 2002. 61(7): p. 729-36.

220.   Manojlovic, N., et al., *Chemical composition of three Parmelia lichens and antioxidant, antimicrobial and cytotoxic activities of some their major metabolites.* Phytomedicine, 2012. 19(13): p. 1166-72.

221.   Sokolov, D.N., et al., *Anti-viral activity of (-)- and (+)-usnic acids and their derivatives against influenza virus A(H1N1)2009.* Bioorg Med Chem Lett, 2012. 22(23): p. 7060-4.

222.   Bucar, F., et al., *Anti-proliferative lichen compounds with inhibitory activity on 12(S)-HETE production in human platelets.* Phytomedicine, 2004. 11(7-8): p. 602-6.

223.   Einarsdottir, E., et al., *Cellular mechanisms of the anticancer effects of the lichen compound usnic acid.* Planta Med, 2010. 76(10): p. 969-74.

224.   Suleyman, H., et al., *Anti-inflammatory and antiulcerogenic effects of the aqueous extract of Lobaria pulmonaria (L.) Hoffm.* Phytomedicine, 2003. 10(6-7): p. 552-7.

225.   Omarsdottir, S., J. Freysdottir, and E.S. Olafsdottir, *Immunomodulating polysaccharides from the lichen Thamnolia vermicularis var. subuliformis.* Phytomedicine, 2007. 14(2-3): p. 179-84.

226. Neamati, N., et al., *Depsides and depsidones as inhibitors of HIV-1 integrase: discovery of novel inhibitors through 3D database searching.* J Med Chem, 1997. 40(6): p. 942-51.

227. Lai, D., et al., *Phenolic compounds with in vitro activity against respiratory syncytial virus from the Nigerian lichen Ramalina farinacea.* Planta Med, 2013. 79(15): p. 1440-6.

228. Cheng, B., et al., *Identification of anziaic acid, a lichen depside from Hypotrachyna sp., as a new topoisomerase poison inhibitor.* PLoS One, 2013. 8(4): p. e60770.

229. Sultana, N. and A.J. Afolayan, *A new depsidone and antibacterial activities of compounds from Usnea undulata Stirton.* J Asian Nat Prod Res, 2011. 13(12): p. 1158-64.

230. Gianini, A.S., et al., *Activities of 2,4-dihydroxy-6-n-pentylbenzoic acid derivatives.* Z Naturforsch C, 2008. 63(1-2): p. 29-34.

231. Turk, H., et al., *Antimicrobial activity of extracts of chemical races of the lichen Pseudevernia furfuracea and their physodic acid, chloroatranorin, atranorin, and olivetoric acid constituents.* Z Naturforsch C, 2006. 61(7-8): p. 499-507.

232. Kosanic, M., et al., *Evernia prunastri and Pseudoevernia furfuraceae lichens and their major metabolites as antioxidant, antimicrobial and anticancer agents.* Food Chem Toxicol, 2013. 53: p. 112-8.

233. Kosanic, M. and B. Rankovic, *Antioxidant and antimicrobial properties of some lichens and their constituents.* J Med Food, 2011. 14(12): p. 1624-30.

234. Williams, D.E., et al., *Depsides isolated from the Sri Lankan lichen Parmotrema sp. exhibit selective Plk1 inhibitory activity.* Pharm Biol, 2011. 49(3): p. 296-301.

235. Russo, A., et al., *Effect of vicanicin and protolichesterinic acid on human prostate cancer cells: role of Hsp70 protein.* Chem Biol Interact, 2012. 195(1): p. 1-10.

236. Thadhani, V.M., et al., *Antioxidant activity of some lichen metabolites.* Nat Prod Res, 2011. 25(19): p. 1827-37.

237. Lohezic-Le Devehat, F., et al., *Stictic acid derivatives from the lichen Usnea articulata and their antioxidant activities.* J Nat Prod, 2007. 70(7): p. 1218-20.

238. Lopes, T.I., et al., *Radical-scavenging activity of orsellinates.* Chem Pharm Bull (Tokyo), 2008. 56(11): p. 1551-4.

239. Endo, Y., et al., *Confluentic acid and 2'-O-methylperlatolic acid, monoamine oxidase B inhibitors in a Brazilian plant, Himatanthus sucuuba.* Chem Pharm Bull (Tokyo), 1994. 42(6): p. 1198-201.

240. Pejin, B., et al., *A new depsidone of Lobaria pulmonaria with acetylcholinesterase inhibition activity.* J Enzyme Inhib Med Chem, 2013. 28(4): p. 876-8.

241. Pejin, B., et al., *Acetylcholinesterase inhibition activity of acetylated depsidones from Lobaria pulmonaria.* Nat Prod Res, 2012. 26(17): p. 1634-7.

242. Ingolfsdottir, K., et al., *Inhibitory effects of the lichen metabolite lobaric acid on arachidonate metabolism in vitro.* Phytomedicine, 1996. 2(3): p. 243-6.

243. Ingolfsdottir, K., et al., *Inhibitory effects of baeomycesic acid from the lichen Thamnolia subuliformis on 5-lipoxygenase in vitro.* Phytomedicine, 1997. 4(2): p. 125-8.

244. Ichinose, T., M. Miller, and T. Shibamoto, *Inhibition of malondialdehyde formation from liver microsomes by a lichen constituent.* Food Chem Toxicol, 1994. 32(12): p. 1167-8.

245. Oettl, S.K., et al., *Imbricaric acid and perlatolic acid: multi-targeting anti-inflammatory depsides from Cetrelia monachorum.* PLoS One, 2013. 8(10): p. e76929.

246. Werz, O. and D. Steinhilber, *Development of 5-lipoxygenase inhibitors-- lessons from cellular enzyme regulation.* Biochem Pharmacol, 2005. 70(3): p. 327-33.

247.   Pereira, E.C., et al., *Determination of Teloschistes flavicans (sw) norm anti-inflammatory activity.* Pharmacognosy Res, 2010. 2(4): p. 205-10.

248.   Silva, J.A., et al., *Pharmacological properties of lichen Cladonia clathrata.* Pharm Biol, 2010. 48(7): p. 745-52.

249.   Suleyman, H., et al., *An investigation of the antiinflammatory effects of an extract from Cladonia rangiformis HOFFM.* Biol Pharm Bull, 2002. 25(1): p. 10-3.

250.   Tanas, S., et al., *Evaluation of anti-inflammatory and antioxidant activities of Peltigera rufescens lichen species in acute and chronic inflammation models.* J Nat Med, 2010. 64(1): p. 42-9.

251.   Celotti, F. and S. Laufer, *Anti-inflammatory drugs: new multitarget compounds to face an old problem. The dual inhibition concept.* Pharmacol Res, 2001. 43(5): p. 429-36.

252.   Koch, E., *Inhibition of platelet activating factor (PAF)-induced aggregation of human thrombocytes by ginkgolides: considerations on possible bleeding complications after oral intake of Ginkgo biloba extracts.* Phytomedicine, 2005. 12(1-2): p. 10-6.

253.   Diamond, B.J., et al., *Ginkgo biloba extract: mechanisms and clinical indications.* Arch Phys Med Rehabil, 2000. 81(5): p. 668-78.

254.   Ellnain-Wojtaszek, M., Z. Kruczynski, and J. Kasprzak, *Investigation of the free radical scavenging activity of Ginkgo biloba L. leaves.* Fitoterapia, 2003. 74(1-2): p. 1-6.

255.   Kudolo, G.B., et al., *The ingestion of Ginkgo biloba extract (EGb 761) inhibits arachidonic acid-mediated platelet aggregation and thromboxane B2 production in healthy volunteers.* J Herb Pharmacother, 2004. 4(4): p. 13-26.

256.   Kubo, I., H. Muroi, and A. Kubo, *Naturally occurring antiacne agents.* J Nat Prod, 1994. 57(1): p. 9-17.

257.   Itokawa, H., et al., *Antitumor principles from Ginkgo biloba L.* Chem Pharm Bull (Tokyo), 1987. 35(7): p. 3016-20.

258. Lu, J.M., et al., *Ginkgolic acid inhibits HIV protease activity and HIV infection in vitro.* Med Sci Monit, 2012. 18(8): p. BR293-298.

259. Matsumoto, K., et al., *Comparison of the effects of bilobol and 12-O-tetradecanoylphorbol-13-acetate on skin, and test of tumor promoting potential of bilobol in CD-1 mice.* J Toxicol Sci, 1990. 15(1): p. 39-46.

260. Lepoittevin, J.P., C. Benezra, and Y. Asakawa, *Allergic contact dermatitis to Ginkgo biloba L.: relationship with urushiol.* Arch Dermatol Res, 1989. 281(4): p. 227-30.

261. Hecker, H., et al., *In vitro evaluation of the cytotoxic potential of alkylphenols from Ginkgo biloba L.* Toxicology, 2002. 177(2-3): p. 167-77.

262. Oh, J., et al., *Inhibition of fatty acid synthase by ginkgolic acids from the leaves of Ginkgo biloba and their cytotoxic activity.* J Enzyme Inhib Med Chem, 2013. 28(3): p. 565-8.

263. Ilieva, I., et al., *The effects of Ginkgo biloba extract on lipopolysaccharide-induced inflammation in vitro and in vivo.* Exp Eye Res, 2004. 79(2): p. 181-7.

264. Kotakadi, V.S., et al., *Ginkgo biloba extract EGb 761 has anti-inflammatory properties and ameliorates colitis in mice by driving effector T cell apoptosis.* Carcinogenesis, 2008. 29(9): p. 1799-806.

265. Siegers, C.P., *Cytotoxicity of alkylphenols from Ginkgo biloba.* Phytomedicine, 1999. 6(4): p. 281-3.

266. McGettigan, P. and D. Henry, *Cardiovascular risk and inhibition of cyclooxygenase: a systematic review of the observational studies of selective and nonselective inhibitors of cyclooxygenase 2.* JAMA, 2006. 296(13): p. 1633-44.

8 FOOTNOTES

¶ data was determined during my diploma thesis (supervision by Andreas Koeberle) in the lab of Prof. Dr. O. Werz (University Tuebingen, Germany)

9 CONTRIBUTIONS

Determination of activity of isolated human recombinant $cPLA_{2\alpha}$ in all cell-free experiments was performed by Marius Melzer in the lab of Prof. Dr. O. Werz (University of Jena, Germany).

MTT experiments in HL60 cells were performed by Dagmar Blaesius in the lab of Prof. Dr. O. Werz (University of Tuebingen, Germany).

MTT experiments of CFA in A549 cells were performed by Dr. Anja Schaible (University of Jena, Germany).

Experiments of carrageenan-induced pleurisy in rats were performed by Dr. Rossi and Prof. Sautebin (University of Naples, Italy).

Cell-free mPGES-1 experiments for synthsized NSAID derivatives were partially conducted by Giulia Ambrosi (University of Tuebingen, Germany).

10   AKADEMISCHE LEHRER

Dr. Bertolt Gust

Dr. Ulrike Sausbier

Priv. Doz. Dr. Martina Düfer

Priv. Doz. Dr. Matthias Sausbier

Prof. Dr. Gisela Drews

Prof. Dr. J.E. Schultz

Prof. Dr. Lutz Heide

Prof. Dr. Martin Wahl

Prof. Dr. Oliver Werz

Prof. Dr. Peter Krippeit-Drews

Prof. Dr. Peter Ruth

Prof. Dr. Rolf Daniels

Prof. Dr. Stefan Laufer